

A-X Overseer

Striking Lightning at America's Enemies

AIAA UNDERGRADUATE INDIVIDUAL AIRCRAFT DESIGN COMPETITION 2017-2018



KU THE UNIVERSITY OF
KANSAS
AEROSPACE ENGINEERING DEPARTMENT

Pedro Toledo
PEDRO TOLEDO

Dr. R. Barrett-Gonzalez
ADVISOR: DR. R. BARRETT-GONZALEZ



Pedro Toledo

AIAA Member Number: 655253

A handwritten signature in black ink, appearing to read "Pedro Toledo".

**Faculty Advisor:
Dr. Ronald Barrett**

AIAA Member Number: 022393

A handwritten signature in black ink, appearing to read "Ron Barrett".

EXECUTIVE SUMMARY

The need for top of the line aircraft has always been a priority in the United States armed forces. Historically, new aircraft for the military have been introduced at a quickened pace. With the sociopolitical forces in recent decades, this trend has slowed down. This can be seen in the date of introduction for the last five members of the fighter, F, family: F-35 in 2015, F-22 in 2005, F/A-18 E/F in 1995, F/A-18A/B in 1983, F-16 in 1978, and the F-15 in 1976. Similar trends are found in transport, bombers, air support, and trainer aircraft. With a fleet of aging airframes, the feasibility of continuously upgrading Cold War-era aircraft with cutting-edge technology is slowly becoming impractical.

The purpose of this report is to introduce the A-X Overseer as a replacement to the Fairchild Republic A-10 Thunderbolt II. Preliminary sizing, Class I, and Class II design are presented in this design report. The design process started with preliminary weight, wing, and powerplant sizing. Input from A-10 pilots, flight line crew, and ground forces that work alongside the aircraft were consulted. A sweep of potential configurations was undertaken for a final selection. Once a final configuration was selected, Class I and Class II design methods from Jan Roskam's Airplane Design series were performed. The defining feature of the A-X Overseer is the use of the Coandă effect through upper surface blowing and a side-mounted cannon. Two General Electric CF34-3B1 engines power the Overseer. A large wing span of 89.6 ft with a high aspect ratio provides sufficient lift characteristics to meet range and loiter requirements. Supplemented by upper surface blowing, plain flaps provide sufficient lift to accomplish takeoff and landing requirements keeping the aircraft's complexity at a minimum. Flight controls use a fly-by-light system with de facto longitudinal and directional stability. MTOW for the Overseer is 55,000 lb with a maximum fuselage diameter of 76 in, maximum length of 645 in, and wing span of 86.6 ft.

An accompanying website, <https://toledoph.wixsite.com/ae522/>, provides detailed sample calculations and screen shots of programs used.

ACKNOWLEDGMENTS

This author would like to acknowledge the following individuals for their support in the success of this report:

- Dr. Ron Barrett for his insight and guidance through the design process, and for fanning the flame of creative problem solving.
- Col. Roger Disrud and Lt. Col. John Marks for sharing their knowledge on the capabilities of the A-10 and insight on the qualities of a future close air support aircraft.
- Dr. Adrian Lewis for his insight on the needs of a support aircraft from ground forces perspective.
- The pilots and crew members at Whiteman AFB for their insight on the A-10 and thorough discussion of the capabilities of a future replacement.

Table of Contents

1. INTRODUCTION, MISSION SPECIFICATION & PROFILE	1
1.1. DESIGN REQUIREMENTS	1
1.2. MISSION PROFILE, PERFORMANCE, PAYLOAD-RANGE REQUIREMENTS	2
1.3. OVERALL DESIGN METHODS AND PROCESS	3
2. HISTORICAL REVIEW & COMPETITION IN THE MARKET	4
3. DESIGN VECTOR & WEIGHTS ESTABLISHMENT	8
4. WEIGHT SIZING	9
4.1. EMPTY-TO-TAKEOFF WEIGHT RATIO DETERMINATION.	9
4.2. DETERMINATION OF PRELIMINARY DESIGN WEIGHTS	9
5. WING AND POWERPLANT SIZING	10
5.1. DISCUSSION OF PERFORMANCE CONSTRAINTS	10
5.2. SIZING CHART ANALYSIS	11
6. CLASS I CONFIGURATION DOWN SELECTION	13
6.1. CONFIGURATION MATRIX AND OPTIMIZATION FUNCTION.	13
6.2. CONFIGURATION DOWNSELECTION	15
6.4. CARPET PLOTS	16
6.3. SELECTION OF MAJOR WING CHARACTERISTICS	17
7. CLASS I DESIGN	18
7.1. LAYOUT OF THE COCKPIT AND FUSELAGE.	18
7.2. ENGINE INSTALLATION	20
7.3. WING LAYOUT DESIGN	20
7.4. HIGH LIFT DEVICE SIZING	21
7.5. EMPENNAGE DESIGN	22
7.6. LANDING GEAR DESIGN	23
7.7. WEIGHT AND BALANCE.	25
7.8. V-N DIAGRAM	26
7.9. STABILITY AND CONTROL.	27
7.10. DRAG POLAR & PERFORMANCE ANALYSIS.	29
7.11. ANALYSIS OF WEIGHT AND BALANCE AND STABILITY AND CONTROL.	30
7.12. LIFT-TO-DRAG ANALYSIS	30
7.13. STRUCTURAL LAYOUT	31
8. SYSTEMS DESIGN	33
8.1. FUEL SYSTEM	33
8.2. FLIGHT CONTROL SYSTEM	34
8.3. ELECTRICAL SYSTEM	34
8.4. HYDRAULIC SYSTEM	35
8.5. ENVIRONMENTAL CONTROL AND AIR BLEED SYSTEMS	35
9. CLASS II DESIGN	37
9.1. LANDING GEAR.	37
9.2. WEIGHT AND BALANCE.	37

	OVERSEER
9.3. STABILITY AND CONTROL	40
10. UPDATED THREE VIEW AND EXPLODED VIEWS	43
11. ARMAMENTS	45
11.1. BUSHMASTER III CANNON	45
11.2. ORDNANCE	46
11.3. ADVANCED ARMAMENT DEPLOYMENT	46
12. ADVANCED TECHNOLOGIES	47
12.1. UPPER SURFACE BLOWING	47
12.2. ADVANCED COMMUNICATIONS-ELECTRONICS SYSTEMS	48
13. RISK MITIGATION	49
14. MANUFACTURING PLAN	51
15. COST ANALYSIS	56
16. MARKETING PLAN AND PATH FORWARD	57
16.1. MARKETING PLAN	57
16.2. PATH FORWARD	57
17. SPECIFICATION COMPLIANCE	58
REFERENCES	59

List of Figures

Figure 1.1: Overseer Mission Profile [1]	2
Figure 1.2: Field Length Requirements at ICAO Hot Day [1].	2
Figure 1.3: Required/Specified Payload-Range Performance [1]	2
Figure 1.4: Dean E. Ackers Distinguished Professor Emeritus, Dr. Jan Roskam [13].	3
Figure 2.1: Junkers Ju-87 Stuka [15]	4
Figure 2.2: Ilyushin Il-2 Shturmovik [20].	4
Figure 2.3: Republic P-47 Thunderbolt [22]	4
Figure 2.4: Fairchild Republic A-10 Thunderbolt II [25].	5
Figure 2.5: Douglas AC-47 Spooky [29]	5
Figure 2.6: Fairchild AC-119K Stinger [33]	6
Figure 2.7: Lockheed AC-130J Ghost rider [39]	7
Figure 3.1: Col. Roger Disrud [48]	8
Figure 3.2: Lt. Col. John Marks [49]	8
Figure 3.3: Maj. Adrian Lewis [50].	8
Figure 4.1: Empty-to-Takeoff Weight Ratio (Left) and Takeoff Weights (Right) used in STAMPED Analysis	

The aircraft above the red line in the figure demarcate historical aircraft used as reference.	9
Figure 5.1: Preliminary Sizing Drag Polar Estimation	10
Figure 5.2: Sizing Chart With Performance Constraints	12
Figure 6.1: Configuration Sweep	13
Figure 6.2: Configuration 1	14
Figure 6.3: Configuration 2	14
Figure 6.4: Configuration 3	14
Figure 6.5: Configuration 4	14
Figure 6.6: Configuration 5	14
Figure 6.7: Configuration 6	14
Figure 6.8: Configuration 7	15
Figure 6.9: Configuration 8	15
Figure 6.10: Configuration 9	15
Figure 6.11: Effect of Thrust to Weight Ratio and Wing Loading, lb_f/ft^2 , on Takeoff Run, ft.	16
Figure 6.12: Effect of Aspect Ratio and Wing Loading, lb_f/ft^2 , on Takeoff Weight, lbf.	16
Figure 6.13: Effect of Coefficient of Lift and Wing Loading, lb_f/ft^2 , on Minimum Cruise Velocity, kt.	16
Figure 7.1: Forward Cockpit Visibility Diagram. Overseer Visibility Drawn in Red; Recommended Visibility in Black. Background Image from Airplane Design: Part 3 [5].	18
Figure 7.2: Front, Top, and Side View of Fuselage. Scale: Front: 1:100 in. Top/Side: 1:200 in.	19
Figure 7.3: GE CF34-3B1 [63]	20
Figure 7.4: Wing Configuration Scale: 1:100 in.	21
Figure 7.5: Top View of High Lift Devices on Wing and Side View of Flap. Scale: Top: 1:100 in. Side: NTS	22
Figure 7.6: Three View of Empennage. Scale: 1:100 in.	23
Figure 7.7: Lateral Tip-over Criterion. Scale: 1:100 in.	24
Figure 7.8: Front and Side View of Undercarriage. Scale: 1:200 in.	24
Figure 7.9: Landing Gear Retraction. Scale: 1:200 in.	25
Figure 7.10: X CG Excursion Diagram	26
Figure 7.11: V-n Diagram	27
Figure 7.12: Longitudinal X-plot	27
Figure 7.13: Directional X-plot	28
Figure 7.14: Drag Polar	29
Figure 7.15: Fuselage Perimeter Plot	30

Figure 7.16: Structural Layout Overview: NTS.	31
Figure 7.17: Center of Gravity Location of Selected Components. NTS.	32
Figure 8.1: Complete System Overview; NTS	33
Figure 8.2: Fuel System Overview	33
Figure 8.3: Flight Control System Overview	34
Figure 8.4: Electrical System Overview; NTS	34
Figure 8.5: Hydraulic System Overview; NTS	35
Figure 9.1: Updated Center of Gravity Locations	39
Figure 9.2: Class II Center of Gravity Excursion Diagram	39
Figure 9.3: Empty Weight Distribution by Component Category	39
Figure 9.4: Empty Weight Distribution by Component.	40
Figure 9.5: Trim Diagram for 1G Cruise Flight.	42
Figure 10.1: Updated Three View.	43
Figure 10.2: Exploded View of Subcomponents; NTS.. . . .	44
Figure 11.1: Pylon Turn and Pivotal Altitude [56]	45
Figure 11.2: Ordnance Placement.	46
Figure 12.1: Upper Surface Blowing Nozzle and Thrust Reverser on YC-14 [53].	47
Figure 12.2: AN/AAQ-39 MWIR Magnification System [54]	48
Figure 12.3: AN/AAQ-37 EO DAS Detection [57].	48
Figure 12.4: AN/APG-81 Displays on Glass Cockpit [58]	48
Figure 13.1: Schrenk’s Approximation	49
Figure 14.1: Wing Assembly Visualization	51
Figure 14.2: Wing Assembly Flow Chart	52
Figure 14.3: Empennage Assembly Visualization	52
Figure 14.4: Empennage Assembly Flow Chart	53
Figure 14.5: Fuselage Assembly Flow Chart	53
Figure 14.6: Fuselage Assembly Visualization	54
Figure 14.7: Final Assembly Visualization	55
Figure 14.8: Final Assembly Flow Chart	55
Figure 15.1: Aircraft Production Unit Costs	56

List of Tables

Table 1.1: Close Air Support (A-10 Replacement) Technical Requirements [1].	1
Table 1.2: Aircraft Fuel Fraction	2
Table 2.1: Important Weights, Performance & Geometric Characteristics of Related Aircraft.	7
Table 3.1: Weights for Design Vector Variable as per Col. Disrud and Prof. Lewis [51, 52].	8
Table 5.1: Design Point	11
Table 6.1: Wing Characteristics.	17
Table 7.1: Salient Fuselage Characteristics	19
Table 7.2: Salient Engine Characteristics [63]	20
Table 7.3: Wing Characteristics.	21
Table 7.4: Fuel Tank Characteristics	21
Table 7.5: Flap Characteristics	22
Table 7.6: Flap Deflection	22
Table 7.7: Empennage Characteristics	23
Table 7.8: Landing Gear Strut and Tire Load Force and Ratios	24
Table 7.9: Salient Tire Characteristics	25
Table 7.10: Combined Component Weights	26
Table 7.11: Minimum Control Speed with One Engine Inoperative	28
Table 7.12: Overseer Wetted Area	29
Table 7.13: Drag Polar	29
Table 7.14: Lift to Drag Ratios for Flight Stages	30
Table 7.15: Preliminary Structural Characteristics	31
Table 8.1: Electrical System Components	34
Table 8.2: Electrical Load.	35
Table 9.1: Landing Gear Strut and Tire Load Force and Ratios	37
Table 9.2: Salient Tire Characteristics	37
Table 9.3: Landing Gear Strut Sizing	37
Table 9.4: Weight Breakdown.	38
Table 9.5: Static Margins for Loading Conditions	40
Table 9.6: Stability Derivatives	41
Table 9.7: Longitudinal Handling Qualities in Cruise	41

Table 9.8: Lateral Handling Qualities in Cruise 41

Table 11.1: Orbital ATK Bushmaster III Specifications [54] 45

Table 11.2: 35 mm Rounds [55]. 45

Table 14.1: Wing Material Selection 51

Table 14.2: Empennage Material Selection 52

Table 14.3: Fuselage Material Selection 53

Table 15.1: Acquisition Cost (500 Units) 56

Table 15.2: Life Cycle Cost (500 Units) 56

Table 17.1: Specification Compliance Matrix. 58

Table 17.2: Objective Function Overview 58

List of Symbols

AR	Aspect Ratio	~	W	Weight	lb _f
b	Wing Span	ft	W/S	Wing Load	lb _f / ft ²
c	Chord	ft			
C _L	Lift Coefficient	~		Greek Symbols	
C _l	Section Lift Coefficient	~	α	Angle of Attack	°
D	Drag	lb _f	β	Sideslip Angle	°
D _D	Drag Coefficient	~	Γ	Dihedral Angle	°
e	Oswald's Fuel Fraction	~	δ	Deflection Angle	°
L	Lift	lb _f	Δ	Change in a Parameter	~
K _a	Augmentation Feedback Loop	~	ε	Twist Angle	°
M	Mach Number	~	ε	Downwash	~
M _{ff}	Mission Fuel Fraction	~	η	Span-wise Location	~
n	Load Factor	g	λ	Taper Ratio	~
S	Wing Area	ft ²	μ	Friction Coefficient	~
S _L	Landing Distance	ft	Λ	Sweep Angle	°
S _{TO}	Takeoff Distance	ft	ρ	Air Density	slugs / ft ³
S _h	Horizontal Stabilizer Area	ft ²		Subscripts	
S _v	Vertical Stabilizer Area	ft ²	A	Approach	
T	Thrust	lb _f	c/4	Quarter chord	
TSFC	Thrust Specific Fuel Consumption	lb _m / Hr lb _f	cl	Climb	
T/W	Thrust-to-Weight Ratio	~	cr	Cruise	
V _h	Horizontal Tail Volume Coefficient	~	D	Drag	
V _v	Vertical Tail Volume Coefficient	~	E	Empty	
V	Velocity	ft/s kt mi/hr	F	Friction	
V _H	Maximum Level Speed	ft/s kt mi/hr	FF	Fuel Fraction	
V _L	Maximum Design Speed	ft/s kt mi/hr	f	Fuel, Flaps	
V _S	Stall Speed	ft/s kt mi/hr	g	Ground Friction	
			i	Inboard	
			L	Lift	

max	Maximum	STOL	Short Takeoff and Landing
mc	Minimum Control	USB	Upper Surface Blowing
o	Outboard	WL	Water Line
OE	Operating Empty	WSO	Weapons System Officer
PL	Payload		
r	Root, Rudder		
s	Stall		
tfo	Trapped Fuel and Oil		
TO	Takeoff		
TOG	Takeoff Ground		
w	Wing		

Acronyms

AAA	Advanced Aircraft Analysis
AAO	Aerial Armed Overwatch
AEI	All Engines Inoperative
AEO	All Engines Operative
AESA	Active Electronically Scanned Array
AFB	Air Force Base
AHEAD	Advanced Hit Efficiency And Destruction
APDC-T	Armor Piercing Discard Sabot
BL	Butt Line
CAS	Close Air Support
CG	Center of Gravity
CGR	Climb Gradient Requirement
CONOPS	Concept of Operations
EO DAS	Electro-Optical Distributed Aperture System
FAA	Federal Aviation Administration
FAR	Federal Aviation Regulation
FLIR	Federal Air Regulation
FS	Forward Looking Infrared Radar
GMS2	Gunship Multispectral Sensor System
HEI	High Explosive Incendiary
I ₂ TV	Two Image Intensified Television
IR	Infrared
IRST	Infrared Search and Track
ISA	International Standard Atmosphere
JDAM	Joint Direct Attack Mission
MWIR	Midwave Infrared
NIR	Near Infrared
NTS	Not to Scale
OEI	One Engine Inoperative
RFP	Request for Proposal
SAR	Synthetic-Aperture Radar
SLAR	Side Looking Airborne Radar

1. INTRODUCTION, MISSION SPECIFICATION & PROFILE

Introduced in 1975, one of the most effective ground-attack CAS aircraft in the history U.S. Air Force has been the Fairchild Republic A-10 Thunderbolt II. However, outdated engines and old airframes are a looming problem [1]. AIAA released a RFP looking for a replacement CAS aircraft. The mission specifications and general design requirements propose significant improvements to the current capabilities of the A-10. The overall mission goal the proposed CAS aircraft will be to provide continuous airborne armed overwatch (AAO) to ground forces and provide support as an observation, detection, and targeting imaging aircraft. Furthermore, CAS aircraft are requested at a moment's notice, thus the ability to operate out of unimproved airstrips at the front line is paramount to mission success. Although in-fuselage cannon configuration has been proven very effective with the A-10, this author believes the concept of a gunship is able to better perform and meet the criteria of the RFP. First proposed in Vietnam, the gunship concept has gone through three iterations in the Air Force with the latest installation, the AC-130, serving as long as the A-10. The mode of attack in an A-10, strafing, brings the aircraft to lower altitudes to increase accuracy, however the risk of taking ground fire is also increased. Strafing further requires repositioning the aircraft for another run leaving a period of time for enemy forces to recuperate and potentially open fire at ground forces. The use of a gunship positions the aircraft, typically, in a 30° banked turn orbiting around a target providing continuous suppressive fire.

1.1. DESIGN REQUIREMENTS

The target mission specifications are presented in the RFP given by AIAA for the 2017-2018 Undergraduate Individual Aircraft Design Competition [2]. Other design specifications and requirements are provided by Aircraft Design Pt. 1 [1]. Table 1 below gives the target mission specifications presented in the RFP.

Table 1.1: Close Air Support (A-10 Replacement) Technical Requirements [1]

Combat Mission Requirements	
Airborne Armed Overwatch	4 Hours at 500 nmi radius
Weapons Payload	1x 35 mm cannon with 750 rounds and 14,000 lbf of stores
Performance Requirements	
Max Speed	At least 300 KTAS
Cruise Speed	At least 200 KTAS
Ceiling	45,000 Feet
Minimum Runway Length	6,000 Feet
Maximum Design Load Factor	8g
Entry Into Service	2025
Additional Considerations	
Crew	1-2
Fly-Away Cost	\$40 Million
Direct Operating Cost	\$3000 per hour
Systems	Electro-optical targeting system and advanced communications array

1.2. MISSION PROFILE, PERFORMANCE, PAYLOAD-RANGE REQUIREMENTS

A mission profile presented in Figure 1.1 was derived from the RFP. The prescribed mission profile follows the heaviest load case scenario where the maximum capabilities of the aircraft are used while maintaining a full payload. Mission specifications require takeoff from unimproved runways at ISA hot day conditions (+20°F) at an elevation of 5,000 ft with a maximum balanced field length of 6,000 ft, Figure 1.2. A payload-range performance diagram is presented in Figure 1.3.

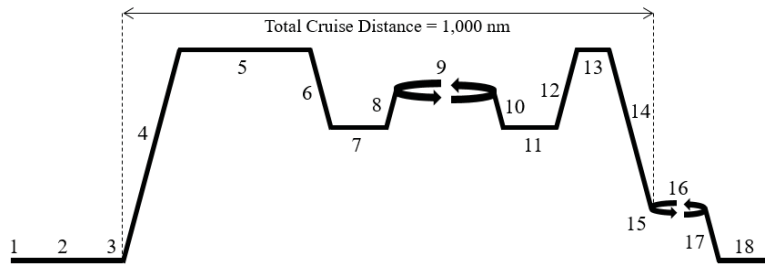


Figure 1.1: Overseer Mission Profile [1]

Mission Segment	Fuel Fraction
1 - Engine Start & Warm up	0.990
2 - Taxi	0.990
3 - Take-off	0.990
4 - Climb	0.998
5 - Cruise	0.978
6 - Descent	0.990
7 - 5 min. Ground Attack	0.997
8 - Climb	0.998
9 - 4 hour AAO	0.923
10 - Descent	0.990
11 - 5 min. Ground Attack	0.997
12 - Climb	0.998
13 - Cruise	0.978
14 - Descent	0.990
15 - Aborted Landing	-
16 - 30 min. Loiter	0.990
17 - Descent	0.990
18 - Landing	0.995



Figure 1.2: Field Length Requirements at ICAO Hot Day [1]

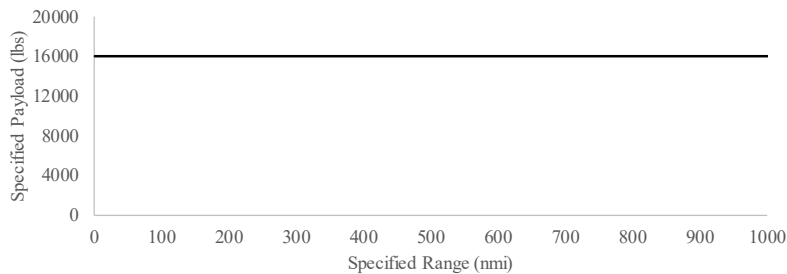


Figure 1.3: Required/Specified Payload-Range Performance [1]

1.3. OVERALL DESIGN METHODS AND PROCESS

The design and analysis methods employed throughout the design process were developed by Dr. Jan Roskam: *Aircraft Design* series, References 3-10. John Anderson's *Introduction to Flight*, Reference 11, and *Fundamentals of Aerodynamics*, Reference 12, were also consulted. Software used included Microsoft Office, OpenVSP, Siemens NX, and MathWorks MATLAB. Adobe InDesign and Photoshop were used for document assembly. Advanced Aircraft Analysis (AAA) was heavily used for stability and control. The design philosophy followed is delineated below:

1. Mission Specification and Identification

The first step is identifying the general design requirements and project objectives as dictated in the RFP.

2. Historical Overview

A number of aircraft are thoroughly researched and studied to understand the evolution of the air frame's primary mission. Historical data provide testimonials of both effective and ineffective design choices. The historical overview is presented in Chapter 2.

3. Statistical Time and Market Predictive Engineering Design (STAMPED) Analysis

STAMPED analysis allows for a preliminary design point to anticipate market trends and produce an aircraft that caters to the market when the aircraft is introduced. STAMPED analysis is further explained in Reference 14.

4. Class I Design, Configuration Design, and Down Selection

Class I design calculations are conducted providing preliminary weight and performance estimates. Exploratory configuration design follows Class I design where designs are filtered down to a final configuration based on specific design criteria.

5. Class II Design

Class II calculations are performed on the selected configuration followed by cost estimates and manufacturing selections.



**Figure 1.4: Dean E. Ackers
Distinguished Professor Emeritus,
Dr. Jan Roskam [13]**

2. HISTORICAL REVIEW & COMPETITION IN THE MARKET

Initially developed for a light bomber program for the secret German Defense and Aerospace Ministry, the Junkers Ju-87 Stuka was a successful attack aircraft for the Luftwaffe. The Ju-87 was structurally rugged allowing



Figure 2.1: Junkers Ju-87 Stuka [15]

6 g's to be pulled out of dives. Special automatic pull-up systems were integrated into the Ju-87 due to the high number of pilots losing consciousness during dives [16, 17] The final deployment version was the Ju-87G, nicknamed "Tank Buster." The Ju-87G, featured two 37 mm Bordkanone (BK

3.7) cannons under the wings. The BK 3.7 was fed by six round clips with an armor-piercing shell muzzle velocity of 2,790 feet per second. The overall combat capabilities of the Stuka as a ground attack aircraft were unmatched in the first half of World War II. However, with the rapidly advancement of aircraft technology, fast planes were able to take advantage of the Ju-87's low top speed of 190 kts [18, 19].

One of the primary main aerial opponents of the Ju-87 Stuka was the Soviet Ilyushin Il-2 Shturmovik. As



Figure 2.2: Ilyushin Il-2 Shturmovik [20]

the most manufactured aircraft of WWII, the Il-2 proved to be robust even with its wood-metal mixed structure. The forward fuselage was constructed entirely of metal with varying thicknesses to protect crucial systems. Although its heavy armor plating withstood machine gun and 20 mm cannon fire,

the aft of the aircraft was highly susceptible to gunfire, leading to the addition of an aft cockpit gunner [21].

The Republic P-47 Thunderbolt was quickly conceived following a call from the United States Army Air Corps for an airframe capable of 400 mph TAS at 25,000 ft, six .50 caliber machine guns with a preference for eight, armor plating, and 315 gal self-sealing fuel tanks [23]. Designed by Alexander Kartveli, the XP-47B prototype featured eight



Figure 2.3: Republic P-47 Thunderbolt [22]

.50 caliber machine guns and a newly developed 2,000 HP Pratt & Whitney XR-2800-21 eighteen cylinder radial engine. The design also featured a highly efficient supercharging duct, forcing the fuselage to be designed around it. Although high in weight and initially filled with flaws, the P-47 proved highly

effective as an escort to bombers and ground-attack aircraft [24].

The development of the A-10 Thunderbolt II started in the 1960s with study contracts defining the requirements of a new rugged and survivable CAS as part of the A-X program. The initial specifications called for high loiter time, maneuverability, cannon firepower, and survivability. The final RPF designated the GAU-8 as the primary cannon and called for 2 hours of loitering, 16,000 lbs of ordnance, 300 kt cruise, and 400 kt max speed. The primary competitor of

the Fairchild Republic YA-10 was the Northrop YA-9 – both selected for a fly-off competition. Defense analyst Pierre Sprey, who wrote the A-X requirements, praised the planes “responsiveness and simplicity,” allowing it to perform a wide variety of ground support missions and high amount of sorties while providing easy maintainability. While not all of the specifications were met – the takeoff distance exceeded the goal by 50 feet, and maximum speed was lower than specified – the YA-10 was deemed superior to the YA-9 due to design elements such as engine location, pylon spacing, ease of maintainability, and overall survivability [26]. Two GE TF-34-GE-100 engines provide 18,000 lb_t of thrust. Mounted above and slightly aft of the wings, the engine location reduces the risk of foreign object ingestion and forces exhaust gases over the horizontal stabilizer minimizing IR signature. Yawing moment introduced with engine failure is also minimized due to engine proximity to the fuselage. Pylon spacing underneath the wing allowed for a variety of armaments to be installed, including “general purpose bombs, cluster bombs, laser guided bombs, Joint Direct Attack Munitions (JDAM), Wind Corrected Munitions Dispenser (WCMD), AGM-65 Maverick and AIM-9 sidewinder missiles, 2.75 inch rockets, and illumination flares.” Designed for ease in maintainability, the A-10 features interchangeable engines, main landing gears, and vertical stabilizers. The high aspect ratio, unswept wings of the A-10



Figure 2.4: Fairchild Republic A-10 Thunderbolt II [25]

provided high maneuverability in low speeds and contributed to its short take off ability. Survivability is provided through a titanium bathtub around the cockpit and triple redundant flight systems – two hydraulic and a mechanical backup capable of absorbing 23 mm armor-piercing rounds. Although a low top speed of 380 kt was detrimental to its survivability, the A-10 has only operated in complete air superiority. Numerous upgrades since its introduction has allowed the A-10 to stay competitive with Generation 4 and 5 fighters in ground support capabilities. The A-10C entered service in 2007 with the latest batch of upgrades [27, 28].

The AC-47 Spooky was the first gunship in the USAF and was highly successful despite initial skepticism at the foreign concept. Converted from the C-47, the AC-47 featured three GAU-2 7.62 mm miniguns with firing modes of 50 or 100 rounds per second and 24,000 rounds. Placed at the cargo bay door and aft windows on the port side of the fuselage, the low wings of the AC-47 hindered the field of fire of the GAU-2 [30]. Combat missions were performed at an altitude of 2,500-3,000 ft and an airspeed of 120 kts with enough fuel for 7 hours of combat. The AC-47 flew toward its target on the outside and forward of the left side followed by a 30° bank once the target passed below. This maneuver



Figure 2.5: Douglas AC-47 Spooky [29]

allowed weapons to be fired in 3-7 second bursts [31-32].

Due to the success and age of the AC-47, a newer gunship was needed as part of Project Gunship II – the forerunner being the C-130. However, production numbers were low and the primary mission of the aircraft was as a transport. As an interim gunship, the readily available C-119 Boxcar was converted to the AC-119G Shadow in Project Gunship III. Armed with four 7.62 GAU-2 miniguns and increased ammo capacity of 50,000 rounds, the AC-119G had a 25% increase in efficiency over the AC-47. The addition of a fire control safety display safeguarded



Figure 2.6: Fairchild AC-119K Stinger [33]

the possibility of friendly fire [34-36]. The AC-119G was primarily used in South Vietnam, where its 6 hour endurance played crucial roles in airbase defense and providing support to ground troops [37].

A second variant, the AC-119K Stinger, included two additional J85 jet engines alongside the two original Wright R-3350 radial engines, two 20 mm cannons, improved fire control systems, and forward looking infrared radar (FLIR). Normal combat operations were carried out at 7,000 ft in areas of abundant anti-aircraft weapons, 5,500 ft for a vehicle hunting missions, and 3,500 ft in combat support missions with combat speeds of 180 kts and endurance of 5 hours [38].

The development of Project Gunship II lead to the production of the AC-130A Spectre. The AC-130A armament included four MXU-470 7.62 mm miniguns and four M61A1 20 mm cannons. Compared with its interim predecessor, the AC-130A had upgraded avionics including “night observation devices, FLIR, SLAR, beacon tracking radar, and a fire control computer system.” With a combat speed of 145 kts, the AC-130A flew at 5000 ft during armed reconnaissance and intercept missions, between 6500 and 8000 ft in areas with high anti-aircraft weapons, and at a lower limit altitude of 3500 ft during CAS missions. The AC-130A had an endurance limit of 6 hours with 30 minute reserve. Like the AC-47 attack profile, the AC-130A banked 30° left, allowing the miniguns depressed by 20° to fire on its target. The 20 mm M61A1 cannon was primarily used and sufficient for a single targets. The use of all armaments was only seen when targeting anti-aircraft weapons [40].

An initial batch of eight JC-130s were to be converted into the AC-130A configuration used in testing; this configuration came to be known as Plain Jane [41]. Prior to the start of modifications on the last airframe, the Aeronautical Systems Division successfully proposed to use it as a test bed for new equipment and armaments; this proposal was unofficially nicknamed the “Surprise Package.” The Surprise Package removed the 7.62 mm miniguns and replaced them with two 40 mm Bofors Cannons, a WWII era anti-aircraft weapon used by the US Navy. The Bofors cannon increases the maximum combat altitude to 10,500 ft and boosts the efficiency of destroying light armored vehicles (LAV). The Pave Aegis program aimed to add a large caliber weapon to the airframe. With the 105 mm M102 Howitzer ultimately selected, the aft 40 mm Bofors cannon and beacon tracker radar were replaced by a 72

and 24 round ammunition rack for the M102. A three foot blast deflector was placed atop the gun barrel to shield the wing from blast damages. The cannon had a swivel range of 20° aft and 40° down from horizontal. The introduction of the AC-130H added an in-flight refueling system. Modified from the AC-130H variant, the AC-130U replaced both 20 mm cannons for a 25 mm Gatling gun [42-45]

The AC-130W Stinger II, deployed late 2010, features improved navigation, threat detection, countermeasure, and communication systems. Designed for CAS and air interdiction, the airframes are equipped with a Precision Strike Package that includes precision guided munitions and a tracer-less 30 mm GAU-23 Gatling gun [46]. Set to enter service in 2017, the C-130J Ghostrider will feature two fully integrated digital avionics suites, Universal Air Refueling Receptacle Slipway, and the Precision Strike Package. The C-130J arsenal includes a 30 mm cannon, 105 mm cannon, GBU-39 Small diameter bombs, and AGM-176 missiles [47].



Figure 2.7: Lockheed AC-130J Ghostrider [39]

The table below lists salient weight, performance, and geometric characteristics of aircraft in roles comparable to the design intent. Both jet and prop driven aircraft are presented as well as military and civilian. Aircraft of note are the Antonov AN-72 and Boeing YC-14 due to their use of USB which will be central to the design of the Overseer.

Table 2.1: Important Weights, Performance & Geometric Characteristics of Related Aircraft

	W_E/W_{TO}	W_{TO} (lb _p)	W_E (lb _p)	Payload (lb _p)	Range (nmi)	Cruise Speed (kts)	Thrust (lb _p)	Ceiling (ft)	S (ft ²)	b (ft)
An-72/72	0.55	76,000	42,000	-	2,350	325	28,660	33,000	1,062	107.6
YC-14	0.47	251,000	117,500	69,000	-	390	102,000	45,000	1,762	129
YC-15	0.47	216,680	105,000	69,000	-	470	64,000	30,000	1,740	110.3
C-17	0.48	585,000	282,500	171,000	2,420	450	161,760	45,000	3,800	169.08
AC-47	0.55	33,000	18,080	-	1,890	150	16,000	24,500	987	95
AC-119G	0.65	62,000	38,300	-	1,680	130	38,300	23,300	1,400	109.3
AC-130J	0.46	164,000	75,800	-	-	360	56,500	28,000	-	132.5
AC-130U	0.49	155,000	75,800	-	-	360	55,000	28,000	-	132.5
AC-130W	0.49	155,000	75,800	-	-	360	51,500	28,000	-	132.5
AC-27J	0.56	67,200	37,500	67,200	950	315	43,500	30,000	880	94.1
A-10	0.57	51,000	29,000	16,000	-	300	18,100	45,000	506	57.5

3. DESIGN VECTOR & WEIGHTS ESTABLISHMENT

Prior to performing Class I sizing calculations, target design vectors were established and weighted. For this competition, AIAA has provided an objective function defining the design vectors; however, a weighting factor that precedes each term is left up to the author. The objective function is presented below, Eq. 3.1.

$$OF = \frac{\text{Actual Range with 4 hrs AAO}^2}{500 \text{ nm}} + \frac{\text{Actual Dash Speed}^2}{300 \text{ KTAS}} + \frac{\text{Actual Cruise Speed}^2}{200 \text{ KTAS}} + \frac{\$40M}{\text{Actual Flyaway Cost}} + \frac{\$3000/\text{Hr}}{\text{Actual Direct Operating Cost}} + \frac{6,000 \text{ ft}}{\text{Fully Loaded Minimum Runway Length}} + \frac{\text{Max Positive Load Factor with 50\% Internal Fuel, Gun, and Gun Ammo}^2}{8} + \text{Observable} \quad \text{Eq. 3.1}$$

Several military personnel were consulted in weighing each design vector. The individuals are as follows:

- Col. Roger Disrud (Ret.) Former A-10 Pilot & 1992 Gunsmoke Winner.
- Lt. Col. John Marks A-10 Pilot with ~6200 flight hours.
- Dr. Adrian Lewis (Ret.) KU History Professor & Ret. Army Ranger



Figure 3.1: Col. Roger Disrud [48]

Col. Disrud, and Dr. Lewis provided quantitative analysis; Lt. Col. Marks provided a qualitative assessment. Table 3.1 shows the quantitative weighing results. Interviews with both A-10 pilots displayed concern with loiter time and mission radius. Col. Disrud noted, “Why [do] you want four hours? You’re not going to have enough ordnance.” Similar sentiments are felt by Lt. Col. Marks, “Four hours is very optimistic for loiter time with all the other requirements, especially at 500 nm – I don’t know how you would



Figure 3.2: Lt. Col. John Marks [49]

do that, which would essentially be a 5 to 6-fold increase or so over the A-10.” Furthermore, both pilots agreed that an increase in caliber size is not a necessity. Lt. Col. Marks remarked,

“I’m not sure why they would want an increase to 35 mm, but I think a 25-30 mm gun with 750-1000 round would be a good starting point ... I don’t think the gun needs to be able to kill all armored vehicles – I would specify ‘SSVs’ or soft-skinned vehicles, possibly APCs. There are numerous other weapons that could be used to take out main battle tanks more efficiently than when the A-10 was designed.”



Figure 3.3: Maj. Adrian Lewis [50]

Table 3.1: Weights for Design Vector Variable as per Col. Disrud and Prof. Lewis [51, 52]

Design Variable	Col. Disrud	Prof. Lewis	Average
Actual Range with 4 hours AAO	0.10	0.10	0.10
Actual Dash Speed	0.20	0.10	0.15
Actual Cruise Speed	0.20	0.10	0.15
\$40 M Fly-Away Cost	0.05	0.10	0.075
\$3000/hour Actual Direct Operating Cost	0.05	0.10	0.075
6,000 Ft. Runway	0.20	0.20	0.20
8g Load Factor	0.20	0.10	0.15
Observables	0.00	0.20	0.10

4. WEIGHT SIZING

The purpose of this chapter is to present a preliminary weight sizing of the aircraft.

4.1. EMPTY-TO-TAKEOFF WEIGHT RATIO DETERMINATION

A group of historical and contemporary aircraft in a similar role and/or configuration were selected for STAMPED analysis (Further information on STAMPED analysis is found in Reference 14. Figure 4.1 shows empty-to-takeoff weight ratios and takeoff weights for each aircraft. Given the relative variety of aircraft types listed in Figure 4.1 – prototypes, gunships, passenger transport, and military transport, as well as prop and jet driven aircraft – a traditional STAMPED analysis was not ideal. Rather than making a market predictive plot, each aircraft’s empty-to-takeoff weight was given an equal market share and analyzed on their age, mission, and configuration. The primary aircraft used as starting references are located below the red line. The aircraft above the red line were placed for reference as historical aircraft in a similar role powered by turboprops.

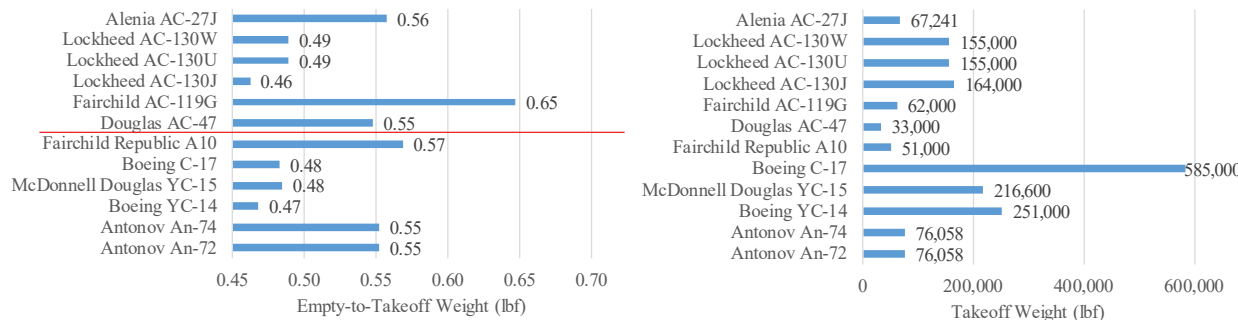


Figure 4.1: Empty-to-Takeoff Weight Ratio (Left) and Takeoff Weights (Right) used in STAMPED Analysis
 The aircraft above the red line in the figure demarcate historical aircraft used as reference.

4.2. DETERMINATION OF PRELIMINARY DESIGN WEIGHTS

Determination of preliminary design weights followed the guidelines shown in Chapter 1 of Roskam’s *Airplane Design: Part I* [3]. Calculation of fuel weight was done by using the fuel fraction method. The Breguet range and endurance equations are used to calculate cruise and loiter fuel fractions. Estimate for other profile segments are taken from Table 2.1 of *Airplane Design: Part I* [3]. Figure 1.1 shows the complete mission profile the aircraft was sized to. Through the advice of Dr. Ron Barrett, optimistic lift-to-drag ratios and thrust specific fuel consumption (TSFC) were used in the fuel fractions method; a lift-to-drag ratio of 20, and TSFC of $0.4 \text{ lb}_m / \text{hr} \cdot \text{lb}_f$ [53]. These values were chosen given the time since an aircraft of this configuration has been introduced and the technological advances in turbofan engines. The final preliminary design weights are as follows:

$$\begin{aligned}
 W_{TO} &: && 58,000 \text{ lb}_f \\
 W_{TE} &: && 29,000 \text{ lb}_f \\
 W_f &: && 12,500 \text{ lb}_f \\
 W_E/W_{TO} &: && 0.50
 \end{aligned}$$

5. WING AND POWERPLANT SIZING

The purpose of this chapter is to size the aircraft to the design requirement using methods from *Airplane Design: Part I* [3].

5.1. DISCUSSION OF PERFORMANCE CONSTRAINTS

Design specifications are plotted on the Sizing Chart in Figure 5.2 on page 12. Performance constraints used in the sizing chart are as follows:

- Take-off field length of 6,000 ft (ISA Hot Day at 5,000 ft altitude);
- Ceiling of 45,000 ft;
- Maneuver load of 8g, sustained;
- Maximum speed 400 KTAS
- Cruise speed of 350 KTAS

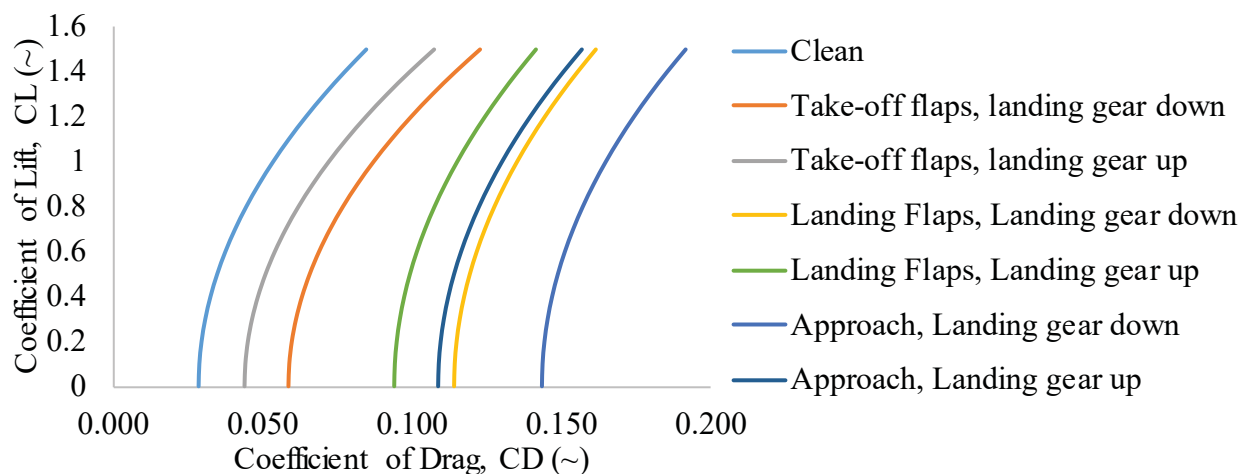


Figure 5.1: Preliminary Sizing Drag Polar Estimation

Drag polars for drag coefficients are presented in Figure 5.1. Calculation of wetted area, S_w , and parasite area, f , were performed following *Airplane Design: Part I* [3]. A value of 0.0040 was selected for equivalent skin friction coefficient, c_f ; due to the nature of the Overseer’s combat operations (This will be further discussed in Chapter 6) the aircraft was designed with maximizing lift and minimizing drag in mind including the use of low friction skin panels at the expense of increased production cost.

A skin friction coefficient, μ_G , of 0.1 was selected for simulating unimproved airstrips to be used by the Overseer. In addition to meeting design specifications, all military aircraft must adhere to military specifications. For climb requirements, FAR 25 certification was used instead. FAR 25 requirements are shown in Section 3.4.6 of *Airplane Design: Part I* [3]. The following six climb gradients requirements (CGR) must be met for one engine inoperative (OEI) or all engines inoperative (AEI):

FAR 25.111 Initial Climb	(OEI)	< 0.012
FAR 25.121 Transition Segment	(OEI)	< 0
FAR 25.121 Second Climb	(OEI)	< 0.024
FAR 25.121 En-Route Climb	(OEI)	< 0.012
FAR 25.119 Landing Climb	(AEI)	< 0.032
FAR 25.121 Balked Landing	(OEI)	< 0.021

Per the insight of Col. Disrud and Lt. Col. John Marks, maneuverability calculations are performed for an instantaneous 8g load factor. Wing and powerplant sizing calculations are provided in the accompanying website, <https://toledoph.wixsite.com/ae522/preliminary-wing-and-powerplant-siz>.

5.2. SIZING CHART ANALYSIS

Figure 6.1 shows the Sizing Chart with each constraint line. Examination of Figure 5 shows a standard deviation box of the aircraft used in STAMPED analysis. As discussed in Section 4.1, due to the variety of aircraft used the STAMPED data provides a rough design point location. Higher emphasis was placed on individual aircraft location in the Sizing Chart. The selected design point lead to the following design characteristics:

Table 5.1: Design Point

Parameter	Value
W/S	120 lb _f /ft ²
T/W	0.30
S	500 ft ²
T _{TO}	17,400 lb _f
AR	15
Wb	84.4 ft
C _{L,MAX CLEAN}	1.8
C _{L,MAX LANDING}	3.0
C _{L,MAX TO}	4.0

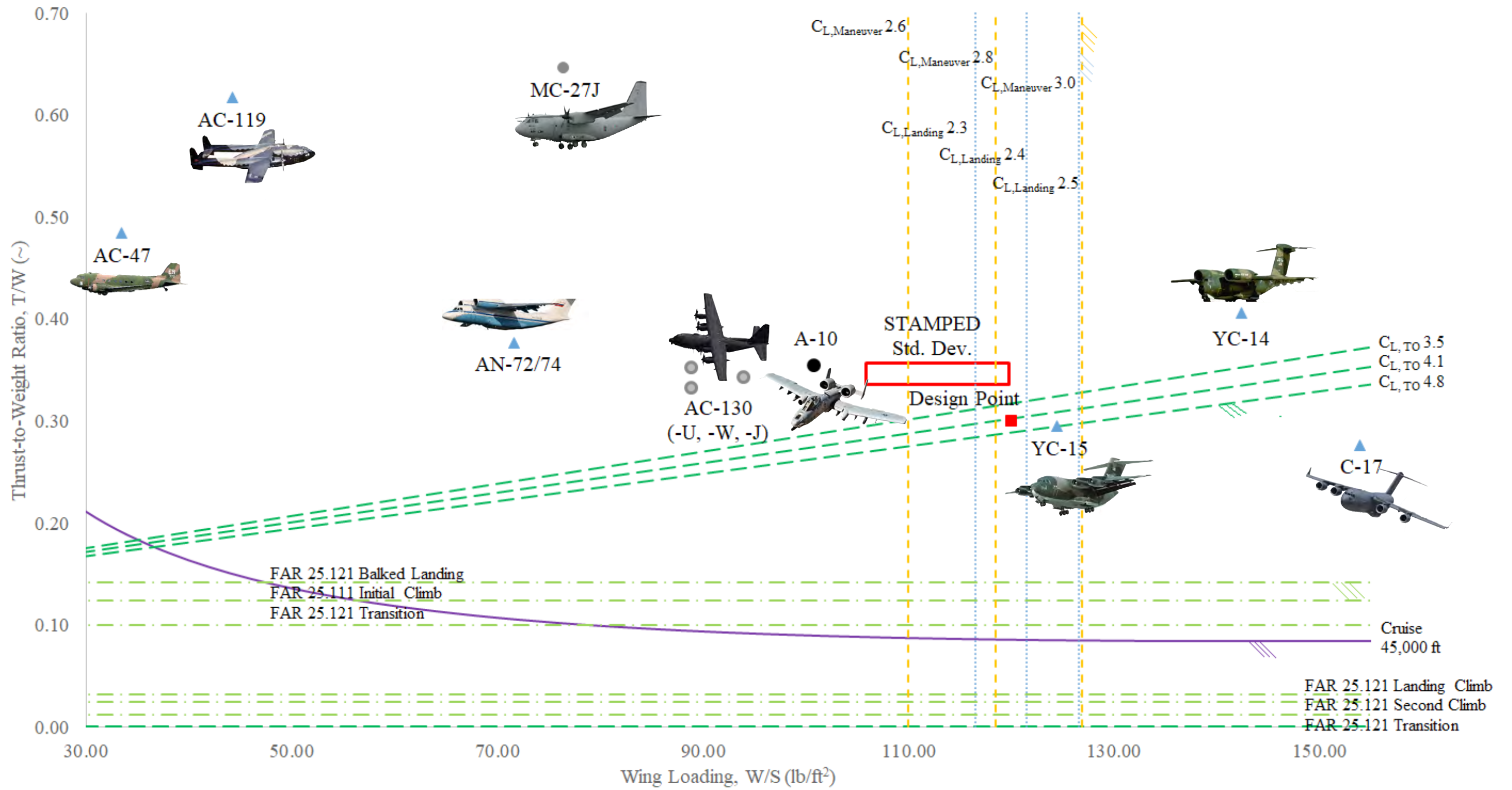


Figure 5.2: Sizing Chart With Performance Constraints

6. CLASS I CONFIGURATION DOWN SELECTION

The first step in the design of the Overseer was the determination of a configuration viable for Class I Design. A sweep of configurations were modeled and rated based on perceived characteristics. A variety of conventional and radical configurations were considered as shown below. Each design attempts to maximize a specific flight function.

6.1. CONFIGURATION MATRIX AND OPTIMIZATION FUNCTION



Figure 6.1: Configuration Sweep

Each preliminary configuration was rated through a pros and cons list. The characteristics of each design analyzed were based on the state of the configuration as shown in Figure 6.1. Solutions or alterations to any potential configurations problems were not taken into account at this stage.

Configuration 1 – Low Wing Upper Surface Blowing

- | | |
|---|-------------------------|
| + High Aspect Ratio (Low Induced Drag / High L/D) | - Gun Gas Ingestion |
| + Coandă Effect | - Wing Fuel Volume |
| + Empennage Out of Jet Wash | - Wing Weight |
| + Low Landing Gear Weight | - Foreign Object Debris |
| | - Nacelle Weight |
| | - Stores Accessibility |



Figure 6.2: Configuration 1

Configuration 2 – High Wing, Conventional

- | | |
|------------------------|----------------------------|
| + High Aspect Ratio | - Landing Gear Integration |
| + Engine Accessibility | - Wing Weight |
| + Stores Accessibility | - Tip Stall |
| | - Exposed Engines |

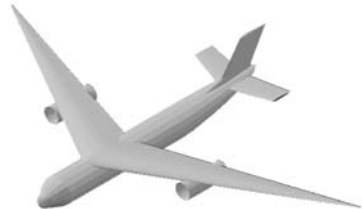


Figure 6.3: Configuration 2

Configuration 3 – Swept Upper Surface Blowing

- | | |
|---------------------------|-------------------------|
| + Coandă Effect | - Gun Gas Ingestion |
| + End Plating Effect | - Wing Fuel Volume |
| + Low Landing Gear Weight | - Foreign Object Debris |
| | - Potential Deep Stall |

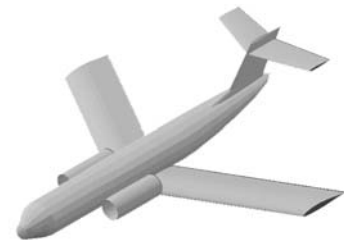


Figure 6.4: Configuration 3

Configuration 4 – Forward Swept Upper Surface Blowing

- | | |
|----------------------------------|------------------------|
| + Coandă Effect | - Gun Gas Ingestion |
| + Low Compressibility Drag | - Wing Fuel Volume |
| + Superior Stall Characteristics | - High Wing Weight |
| + Low Landing Gear Weight | - Empennage Jet Wash |
| | - Stores Accessibility |



Figure 6.5: Configuration 4

Configuration 5 – Conventional Straight Wing

- | | |
|-------------------------|------------------------------|
| + Conventional Design | - Low Maneuverability |
| + Low Wing Loading | - Low Attainable Load Factor |
| + Low Interference Drag | - Stores Accessibility |
| + Low Cost | - Inlet in Downwash Field |
| + Continuous Spar | |



Figure 6.6: Configuration 5

Configuration 6 – Low Delta, Inverted U-Tail

- | | |
|-------------------------|------------------------|
| + Delayed Stall | - Engine Accessibility |
| + Transonic Performance | - Empennage Jet Wash |
| + Redundant Tails | |
| + End Plating Effect | |

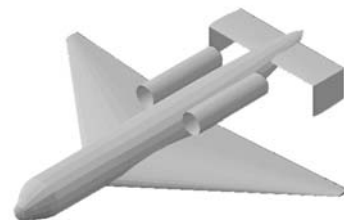


Figure 6.7: Configuration 6

Configuration 7 – High Delta, U-Tail

- | | |
|-------------------------|----------------------------|
| + Delayed Stall | – Gun Gas Ingestion |
| + Transonic Performance | – Landing Gear Integration |
| + Stores Accessibility | – Foreign Object Debris |
| + Engine Accessibility | – Exposed Engines |
| + Redundant Tail | |



Figure 6.8: Configuration 7

Configuration 8 – Dihedral Delta, V-tail

- | | |
|-------------------------|------------------------------|
| + Delayed Stall | – Landing Gear Integration |
| + Transonic Performance | – Inlet in Downwash Field |
| + Smaller Wetted Area | – Decreased Ground Clearance |

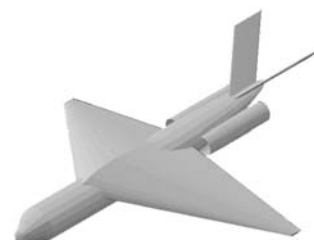


Figure 6.9: Configuration 8

Configuration 9 – Gun Ship

- | | |
|--------------------------|----------------------------|
| + High Aspect Ratio | – Wing Fuel Volume |
| + Coanda Effect | – Wing Weight |
| + Stores Accessibility | – Interference Drag |
| + End Plating Effect | – Nacelle Weight |
| + Multiple Gun Locations | – Landing Gear Integration |
| + Continuous Spar | |



Figure 6.10: Configuration 9

6.2. CONFIGURATION DOWNSELECTION

Of the nine configurations presented, several designs show inherent drawbacks to the RFP mission requirement. The single most important factor in the selection of a final configuration was simplicity and reparability of design. Given the mission specifications, the aircraft design must be able to endure less than ideal conditions and continuously perform at maximum capacity. To maintain mission ready status maintenance and repairs must be able to be performed at forward operating status in addition to major Air Force bases (AFB). Each of the presented designs are aerodynamically symmetrical about the butt line; this excludes any external stores or canon location. The use of a high wing potentially increases accessibility to store if externally mounted; however, potentially long, and heavy landing gears may be required. Placement of engines above or near the top of the fuselage decrease the risk of small arms ground fire.

Figures 6.11-6.13 display basic carpet plots for takeoff run, take off weight and minimum level flight velocity. As expected a higher thrust to weight ratio decreases takeoff run requirement; similarly, wing loading shows a small increase with increasing values. The selected design point falls within acceptable values without reaching extreme values of thrust to weight, or wing loading.

Configuration nine was selected to proceed to Class I design. A variety of characteristics make this configuration fundamentally superior. The high wing placement allows for placement of the canon on the belly of the aircraft, as

6.4. CARPET PLOTS

Three carpet plots are presented below displaying trade studies performed for design optimization.

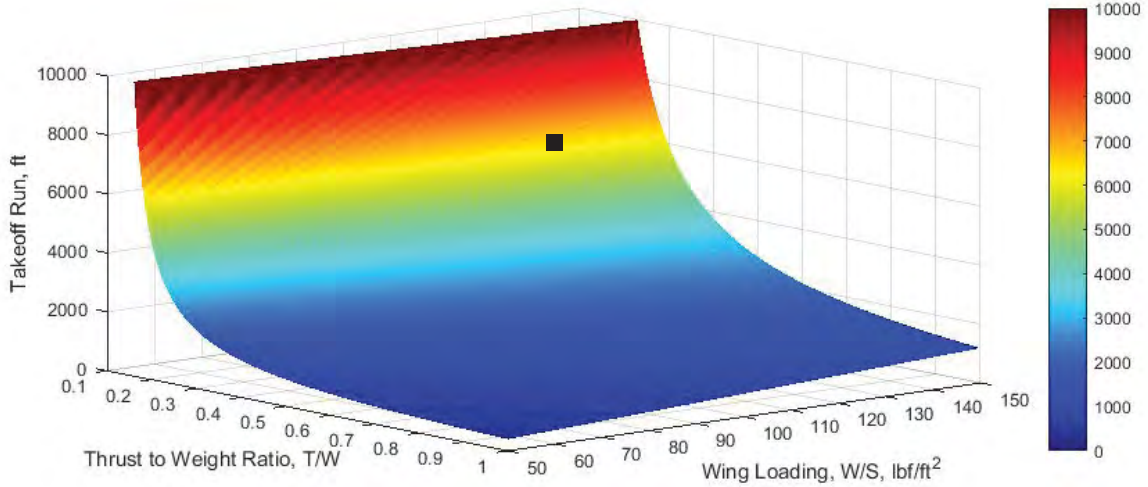


Figure 6.11: Effect of Thrust to Weight Ratio and Wing Loading, lb/ft², on Takeoff Run, ft.

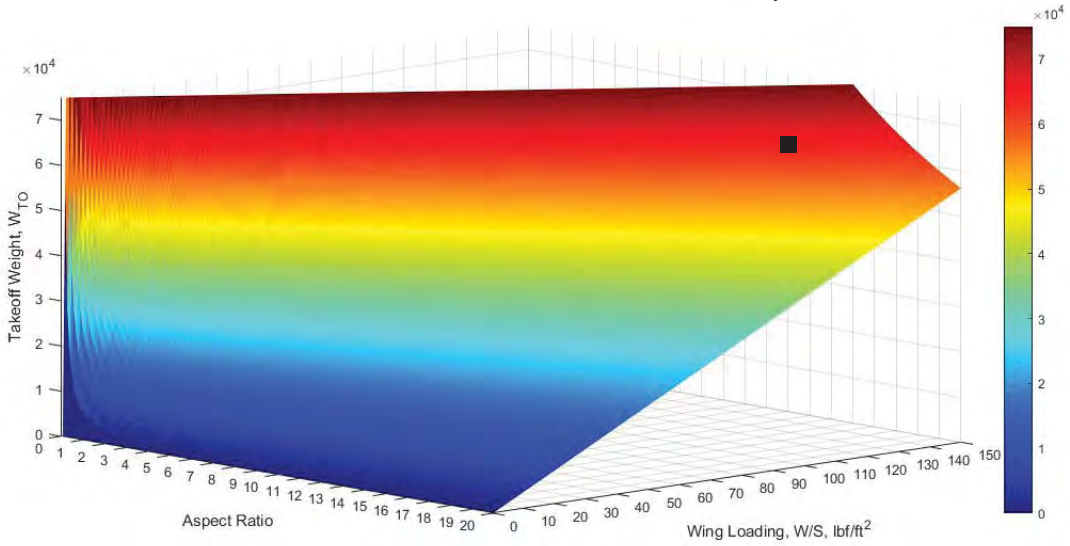


Figure 6.12: Effect of Aspect Ratio and Wing Loading, lb/ft², on Takeoff Weight, lbf.

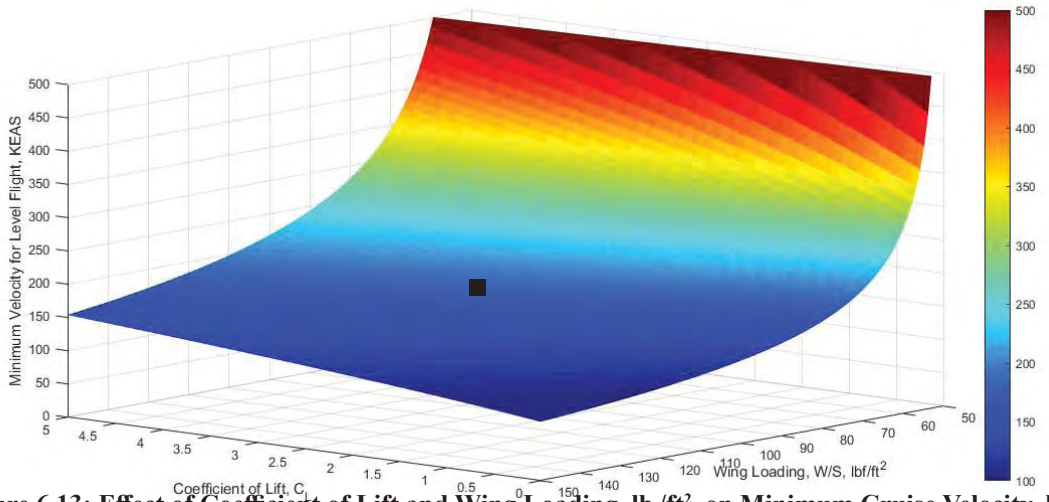


Figure 6.13: Effect of Coefficient of Lift and Wing Loading, lb/ft², on Minimum Cruise Velocity, kt.

well as the side. Engine placement on the leading edge takes full advantage of the Coanda effect and places the inlet out of gun gas ingestion and foreign object debris range. Exhaust gases passing over the wing are also out of line of sight from ground based IR-locking anti-aircraft weaponry. Although a high wing placement generally means heavier main landing gear, the addition of an aerodynamic fairing attached to the bottom of the aircraft provides housing for the landing gear system. Discussion on the selection of wing characteristics are presented in the following section. The defining characteristics of this configuration is the ability to place the cannon on the side of the aircraft. This provides an ability to provide CAS through orbital maneuvers above the target in addition to conventional strafing runs as seen in the A-10. In contrast to strafing runs that require an aircraft to circle back to set up another strafe line thus disengaging from suppressive fire, pylon turns allows for sustained suppressive fire. Armaments are further discussed in Chapter 11.

6.3. SELECTION OF MAJOR WING CHARACTERISTICS

The selection of wing characteristics revolved around designing a wing for maximizing the objective function, Equation 3.1. A straight, unswept single panel wing was chosen due to favorable low to medium speed characteristics. The use of a delta wing is primarily seen in supersonic aircraft, as such, the enhanced supersonic characteristics provides no value for the proposed flight speeds. Similarly, flight benefits of swept wings were also determined to provide little benefit. With expected cruise conditions out of the transonic range, the favorable compressibility effects gained through wing sweep were deemed insufficient for the weight trade off. The lack of wing sweep maintains a high $C_{L\alpha}$ increasing load factor reaction to turbulence; however, this is counteracted by high wing loading. By keeping an unswept wing at initial configuration design allowed for future weight and balancing issues to be fixed through small wing sweep changes. An unswept wing concept also allows for a single, or both spars to be spar throughout the entire span. A small taper ratio was also prescribed to achieve a near ideal Oswald efficiency factor similar to an elliptical wing. A very high aspect ratio was selected for increased lift and low speed performance. Typical airport wing span constraints were not considered in the selection of aspect ratio and its effect of wing span.

The NASA/Langley Medium Speed 0317 airfoil was chosen for both the root and tip. A high thickness ratio was required to maximize wing fuel volume due to the high aspect ratio. A high inherent C_L was also necessary to achieve the required $C_{L,max}$ and L/D values at combat speeds and maximize STOL capabilities.

Table 6.1: Wing Characteristics

Wing Area	S	500 ft ²
Aspect Ratio	AR	15
Span	b	86.6 ft
Sweep Angle	$\Lambda_{c/4}$	0°
Root Thickness Ratio	$(t/c)_r$	17%
Tip Thickness Ratio	$(t/c)_t$	17%
Taper Ratio	λ	0.4
Dihedral Angle	Γ_w	0°
Airfoil		MS-0317

7. CLASS I DESIGN

The purpose of this chapter is to present overall Class I Design of the Overseer. Class I Design establishes preliminary geometric characteristics, initial order of magnitude weight and balance analysis, and empennage sizing using stability and control derivatives. Methods used are found in *Airplane Design: Part I* [3], *Airplane Design: Part II* [4], and *Airplane Design: Part III* [5].

7.1. LAYOUT OF THE COCKPIT AND FUSELAGE

This section presents the configuration and design of the cockpit and fuselage following the methods from *Airplane Design: Part 2* [4] and *Airplane Design: Part 3* [5]. The foremost concern of the cockpit lay was the selection of a tandem or side-by-side seating arrangement. The primary advantage of a side-by-side cockpit is the increased visibility for both pilot and WSO; this is clearly displayed in aircraft such as the OV-1 Mohawk. The drawback of side-by-side seating is an increase in fuselage width and, by extension, an increase in fuselage drag. Tandem aircraft produce the opposite aircraft. A tandem seating layout was chosen. This decision was driven by the high performance characteristic required for optimal flight determined in Chapter 4. The increased visibility for the WSO is determined to be an insufficient trade off; the primary mode of fire will be the side firing. Targeting by the WSO will be done using as series of instruments rather than direct line of sight. Firing and targeting systems will be further discussed in Chapter 11. The cockpit was designed around a 95th percentile male pilot with proper clearance for ejection seats. Pilot visibility is shown below in Figure 7.1.

The primary goal in the layout of the fuselage is to maximize utility of the available space to maintain a small aircraft size. The use of a tandem cockpit the space behind the aft seat allows for storage of the nose landing gear. Internal stores are used to allow for high lift-to-drag ratios as discussed in Chapter 4. Due to the high armament load

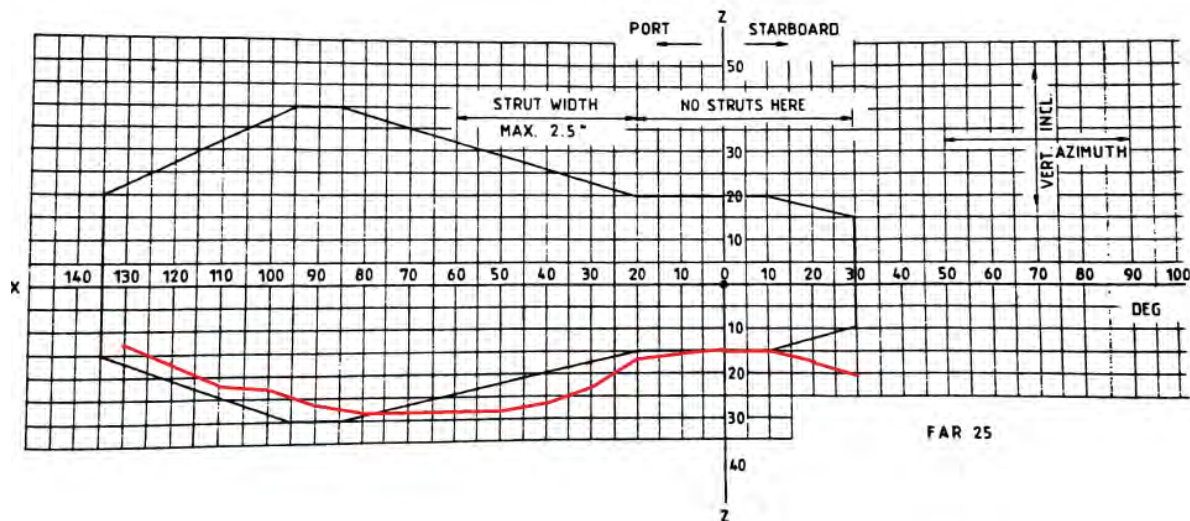


Figure 7.1: Forward Cockpit Visibility Diagram. Overseer Visibility Drawn in Red; Recommended Visibility in Black. Background Image from *Airplane Design: Part 3* [5].

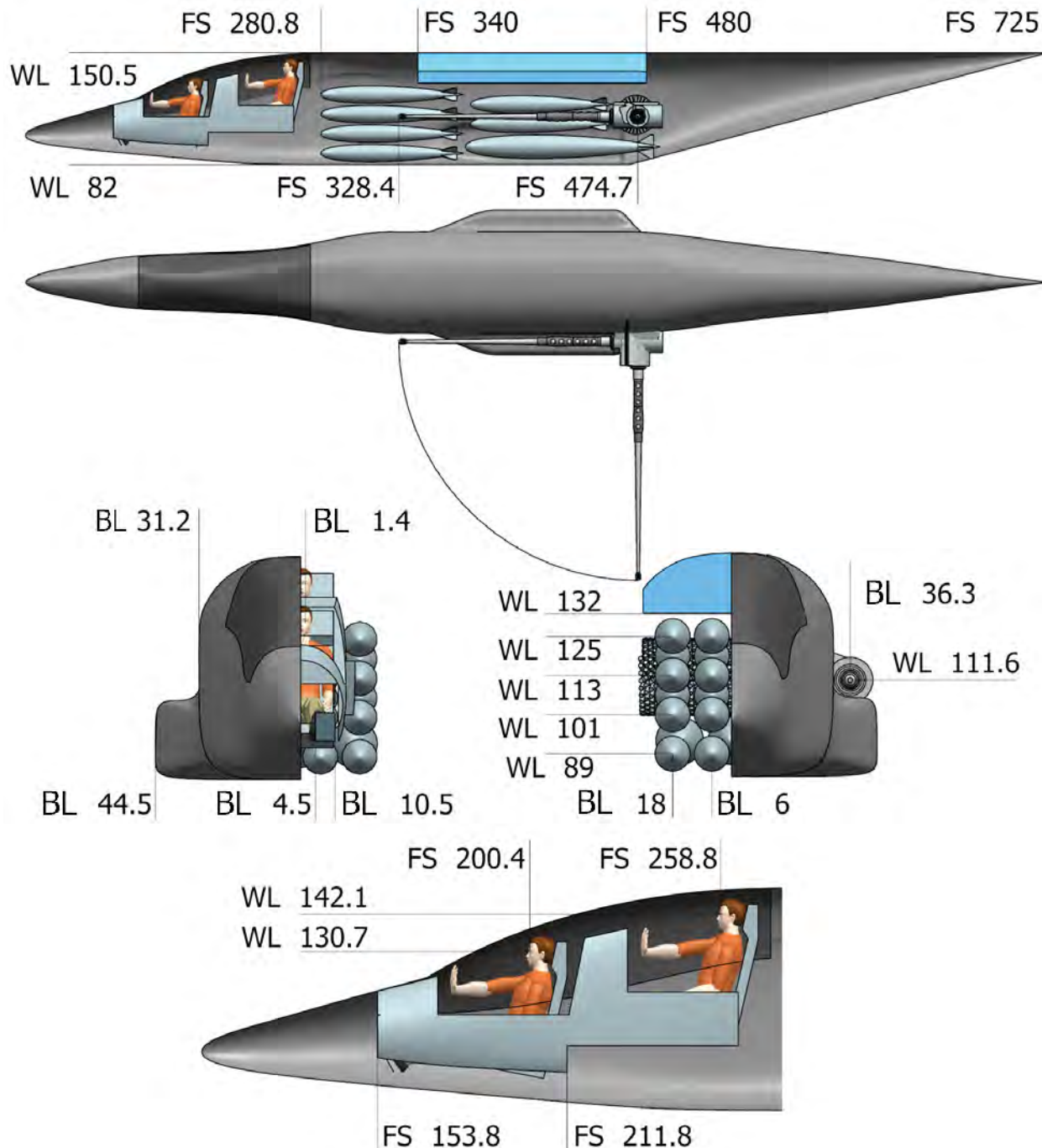


Figure 7.2: Front, Top, and Side View of Fuselage. Scale: Front: 1:100 in. Top/Side: 1:200 in.

requirement, two bomb bays were designed at the center of the fuselage. Spatial limitations allow for a total of 15,000 lb_f of ordnance; the configuration presented in this report specifies the placement of sixteen Mark 82 bombs in the forward bomb bay, and eight Mark 82 with three Mark 83 bombs in the aft bomb bay. The Bushmaster III cannon and its ammunition were placed toward

Table 7.1: Salient Fuselage Characteristics

Length	645 in
Height (Max Clearance)	76 in
Width (Max Clearance)	88.6 in

the aft of the aircraft for weight and balance purposes. Weight and balance will be further discussed in Section 7.7. The placement of the cannon was of major concern to reduce any aircraft dynamic effects such as yawing moment during flight. Weapon provisions and their effects will be further discussed in Chapter 11. A single fuselage fuel tank is placed at the top of the fuselage to minimize risk of ground fire. Fuel tank requirements and placement are further discussed in Section 7.3. Two spousons on either side of the fuselage were placed to house the main landing gear as well as subsystem components. Salient cockpit and fuselage characteristics are shown in Table 7.1. Cockpit and location of internal structures and stores are shown in Figures 7.2.

7.2. ENGINE INSTALLATION

This section presents configuration and installation of the powerplant following methods from *Airplane Design: Part II* [4] and *Airplane Design: Part III* [5]. The selection of a powerplant was determined in Chapter 4 during preliminary powerplant sizing; this sizing called for a minimum required total thrust of 17,400 lb_f. Similarly sized powerplants primarily fell into the business jet market. The selection of a turbofan over a turboprop or piston was based on the rising efficiency of turbofan engines. A selection of the General Electric CF34-3B1 was made due to its favorable TSFC, size, and weight. Table 7.2 presents salient powerplant characteristics.

Each engine is placed above the wing and cantilevered forward of the leading edge allowing for upper surface blowing. The primary purpose of this engine placement is to take advantage of the Coandă Effect as explained in Chapter 6. The exit nozzles were designed to with a half-elliptical exit area as seen on the YC-14, see Figures 6.14 and 6.15. A cross ducting system was designed to bleed air from the engine compressor to opposing wing tips. This is done to reduce yawing moment created in an one engine out situation. See Section 8.6 for further discussion. Powerplant installation on the wing is shown in Figure 7.4 .

7.3. WING LAYOUT DESIGN

This section presents the layout and design of the wing following methods from *Airplane Design: Part II* [4] and *Airplane Design: Part III* [5]. As discussed in Chapter 6, the Overseer was designed with a high wing in mind to prevent possible self-inflicted damage from side firing the Bushmaster III cannon. An airfoil with an inherent high-lift characteristics was chosen to achieve the high coefficient of lift prescribed; NASA/Langley Medium Speed MS-0317.

Table 7.2: Salient Engine Characteristics [63]

Engine	General Electric CF34-3B1
Takeoff Thrust	8,729 lb _f
Bypass Ratio	6.2:1
TSFC (37k/0.74 Mn)	0.69 lb _m / hr lb _f
Length	103 in
Fan Diameter	44 in
Diameter	49 in
Weight	1,670 lb _f

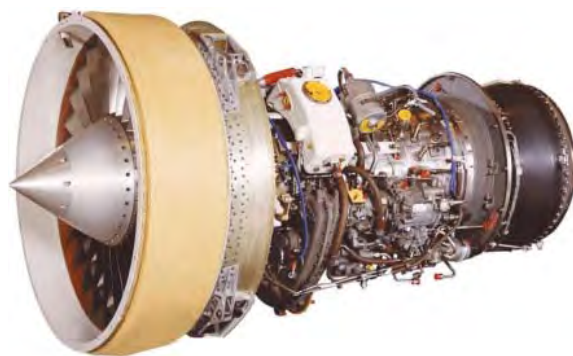


Figure 7.3: GE CF34-3B1 [63]

No wing sweep was prescribed due to the relatively low speeds of operation. A taper ratio of 0.4 was selected to lower wing weight; this choice was made at the cost of wing fuel capacity. No wing twist or dihedral was designed into the wing.

Due to the location of the engine at the root of the wing, a dry bay must be placed around the engine fuselage stations ultimately reducing fuel capacity in the wing. To offset the loss of usable space at the root, the 17% thickness NASA/Langley Medium Speed airfoil was also used at the tip. The wing fuel tanks holds up to 9,512 lb_m of Jet A Fuel. A single fuselage fuel tank was added to store the remaining fuel. To consolidate space, the fuel tank was built around aircraft wing structure using fuel bladders. Figure 7.2 and 7.3 displays fuselage stations, wing stations, and water lines for the wing and fuselage fuel tank, respectively.

Table 7.3: Wing Characteristics

Span	b	86.6 ft
Wing Area	S	500 ft ²
Aspect Ratio	AR	15
Sweep Angle	Λ	0°
Airfoil	Root/Tip	MS 0317
Taper Ratio	λ	0.4
Twist Angle	ϵ_t	0°
Dihedral Angle	Γ_w	0°
Root Chord	C_r	8.17 ft
Tip Chord	C_t	3.30 ft

7.4. HIGH LIFT DEVICE SIZING

This section presents the layout and design of high lift devices following methods from *Airplane Design: Part II* [4]. Flap sizing was performed for take-off condition which requires the highest maximum lift coefficient of 4.2. Plain flaps with upper

Table 7.4: Fuel Tank Characteristics

Required Fuel	12,500 lb _m (1,850 gal)
Wing Fuel Capacity	9,512 lb _m (1,411 gal)
Fuselage Fuel Capacity	2,988 lb _m (439 gal)

surface blowing provide sufficient lift coefficient increment to meet design $C_{L,max}$. Flap deflection angles, δ_f , are shown

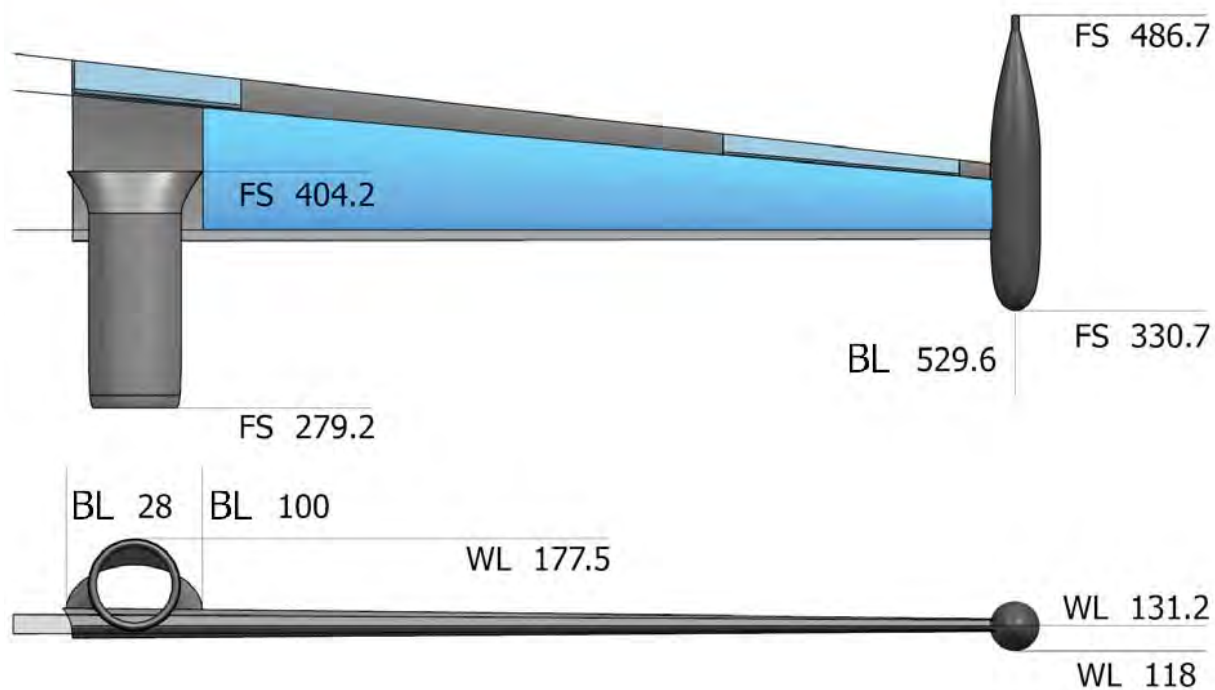


Figure 7.4: Wing Configuration Scale: 1:100 in.

in Table 7.6. Lift coefficient values greater than design values may be achieved at higher flap deflection angles; this author chose to limit flap to conservative angles to prevent premature separation of the Coandă Effect.

Table 7.5: Flap Characteristics

Flap Type	Plain
C_f/C	0.2
S_{wf}/S	0.18
η_i	0.06
η_o	0.2

Table 7.6: Flap Deflection

Flight Phase	δ_f
Takeoff	25°
Landing	15°
Maneuver	10°

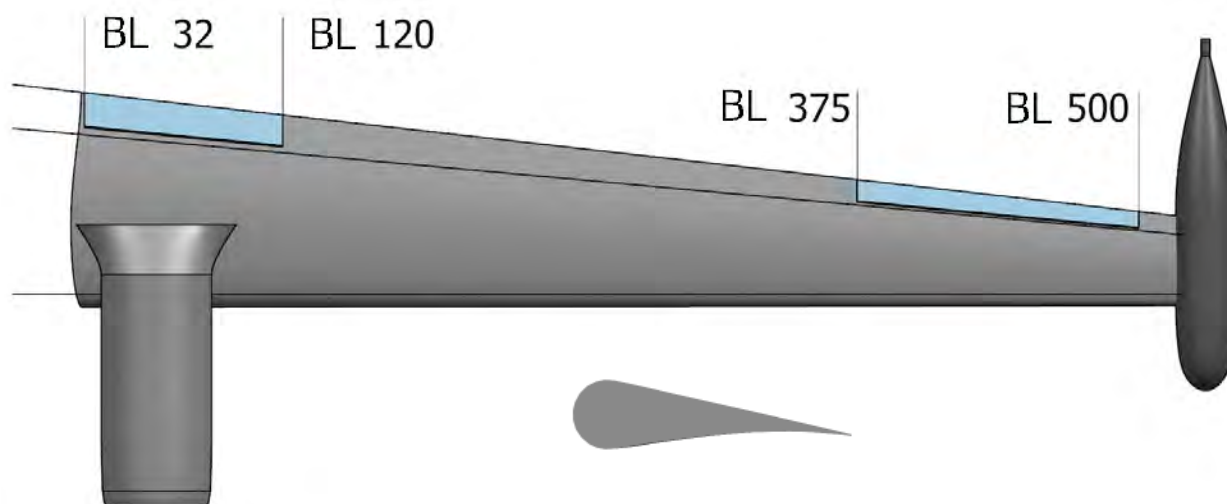


Figure 7.5: Top View of High Lift Devices on Wing and Side View of Flap. Scale: Top: 1:100 in. Side: NTS

7.5. EMPENNAGE DESIGN

This section presents the design of the empennage following methods from *Airplane Design: Part II* [4]. A T-tail configuration is used to minimize the effects of engine downwash over the horizontal stabilizer. The initial sizing was done using the Volume Coefficient Method using historical data in Tables 8.1-8.11 of *Airplane Design: Part II* [4]. Further sizing is done taking stability and control into account; this will be presented in Section 7.9.

Empennage characteristics were selected by reviewing data from comparable aircraft; primarily the C-130H and YC-14. As stated in *Airplane Design: Part III*, the addition of a small anhedral angle reduces horizontal stabilizer weight [5]. To counteract the reaction forces to side firing the Bushmaster III cannon, a double-hinged rudder was used. A correction factor was placed on the vertical stabilizer area to account for increased rudder performance. The purpose of the double-hinged rudder is to improve aircraft control in the event of one engine out at low speeds and decrease vertical stabilizer size.[53].

Table 7.7: Empennage Characteristics

		Horizontal Stabilizer	Vertical Stabilizer
Airfoil	Root/Tip	64A318	NACA 0012
Span	b	23 ft	8 ft
Volume Coefficient	V_v, V_h	1.000	0.065
Wing Area	S_h, S_v	ft ²	ft ²
Control Surface Area Ratio	S_c/S_h S_r/S_v	0.4	0.26
Chord, Root/Tip	C_e, C_r	0.4/0.4	0.38/0.38
Aspect Ratio	AR	4.3	1.1
Taper Ratio	λ	0.65	0.95
Root Chord	C_r	6 ft	7 ft
Tip Chord	C_t	3.9 ft	6.65 ft
Sweep Angle	Λ	25 °	5 °
Twist Angle	ϵ_t	0 °	0 °
Dihedral Angle	Γ_w	-3 °	0 °

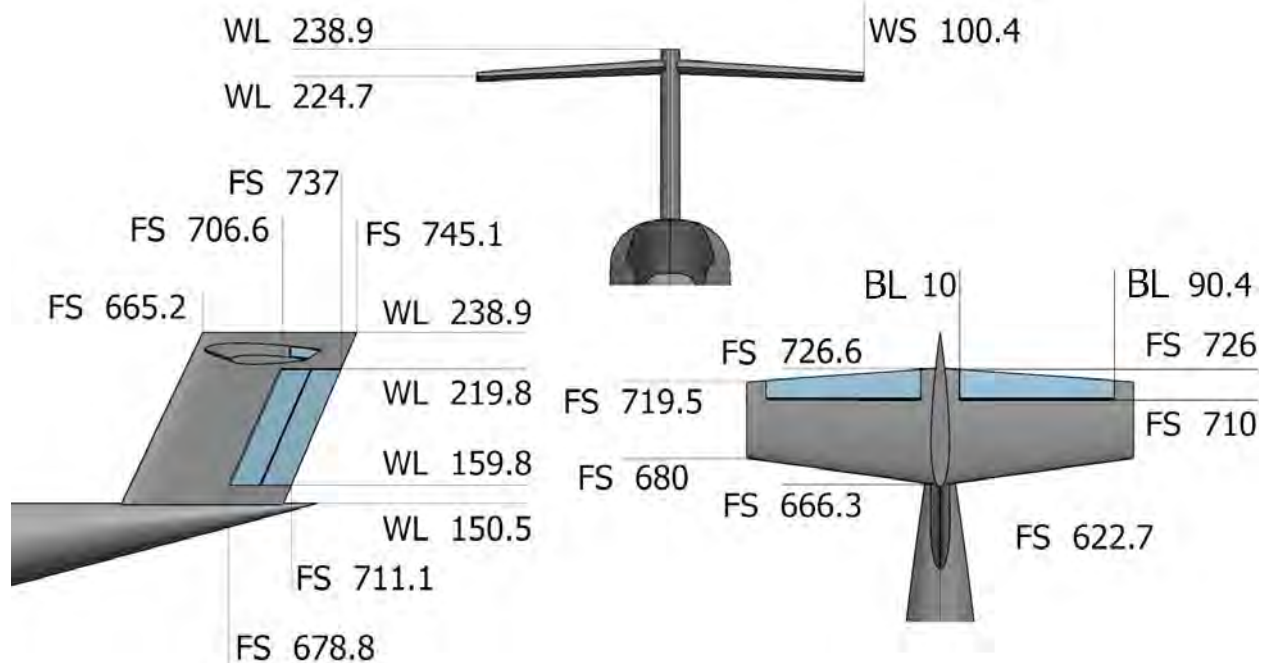


Figure 7.6: Three View of Empennage. Scale: 1:100 in.

7.6. LANDING GEAR DESIGN

This section presents the design of the landing gear and undercarriage following methods from *Airplane Design: Part II* [4] and *Airplane Design: Part IV* [6]. A tricycle configuration with forward retractable nose gear and partial main gear vertical retraction was selected. Hand calculation and AAA model screenshots are presented on the accompanying website, <https://toledoph.wixsite.com/ae522/class-ii-design>.

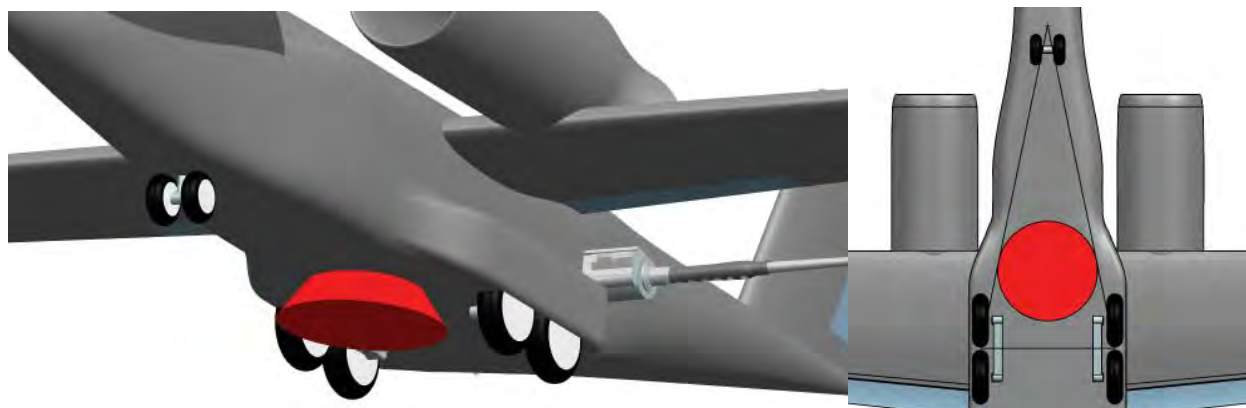


Figure 7.7: Lateral Tip-over Criterion. Scale: 1:100 in.

Of primary importance in landing gear configuration was compliance with longitudinal and lateral tip over criterion. Landing gear contact points were limited to allow for deployment of ordnance from the belly of the aircraft. Due to this requirement, spsonons are added for containment of the main landing gear with two tires placed in tandem .

The locations of the nose and main landing gears were placed to accommodate a 35° cone within a triangular section. This was done to ensure lateral tip-over criterion is met, Figure 7.7. The main landing gear was placed at a 15° angle aft of the aft most CG to prevent longitudinal tip-over, Figure 7.8 (Left). Ground clearance criterion was met by limiting the tail to ground angle to 15° and wingtip to ground angle to a minimum of 5°, Figure 7.8 (Right).



Figure 7.8: Front and Side View of Undercarriage. Scale: 1:200 in.

The static load per strut was calculated based on gear and CG location. As recommended in *Aircraft Design Part IV* [6], both the nose and main gear static loads are increased by a factor 1.25 to allow for growth in aircraft weight. Landing gear strut and tire load forces and ratios are shown in Table 7.8.

Table 7.8: Landing Gear Strut and Tire Load Force and Ratios

	Strut Load (lb _f)	Strut Load (1.25) (lb _f)	Load Ratio	Tire Load (lb _f)
Nose Gear	6,050	7,560	0.1	3,780
Main Gear	26,970	33,720	0.9	16,860

Tires were selected using the Goodyear Aviation Databook, References 64 and 65. Salient tire characteristics are shown in Table 7.9. Retraction mechanism for both nose and main gear are show in Figure 7.9. The nose gear fully retracts forward; this was done for gravity and freestream assisted extension in case of hydraulic malfunction. The main gear partially retracts vertically; this is done for aircraft protection in the event of a belly landing.

Table 7.9: Salient Tire Characteristics

Location	Goodyear Tire Model	Rated Inflation (psi)	Rated Load (in.)	D_t (in.)	b_t (in.)
Nose Gear	459M09B1	90	3822	18.11	7.72
Main Gear	313K02-1	155	17200	31	13

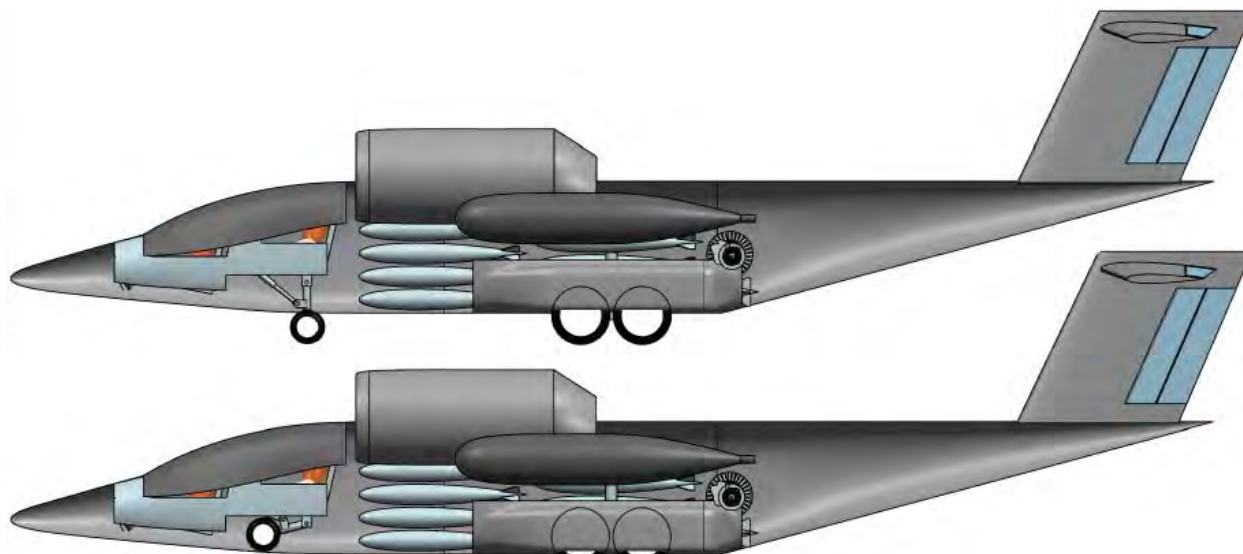


Figure 7.9: Landing Gear Retraction. Scale: 1:200 in.

7.7. WEIGHT AND BALANCE

This chapter presents Class I weight and balance analysis. Procedures follow methods from *Airplane Design: Part V* [7]. A preliminary three-view with CG locations is shown in Figure 7.16 on page 30. Calculation of component weights were done using historical data following the methods of *Airplane Design: Part V* [7]. The weight of similar aircraft are broken down into component weight fractions; component weight divided by gross weight. The weight fractions of historical aircraft are applied to the Overseer resulting in a preliminary weight statement. Weight adjustments are made by adding and removing weight to component groups based on the Overseer’s design compared to historical values.

The two aircraft chosen as baseline weight models are the Boeing YC-14 and the Lockheed Martin C-130H. Each of these aircraft posses features that are complimentary to the Overseer: the YC-14 was selected due to the use of USB and the C-130H was selected as it is the base model of the AC-130 variants - data for the AC-130 was not readily found, thus this author chose to use the C-130H as a comparable model. Substantial weight was added to the engine section due to the extra structure for cantilivering the engines.

Using a coordinate system origin at FS 0, WL 0, and WS 0, Table 7.10 shows weights and CG locations for different weight conditions; a loading condition with full payload is used in determining CG locations.

Table 7.10: Combined Component Weights

Condition	Weight (lb.)	X CG (in)	X CG (% MAC)	Y CG (in)	Z CG (in)
W_E	27,900	401	46.2%	0.6	139
W_{OE}	28,900	398	42.5%	0.6	139
$W_{OE+Fuel}$	41,100	399	42.3%	0.4	139
W_{TO}	61,100	396	39.1%	0.3	130
$W_{OE+Load}$	48,900	396	38.4%	0.4	127

A CG excursion diagram was created by plotting each CG at a given weight condition. The maximum ground CG excursion is 5.2 in. (7.7% MAC); the maximum flight CG excursion is 2.6 in (3.8% MAC). As shown in Figure 7.10, a forward CG excursion occurs from W_E to W_{OE} due to the weight of the pilots. The addition of max payload as well as max fuel shifts the CG forward. The weight of the fuel is less than the weight of the payload, thus the combined weight shifts the CG_{TO} closer to $W_{OE+Load}$ CG when both are loaded onto the aircraft. The main gear contact is shown to be well aft of ground CG excursions preventing tipover during ground loading. Both ground and flight CG lie aft of the wing quarter chord location.

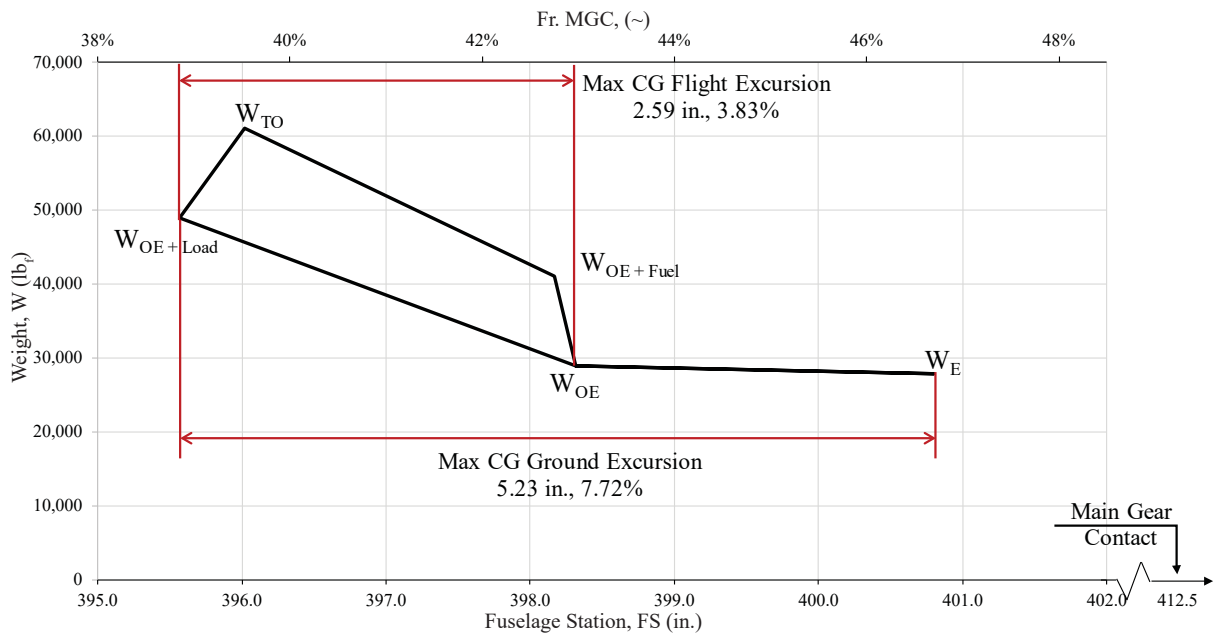


Figure 7.10: X CG Excursion Diagram

7.8. V-N DIAGRAM

This section presents the V-n diagram following the methods from *Airplane Design: Part VI* [8]. The V-n diagram for military type aircraft presents two vertical speed lines: V_H , maximum level speed; and V_L , maximum design speed. The positive load factor, $n_{lim\ pos}$, is prescribed by the RFP as $n_{lim\ pos} = 8.0$ [1]. A negative load factor, $n_{lim\ neg}$, of -3 is selected as directed by Table 4.1 from *Airplane Design: Part II* [4].

The V-n diagram shows that the maximum positive load factor was achievable at 170 KEAS; 130 KEAS below V_H . The maximum negative load factor is achievable at 148 KEAS, 152 KEAS below V_H . Maximum positive

and negative load factor may not be achieved during combat depending on the prescribed combat operational speed; however, the Overseer's CONOPS prevents the need for such maneuvers at low speeds.

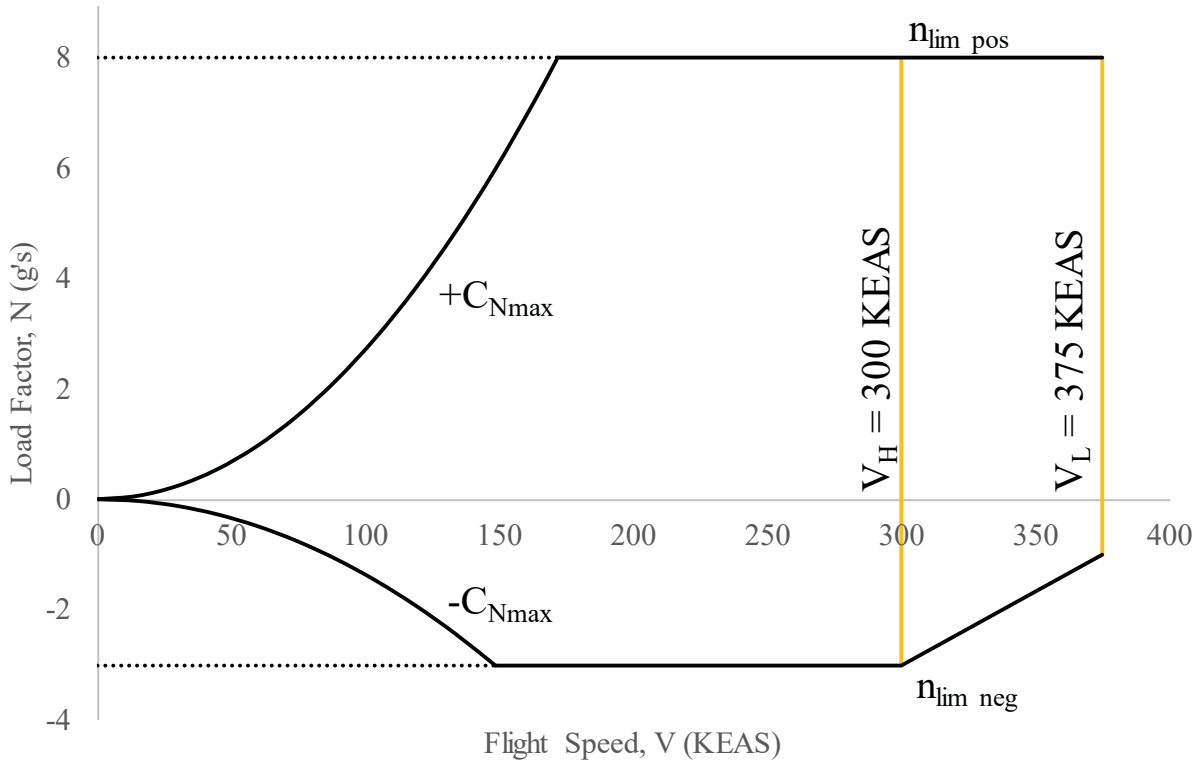


Figure 7.11: V-n Diagram

7.9. STABILITY AND CONTROL

This chapter presents Class I stability and control analysis following methods from *Airplane Design: Part II* [4], and *Airplane Design: Part VI* [8]. For the successful design of a CAS aircraft, a close balance between maneuverability and targeting acquisition must be met. Using values determined from AAA, a longitudinal x-plot was generated to determine horizontal stabilizer size for longitudinal stability; Figure 7.12.

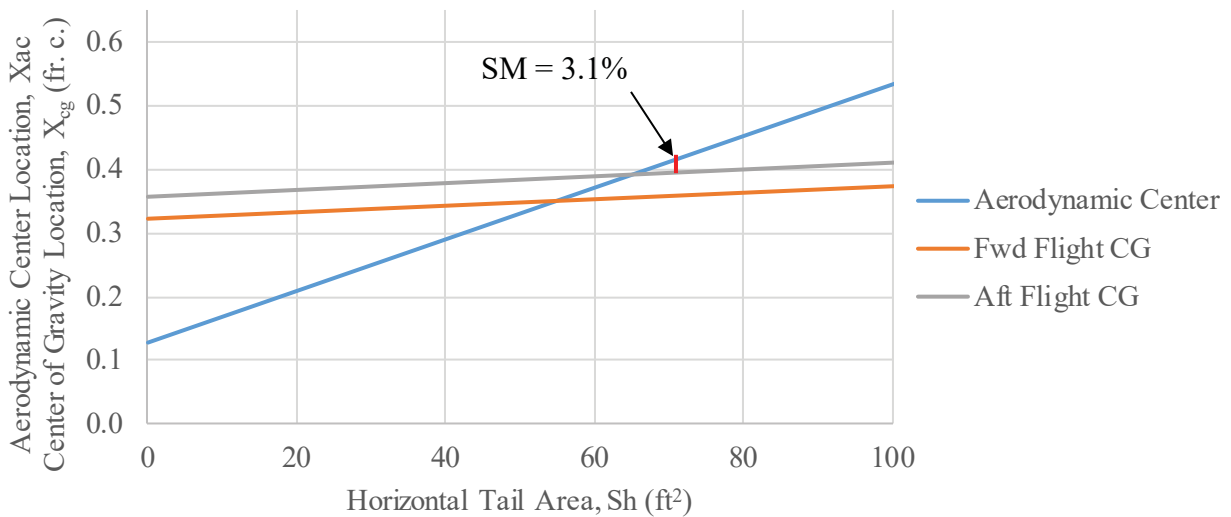


Figure 7.12: Longitudinal X-plot

With a horizontal stabilizer area of 70 ft², a static margin of 3.11% was achieved making the Overseer a stable aircraft. A control augmentation feedback loop, K_c , of -0.14 was determined for a de facto stability of 10%. Directional stability was determined by plotting a lateral x-plot, Figure 7.13. According to Roskam [4], a yawing moment coefficient due to sideslip, $C_{n\beta}$, of 0.001 deg⁻¹ is desirable for military aircraft. To achieve inherent stability a vertical stabilizer with an area of 75 ft² is required. Using AAA, a vertical stabilizer area of 51.35 ft² was determined to achieve a de facto stability with $C_{n\beta}$ equal to 0.00053 deg⁻¹ and a directional SAS feedback augmentation gain of -3.17.

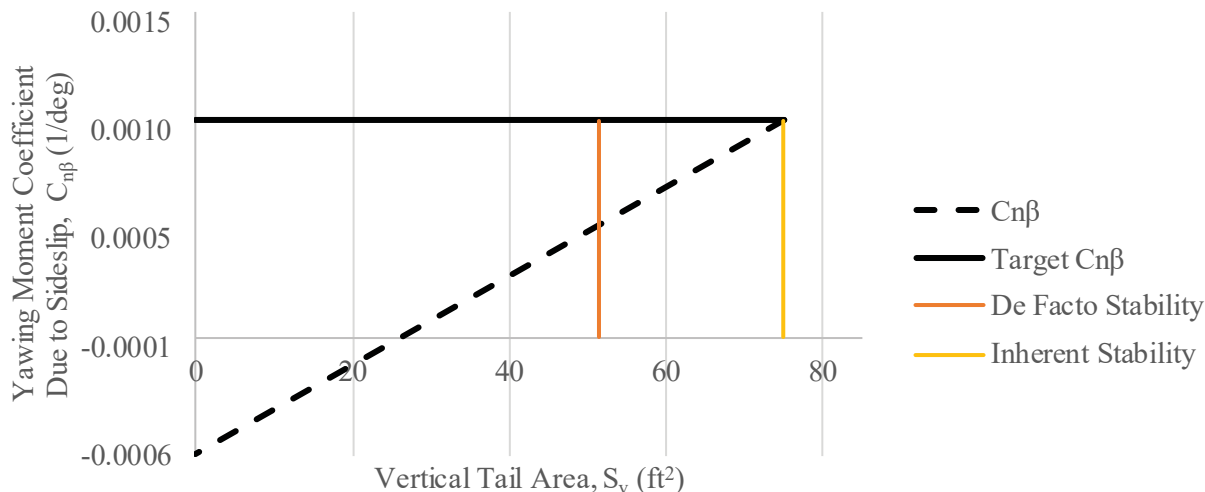


Figure 7.13: Directional X-plot

One engine-out rudder deflection was calculated at takeoff thrust at 5,000 ft and ISA +20°F. Due to the large takeoff thrust on each engine, 9,220 lb_f, an unrealistic rudder size and deflection was required to control the aircraft. A cross ducting system was implemented to significantly circumvent this problem. By bleeding off air at the engine’s compressor to the opposing wing’s tip, the large moment arm due to the wing’s span offsets the lost thrust. A moment balance calculation results in an equivalent takeoff thrust of 2,200 lb_f. Table 7.11 shows calculated values with cross ducted engines. Rudder deflection due to one engine inoperative condition was determined using AAA.

Table 7.11: Minimum Control Speed with One Engine Inoperative

Takeoff Thrust	T_{TO}	2,200 lb _f
Y Location of Inoperative Engine	Y_T	64 in.
Yawing Moment Factor	F_{OEI}	1.15
Critical Yawing Moment due to OEI	N_{TOEI}	5867 ft-lb
Induced Drag due to OEI	D_{OEI}	165 lb _f
Induced Yawing Moment due to OEI	N_{DOEI}	880 ft-lb
Stall Speed	V_S	118 kts
Minimum Control Speed	V_{mc}	141.6 kts
Rudder Deflection	δ_r	18.42°

7.10. DRAG POLAR & PERFORMANCE ANALYSIS

This chapter presents Class I drag polar and performance analysis performed following the methods from *Airplane Design: Part II* [4], and *Airplane Design: Part VI* [8]. Wetted area calculations were performed using AAA and doubled checked with CAD values. The reported wetted areas presented in Table 7.12 were determined using Siemens NX. Using the measured wetted area, the aircraft friction coefficient was accurately recalculated. A skin friction coefficient, C_f , of 0.004 was selected to achieve a high lift to drag ratio value. This value is assumed to be neither conservative nor extraneously liberal. The parasite area was calculated to be 9.5 ft² using Figure 3.21c Ref. 3. This results in a zero-lift drag coefficient, C_{D0} , of 0.019. The calculated drag polars are presented in Table 7.13 and Figure 7.14.

Table 7.12: Overseer Wetted Area

Component	Wetted Area (ft ²)
Fuselage	695
Wing	955
Horizontal Stabilizer	138
Vertical Stabilizer	107
Nacelles	225
Total	2121

Table 7.13: Drag Polar

Configuration	ΔC_{D0}	e	Drag Polar
Clean	0.000	0.85	$C_D = 0.0225 + 0.0248 C_L^2$
Take-off Flaps, Gear Down	0.02	0.80	$C_D = 0.0371 + 0.0263 C_L^2$
Take-off Flaps, Gear Up	0.01	0.80	$C_D = 0.0271 + 0.0263 C_L^2$
Landing Flaps, Gear Down	0.07	0.75	$C_D = 0.0871 + 0.0281 C_L^2$
Landing Flaps, Gear Up	0.06	0.75	$C_D = 0.0721 + 0.0281 C_L^2$

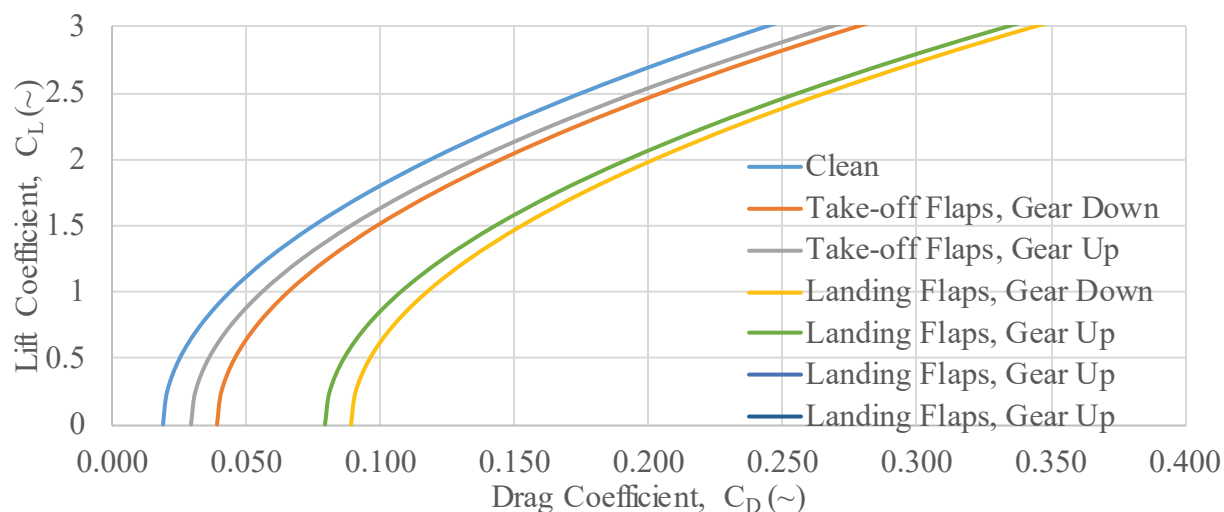


Figure 7.14: Drag Polar

Incremental zero-drag lift coefficient, ΔC_{D0} , values were determined using the assistance of Table 3.6 from *Airplane Design: Part I* [3]. Flap type, flap deflection angle, and landing gear deployment status were used to determine ΔC_{D0} and Oswald's efficient factor, e, at each configuration. More liberal values are used due the use of single flaps, small deflection angles, and small exposure of the main landing gear to the free stream.

7.11. ANALYSIS OF WEIGHT AND BALANCE AND STABILITY AND CONTROL

Weight and balance results presented in Section 7.7 are satisfactory for a military fighter aircraft. A CG excursion is present, however both ground and flight changes are limited to under 10%. The overall center of gravity excursion is consistent with longitudinal, and lateral tip over conditions. Although *Airplane Design* series allows a negative static margin for superior maneuverability in military aircraft, the nature of the Overseer’s mission poses a threat to enemy fire. A small positive static margin was selected with feedback augmentation system in the event of control surface damage.

7.12. LIFT-TO-DRAG ANALYSIS

Validation of lift to drag ratios was performed to confirm initial design selection presented in Chapter 5. The lift to drag ratios selected for the following flight conditions were: cruise, 20; loiter, 20; pylon turn, 18; and strafe, 16. Table 7.7 below show maximum lift to drag ratio for a given drag polar using Equation 18.1

Table 7.14: Lift to Drag Ratios for Flight Stages

Configuration	ΔC_{D0}	$1/\pi Ae$	e	L/D_{max}
Clean	0.00	0.0249	0.85	23.0
Take-off Flaps, Gear Down	0.02	0.0265	0.80	15.5
Take-off Flaps, Gear Up	0.01	0.0265	0.80	18.0
Landing Flaps, Gear Down	0.07	0.0283	0.75	10.0
Landing Flaps, Gear Up	0.06	0.0283	0.75	10.6

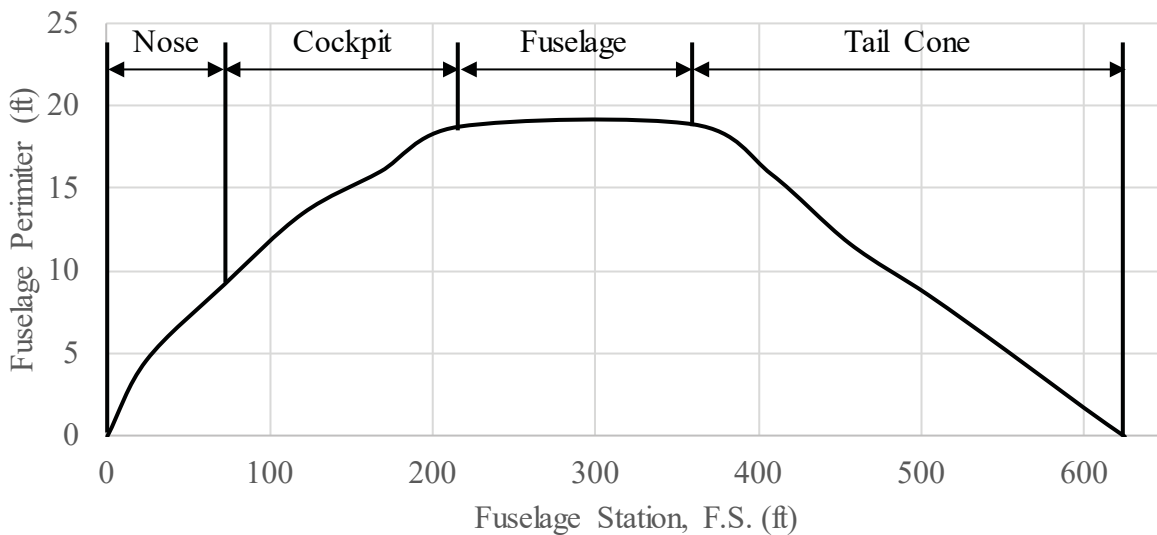


Figure 7.15: Fuselage Perimeter Plot

The calculated Overseer lift to drag ratio is greater than the initially prescribed value. Resizing of the aircraft based on this higher lift to drag ratio is possible, however the change in fuel consumption was deemed to be offset by engine specific fuel consumption at the different flight stages.

7.13. STRUCTURAL LAYOUT

The purpose of this section is to present preliminary structural layout of the Overseer. The methods used in this section follow guidelines presented in *Airplane Design: Part III* [5].

Table 7.15: Preliminary Structural Characteristics

Component	Structural Characteristic
Wing	Spar Location: 14% & 83% Rib Spacing: 21 in.
Horizontal Stabilizer	Spar Location: 20% & 68% Rib Spacing: 18 in.
Vertical Stabilizer	Spar Location: 18% & 66% Rib Spacing: 16.5 in.
Fuselage	Frame Depth: 2 in. Frame Spacing: 10.5 - 25 in.. Longeron Spacing: 10 - 15 in.

In addition to the preliminary structure show below in Figure 7.16 several armor plating component are placed throughout the aircraft. A titanium “bathtub” encompasses the outer perimeter of the cockpit providing protection from high caliber ground fire. Two armored tip pods provide protection for fuel tanks from perpendicular fire during pylon turns and tip lightning strikes.

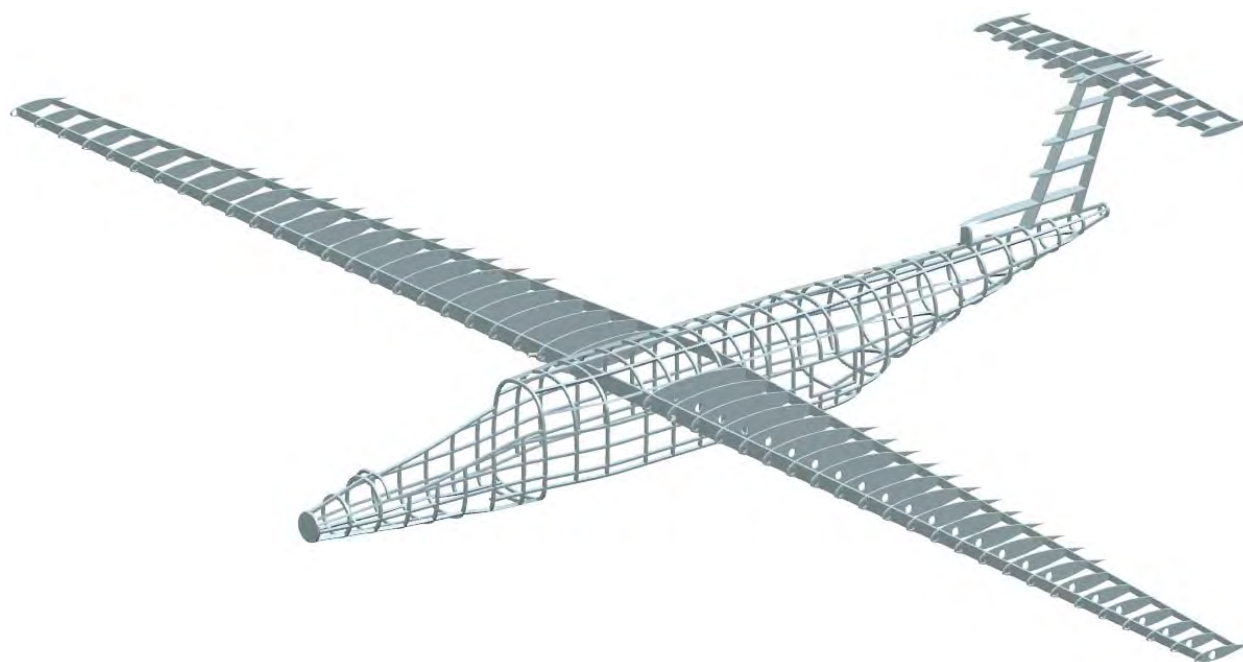


Figure 7.16: Structural Layout Overview: NTS.

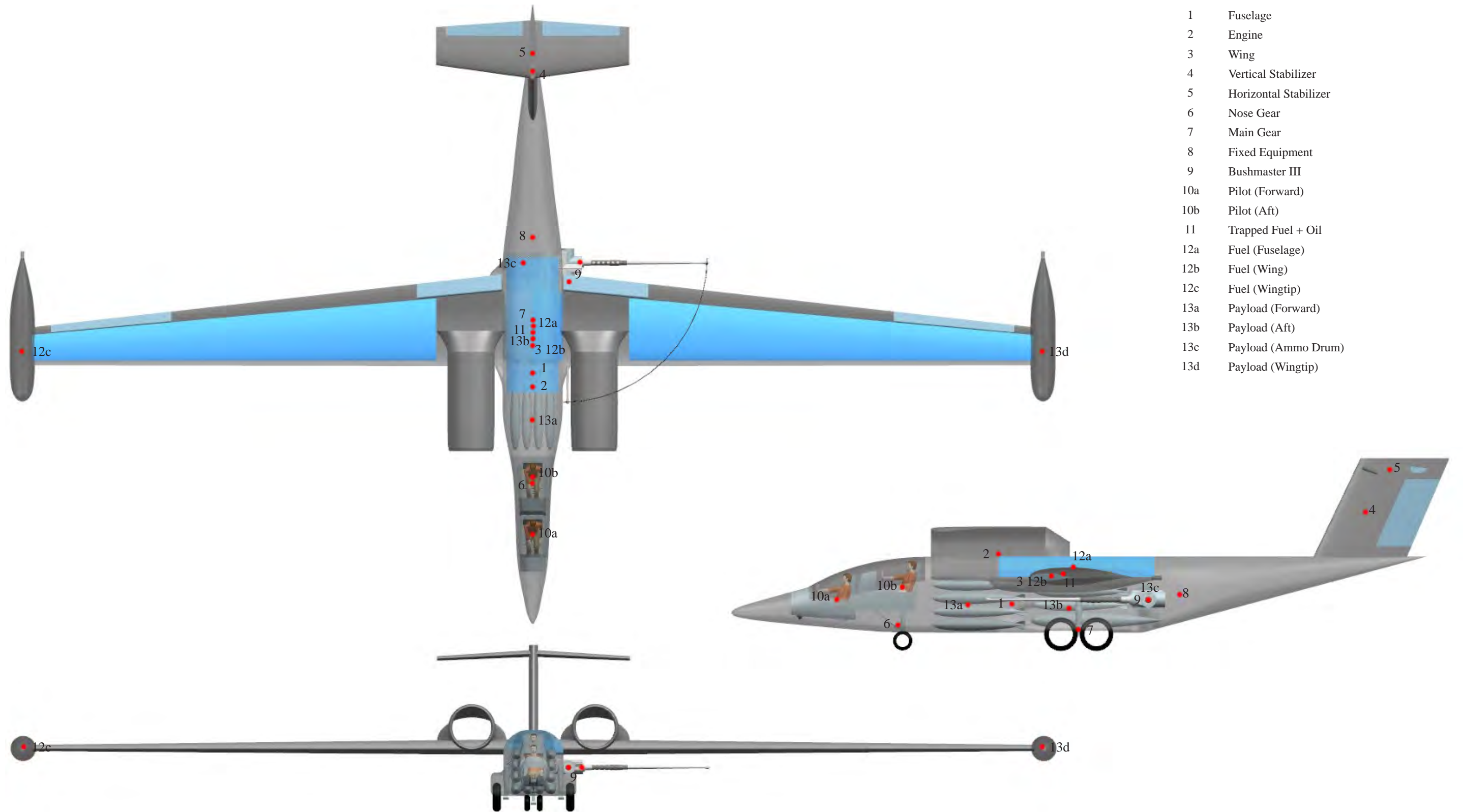


Figure 7.17: Center of Gravity Location of Selected Components. NTS.

8. SYSTEMS DESIGN

The purpose of this chapter is detail the systems installed on the aircraft. The methods used in the chapter are from *Airplane Design: Part IV* [6].

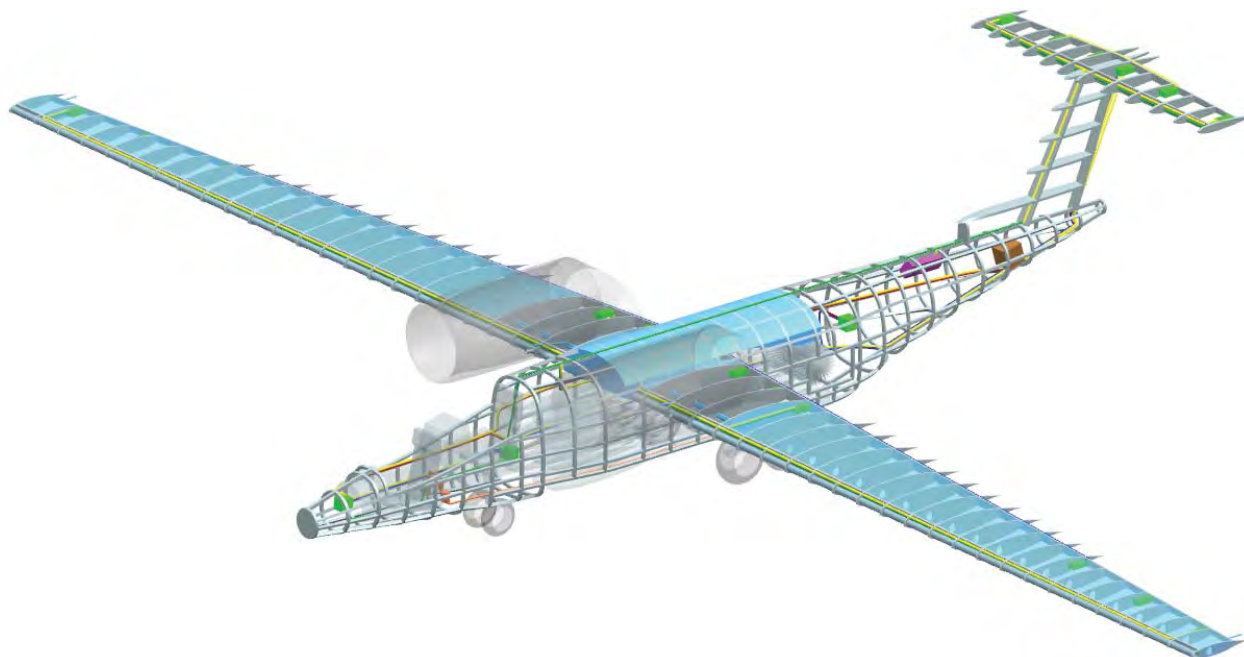


Figure 8.1: Complete System Overview; NTS

8.1. FUEL SYSTEM

The primary purpose of the fuel system is to store and deliver fuel to the engines. Due to the high aspect ratio of the wings the required mission fuel volume mandated a fuselage tank. Dry bays were placed behind the leading edge mounted engines in case of engine fire as recommended by Roskam [6].

The fuselage fuel tank was placed at

the same center of gravity location as the wing fuel tanks to minimize center of gravity excursion in the event of fuel jettison between tanks. As is shown in the figure below, the entire span of the wing is used to maximize wing fuel volume. Structural precautions are considered for wing tip lightning strikes. Fuel pumps are located at the dry bays, mid wing span, and in the fuselage tank. A maximum 9,681 lb_m/hr fuel flow rate is expected during takeoff. Fuel piping is located behind the forward wing spars for protection from leading edge damage. A single point refueling system is located at the aft starboard side of the fuselage. Armor plated tip pods were included for housing fuel dumping system

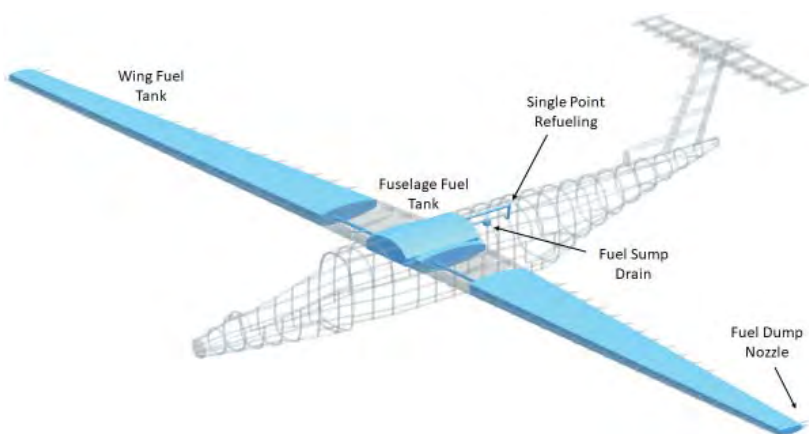


Figure 8.2: Fuel System Overview

and providing fuel tank protection.

8.2. FLIGHT CONTROL SYSTEM

Given the mission specification of the Overseer, the flight control system utilizes three independent flight control systems for redundancy. Three flight computers are utilized to control a section of each control surface. This allows for complete redundancy over the use of a three flight controls and a single voting network. Wiring and flight computer of each system were placed to minimize the possibility more than a single system failing per given event. Wiring lines are placed on the starboard side of the aircraft away from ground fire during pylon turns. Figure 8.2 shows each of the three system wiring lines in green, red, and blue. The three flight computers are also shown forward and aft of the cockpit and at tail of the aircraft.

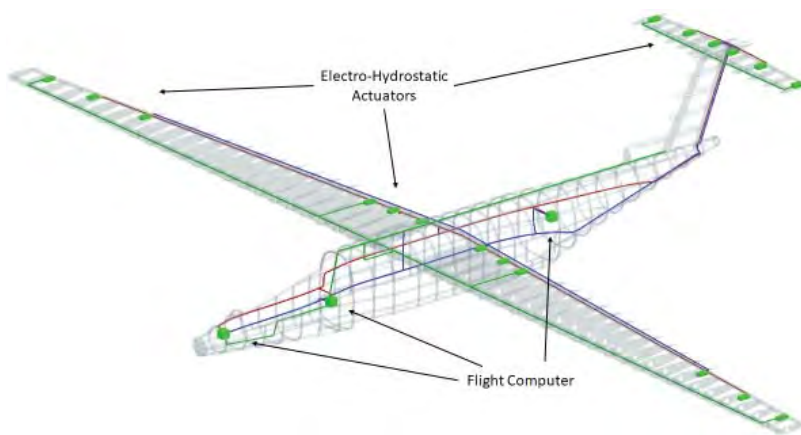


Figure 8.3: Flight Control System Overview

8.3. ELECTRICAL SYSTEM

The primary purpose of the electrical system is supply power to the aircraft throughout flight. The electrical system was also designed to be triply redundant. Each electrical wiring line is connected to three batteries placed on the starboard side of the aircraft. Table 8.2 provides estimated power consumption of the Overseer scaling from McDonnell-Douglas DC-10 consumption values provided in *Airplane Design: Part IV* [6]. Given the dissimilarities between the two aircraft, electrical load used for passenger spaces were omitted, and the final load doubled for a conservative estimate.

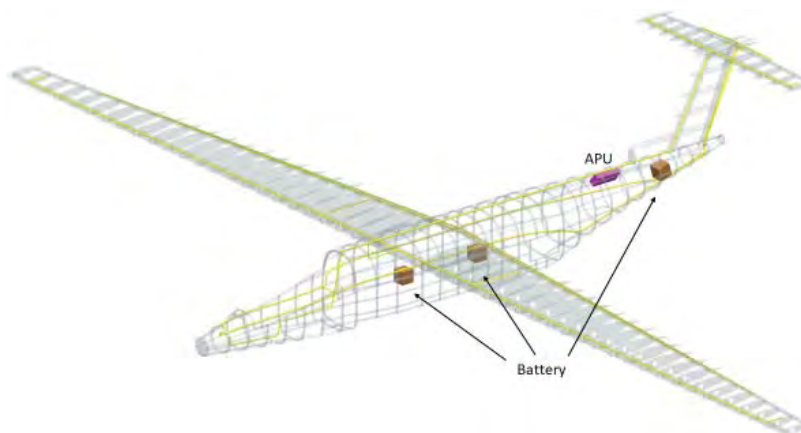


Figure 8.4: Electrical System Overview; NTS

Table 8.1: Electrical System Components

Control Surface Actuators	Fly-by-Light System
Environmental Control System	Flight Computers
Communication Systems	Avionics
Radar and Targeting Systems	Batteries
Internal/External Lighting	Instrument Heating

Table 8.2: Electrical Load

	Ground		TO/Climb		Cruise	
	V.A.	%	V.A.	%	V.A.	%
Exterior Lighting	2600	6.4%	3850	4.2%	200	0.3%
Cockpit Lighting	650	1.6%	1200	1.3%	1200	1.9%
Windshield Heating	1000	2.4%	6000	6.6%	7200	11.2%
Avionics	5300	13.0%	7400	8.1%	7250	11.3%
Environmental System	1600	3.9%	1600	1.8%	1600	2.5%
Fuel System	0	0.0%	6500	7.1%	6500	10.1%
Hydraulic system	0	0.0%	8800	9.7%	0	0.0%
Flight control System	1200	2.9%	2000	2.2%	2000	3.1%
D/C Power	7900	19.3%	7900	8.7%	6000	9.3%
Miscellaneous	200	0.5%	250	0.3%	250	0.4%
Total	40900		91000		64400	

8.4. HYDRAULIC SYSTEM

The purpose of the hydraulic system is to operate the landing gears of the aircraft. The system is heavily simplified due to the use of electro-hydrostatic actuators for control surface rather than hydraulics. The hydraulic system is also used for opening and closing bomb bay doors. A doubly redundant system is placed to ensure mission go-ahead in the event of a hydraulic failure.

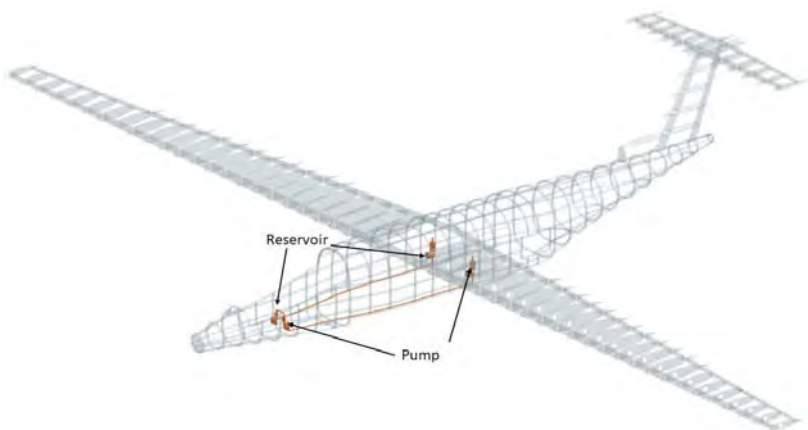


Figure 8.5: Hydraulic System Overview; NTS

8.5. ENVIRONMENTAL CONTROL AND AIR BLEED SYSTEMS

The purpose of the environmental control and oxygen systems is to provide comfort to the pilots and keep flight critical systems within rated temperatures. Bleed air from the engines are used for cockpit pressurization and oxygen. An emergency oxygen system is also placed behind the aft pilot seat.

A second air bleed system is installed on the engines to provide thrust. A cross ducting system is placed to bleed 10% of compressed air from each engine to the opposite wing tip. Ducts run along the leading edge of the wing into the wing tip pods where it is diverted to a nozzle at the end of each pod. The duct radius is the same as the leading edge radius and is placed in front of the leading edge spar. This system is in place to provide a moment balance in the event of one engine out. By cross ducting the bleed air, in the event of Engine 2 failure, the long moment arm from the starboard wing tip to Engine 1 provide enough distance for a small thrust to greatly decrease required rudder

deflection. This system alongside end plating effect of a T-tail greatly decreases vertical stabilizer size.

The high temperature bleed air running along the leading edge of the wing also functions as a component of the anti-icing and de-icing system. An indirect de-icing component such as ultrasonic de-icing or pulse electro-thermo-de-icing (PETD) were also looked into for use on the Overseer. Both of these new technologies offer high efficient, low power consumption, low cost, and reliable operation [59, 60]. These components make use of the already existing electrical wiring running through the entirety of the aircraft. The multiple redundancy of the electrical system thus provides redundancy to the de-icing system.

9. CLASS II DESIGN

Multiple design changes were to the geometric characteristic of the Overseer from Class I to Class II design. This chapter presents Class II Design and updated geometric characteristics due to Class II changes. Methods used are found in *Aircraft Design: Parts III - VI* [3-8]; Perry Rae of Boeing Aerosystems, and Dr. Richard Hale of The University of Kansas were also consulted.

9.1. LANDING GEAR

The determination of landing gear strut sizing follows methods presented in *Aircraft Design: Part IV* [6]. Hand calculation are presented in the accompanying website: <https://toledoph.wixsite.com/ae522/class-ii-design>

Updated tire selection and strut sizing are presented in the following tables.

Table 9.1: Landing Gear Strut and Tire Load Force and Ratios

	Static Strut Load (lb _p)	Static Strut Load (x1.25) (lb _p)	Dynamic Strut Load (lb _p)	Dynamic Strut Load (x1.25) (lb _p)	Load Ratio	Tire Load (lb _p)
Nose Gear	5,439	6,799	11,901	14,876	0.1	7,438
Main Gear	24,781	30,976	-	-	0.9	15,488

Table 9.2: Salient Tire Characteristics

Location	Tire Model	D _t (in.)	W _t (in.)	Rated Load (in.)	Rated Inflation (psi)	Loaded Radius (in.)	Rated Speed (kts)	V ^{sl} (kts.)	V ^{sto} (kts.)
Nose Gear	220K28-1	22	8	7,900	135	9	184	153.4	167.4
Main Gear	313K02-1	30	13	17,200	155	12.4	259	215.8	235.4

Shock absorber deflection, S_t, shock absorber stroke, S_s, and shock absorber diameter, D_s, are presented below for both landing gears. A load factor of 3g and a vertical touch down rate of 10 ft/s was assumed for both landing gears.

Table 9.3: Landing Gear Strut Sizing

	S _t (in.)	S _s (in.)	D _s (in.)
Nose Gear	3.1	9.38	4.83
Main Gear	2.0	8.46	5.21

9.2. WEIGHT AND BALANCE

This section presents Class II weight and balance analysis. The general, order of magnitude values calculated in Section 7.7 were further analyzed using methods from *Airplane Design: Part V* [7] and AAA software. AAA screenshots are presented in the accompanying website: <https://toledoph.wixsite.com/ae522/class-ii-weight-and-balance>. Table 9.4 shows weight and center of gravity locations for the following three weight conditions: empty, operational empty, and takeoff.

Table 9.4: Weight Breakdown

#	Component	Weight (lbs.)	X _{CG} (in.)	Y _{CG} (in.)	Z _{CG} (in.)
1	Wing	7,208	373	0	142
2	Horizontal Tail	357	693	0	229
3	Vertical Tail	315	662	0	189
4	Ventral Fin	19	649	0	133
5	Fuselage	3,378	352	0	116
6	Nacelle	556	320	0	152
7	Nose Landing Gear	263	249	0	89
8	Main Landing Gear	1,215	420	0	94
9	Engine	3,340	331	0	163
10	Fuel System	391	413	0	132
11	Air Induction System	4	350	0	150
12	Propulsion System	391	345	0	150
13	Flight Control System	1,060	450	-5	135
14	Hydraulic/Pneumatic System	593	343	0	92
15	Instruments/Avionics/Electronics	885	204	0	122
16	Electrical System	689	500	-30	145
17	Air Conditioning and Anti-Icing System	235	530	0	135
18	Oxygen System	58	560	0	145
19	APU	720	575	8	145
20	Furnishings	349	223	0	145
21	Cannon Structure and Targeting System	424	474	-20	80
22	Bushmaster III Cannon	606	474	-35	111
23	Other Items	196	330	0	145
24	Titanium Bathtub	2,000	223	0	113
	Empty Weight	25,252	370.4	-2.0	134.3
25	Crew	400	223	0	116
26	Trapped Fuel and Oil	273	370	0	132
	Operational Empty Weight	25,925	368.2	-1.9	134.0
27	Fuel	10,845	370	0	141
28	Ammo Drum	3,000	474	0	111
29	Fwd Bombs	8,000	317	0	111
30	Aft Bombs	7,000	418	0	111
	Takeoff Weight	54,410	372.4	-0.9	127.6

Center of gravity locations for each of the components are presented in the side view on the following page.

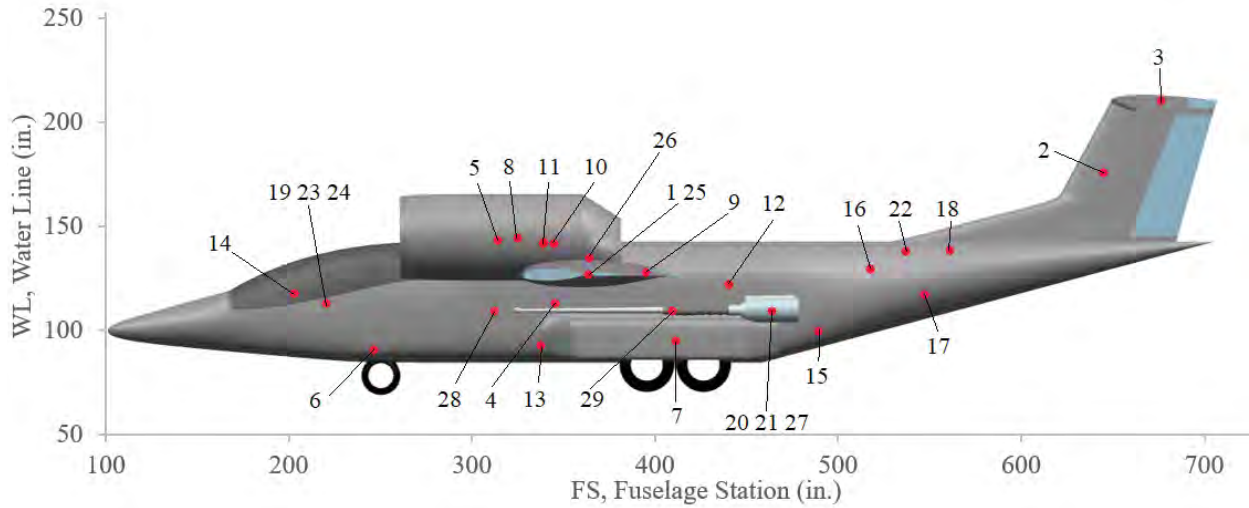


Figure 9.1: Updated Center of Gravity Locations

An updated CG excursion diagram is presented in the following chart. The largest CG excursion occurs during loading and unloading between W_{OE} and $W_{OE+Load}$

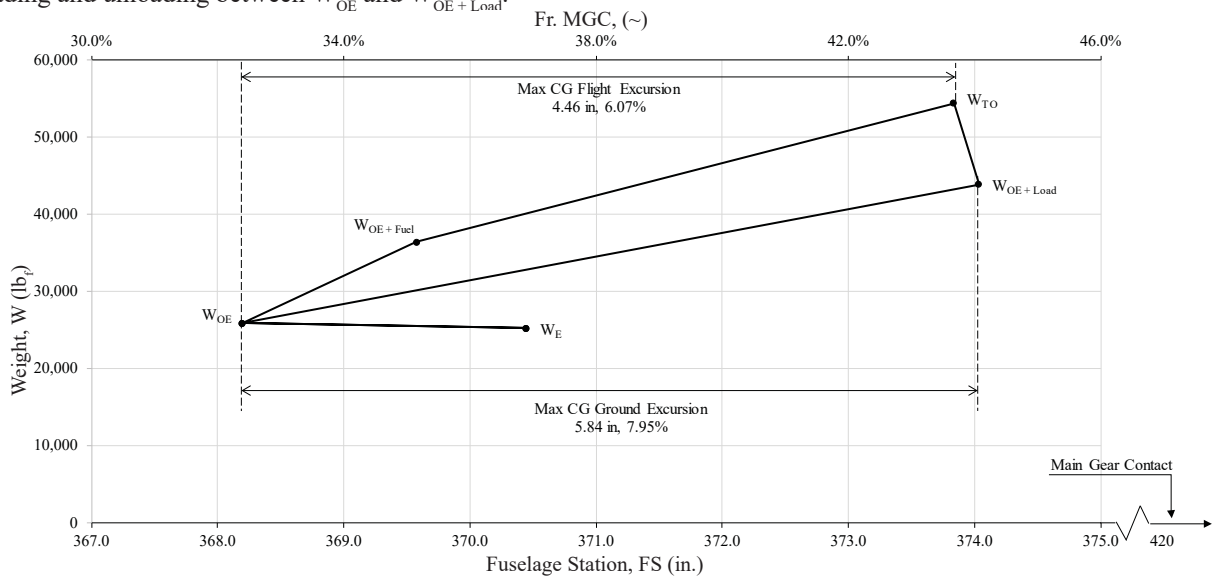


Figure 9.2: Class II Center of Gravity Excursion Diagram

A weight breakdown per component and component category is presented in the following charts:

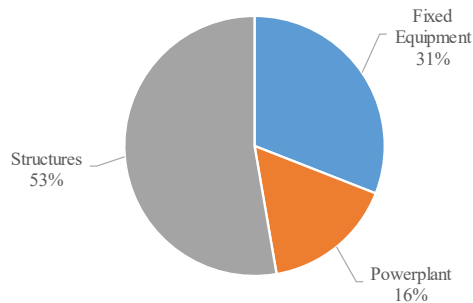


Figure 9.3: Empty Weight Distribution by Component Category

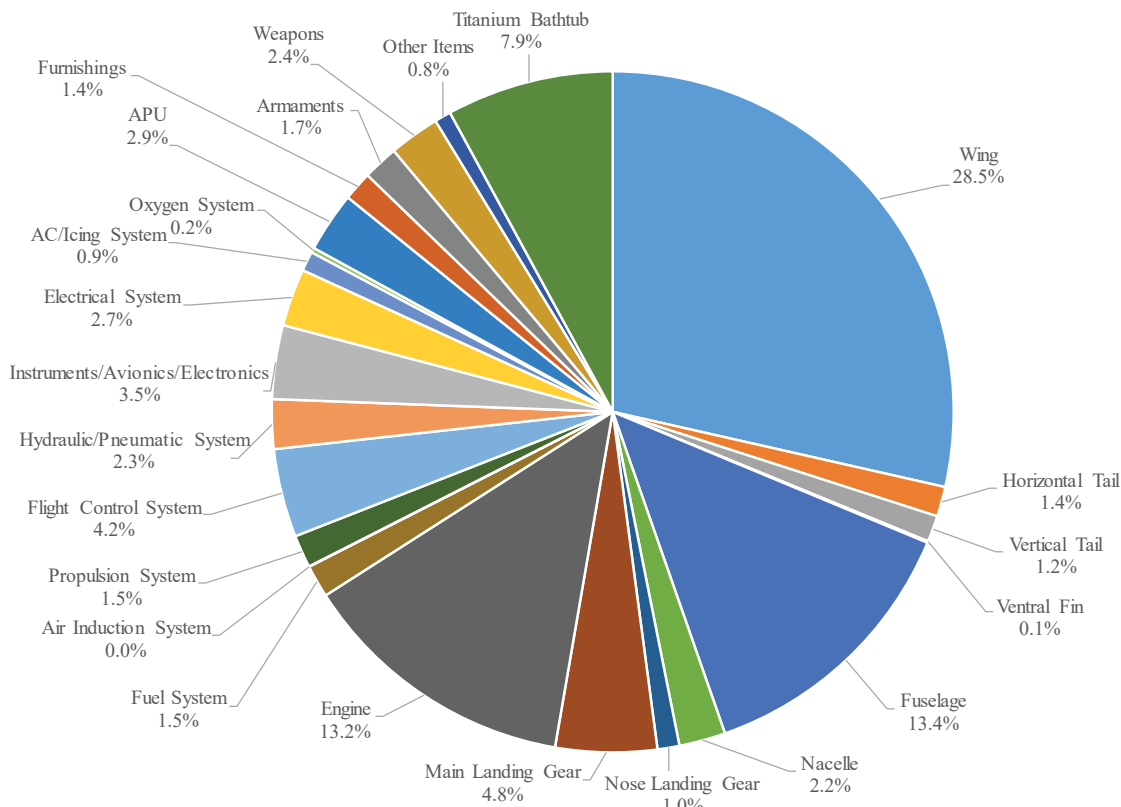


Figure 9.4: Empty Weight Distribution by Component

9.3. STABILITY AND CONTROL

Following Class II Weight and Balance, the static margins for the aircraft are recalculated. Table 8.2 presents static margins for the five primary loading conditions. The static margin change in an mission profile where no payload is dispensed changes for a less stable aircraft; where as the a significantly greater increase occurs due to the deployment of payload. As detailed in *Airplane Design: Part 2* [4] each of the static margins fall within the acceptable range for a fighter aircraft.

Table 9.5: Static Margins for Loading Conditions

	X_{CG} (in.)	Static Margin (%)
W_E	370.4	6.14
W_{OE}	368.2	9.14
$W_{OE + Fuel}$	369.6	7.23
$W_{OE + Pavload}$	373.8	1.52
W_{TO}	374.0	1.25

The table below presents stability derivatives calculated using AAA software. AAA screenshots are presented in accompanying website: <https://toledoph.wixsite.com/ae522/stability-and-control>. Derivatives were determined for cruise, trimmed for 30,000 ft at Mach 0.61 (360 kt).

Table 9.6: Stability Derivatives

	Longitudinal				Lateral		
	Cruise	Takeoff	Landing		Cruise	Takeoff	Landing
$C_{D_u} (1/\text{rad})$	0.2675	0.9333	0.3107	$C_{y_\beta} (1/\text{rad})$	-0.4813	-0.4524	-0.4541
$C_{L_u} (1/\text{rad})$	7.4059	6.6539	6.7244	$C_{l_\beta} (1/\text{rad})$	-0.0284	0.0349	-0.0193
$C_{m_u} (1/\text{rad})$	-0.2233	-0.2101	-0.2046	$C_{n_\beta} (1/\text{rad})$	0.0902	0.0854	0.0821
$C_{D_u} (\sim)$	0.0122	0.0000	0.0000	$C_{y_p} (1/\text{rad})$	0.0197	0.0715	0.0199
$C_{L_u} (\sim)$	0.3830	0.0701	0.0774	$C_{l_p} (1/\text{rad})$	-0.7495	-0.6856	-0.6930
$C_{m_u} (\sim)$	-0.1993	0.0060	0.0067	$C_{n_p} (1/\text{rad})$	-0.0826	-0.3304	-0.1319
$C_{L_q} (1/\text{rad})$	6.5989	5.9152	5.9612	$C_{y_r} (1/\text{rad})$	0.2312	0.2214	0.2159
$C_{m_q} (1/\text{rad})$	-21.047	-19.0056	-19.1462	$C_{l_r} (1/\text{rad})$	0.2026	0.5814	0.2557
$C_{L_a} (1/\text{rad})$	1.1691	0.9298	0.9473	$C_{n_r} (1/\text{rad})$	-0.0702	-0.1177	-0.0708
$C_{m_a} (1/\text{rad})$	-4.960	-3.9468	-4.0199	$C_{y_{\delta_A}} (1/\text{rad})$	0.0000	0.0000	0.0000
$C_{L_{iH}} (1/\text{rad})$	0.5672	0.5133	0.5171	$C_{l_{\delta_A}} (1/\text{rad})$	0.1268	0.1426	0.1415
$C_{m_{iH}} (1/\text{rad})$	-2.4063	-2.1783	-2.1942	$C_{y_{\delta_R}} (1/\text{rad})$	0.1611	-0.4927	0.1826
$C_{L_{\delta_E}} (1/\text{rad})$	0.2021	0.1039	0.2237	$C_{l_{\delta_R}} (1/\text{rad})$	0.0107	-0.0021	0.0117
$C_{m_{\delta_E}} (1/\text{rad})$	-0.8576	-0.4411	-0.9491	$C_{n_{\delta_R}} (1/\text{rad})$	-0.0509	-0.0594	-0.0577

Longitudinal and lateral handling qualities are presented for the cruise condition. Although roll performance and dutch roll damping are Level 2 handling qualities, these values are deemed acceptable for the aircrafts flight mission.

Table 9.7: Longitudinal Handling Qualities in Cruise

$\omega_{n_{SP}}$ (rad/s)	ζ_{SP} (\sim)	$\omega_{n_{P_{long}}}$ (rad/s)	$\zeta_{P_{long}}$ (\sim)	n/a (g/rad)	Level Phugoid Stability	Level Short Period Damping	Level Short Period Frequency
1.22	1	0.067	0.040	10.87	1	1	1

Table 9.8: Lateral Handling Qualities in Cruise

T_R (s)	ζ_D (\sim)	T_{2S} (s)	Level Roll Time Constant	Level Roll Performance	Level Dutch Roll Frequency	Level Dutch Roll Damping	Level Spiral Stability
0.28	0.056	85.879	1	2	1	2	1

A trim diagram is presented on the following page.

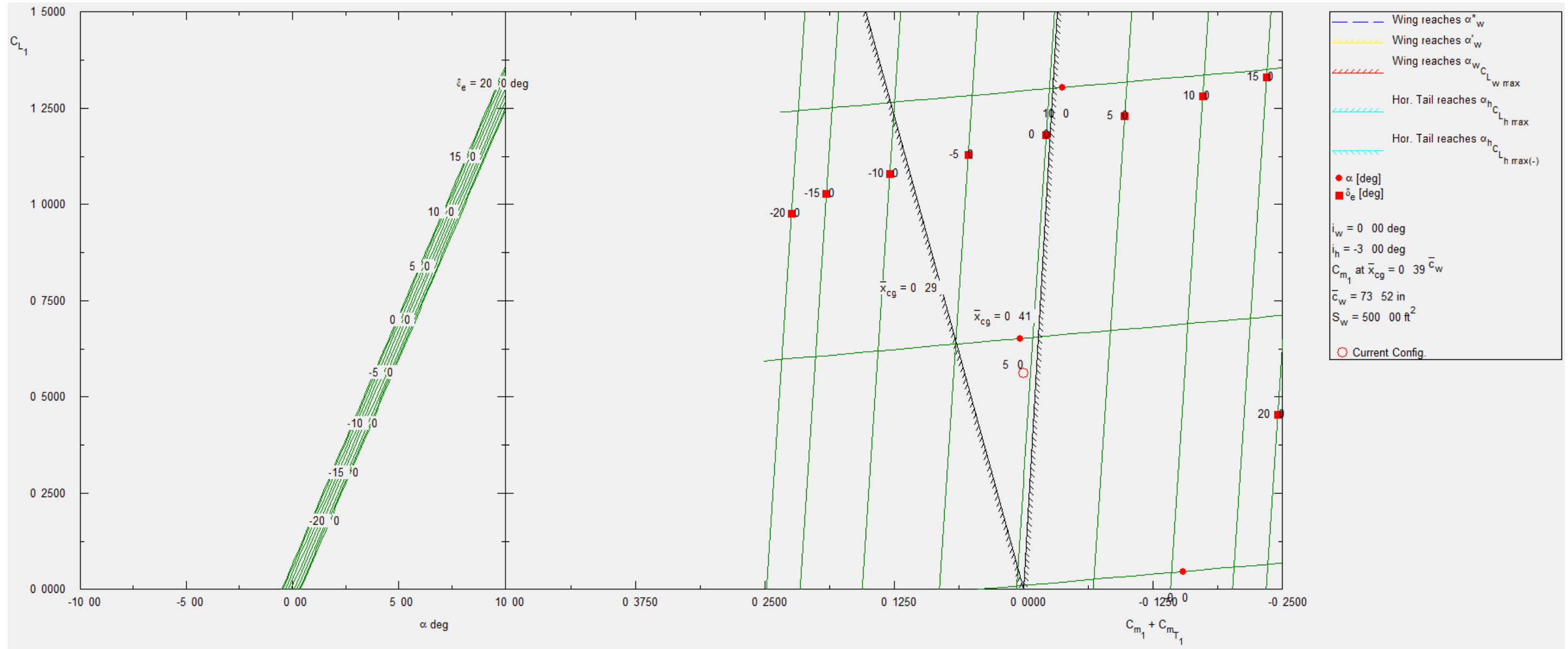


Figure 9.5: Trim Diagram for 1G Cruise Flight

10. UPDATED THREE VIEW AND EXPLODED VIEWS

The purpose of this chapter is to display an updated three view and exploded views of the outer moldline, substructure, and systems. Figure 10.1 shows an updated three view with a table of salient characteristics.

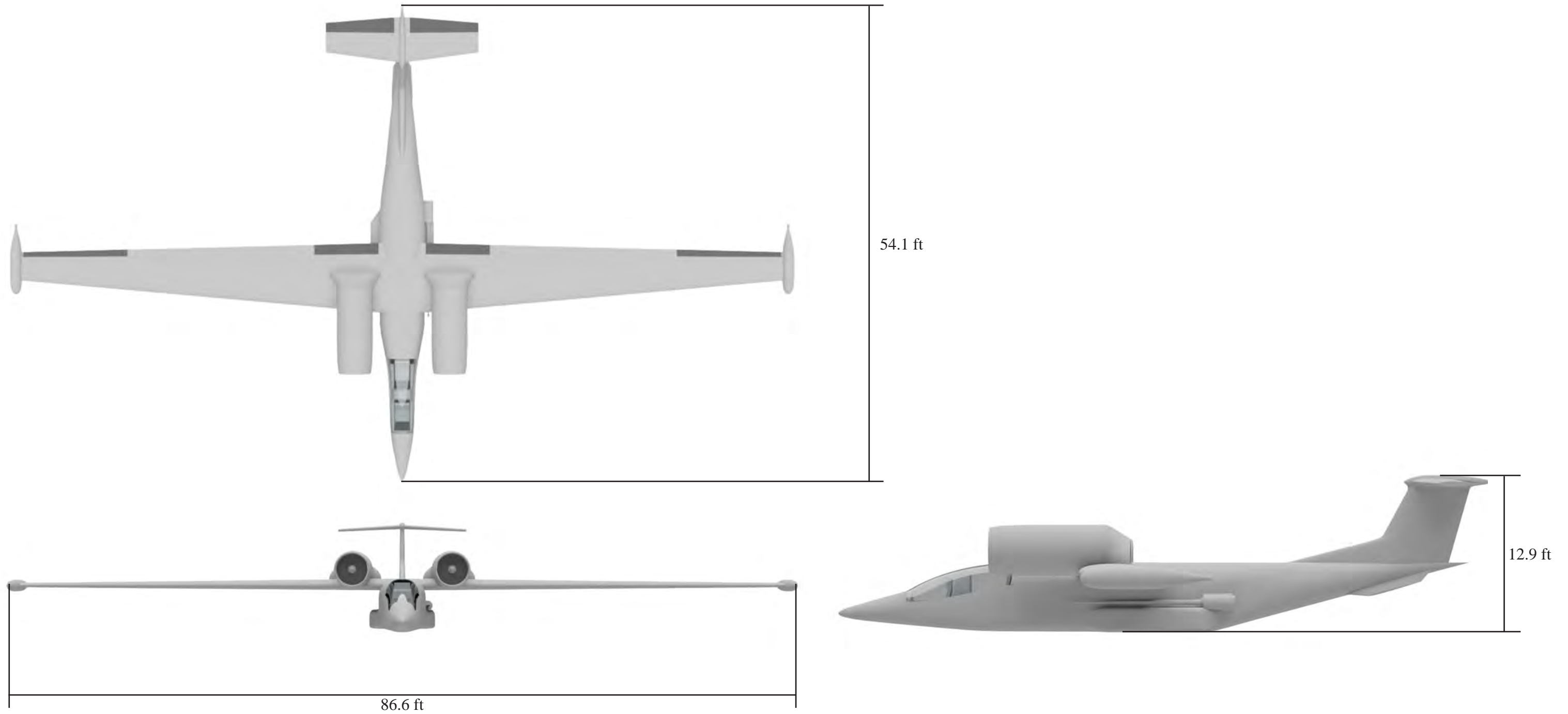


Figure 10.1: Updated Three View

Figure 10.2, below, shows an exploded view of each of the subcomponents of the Overseer.

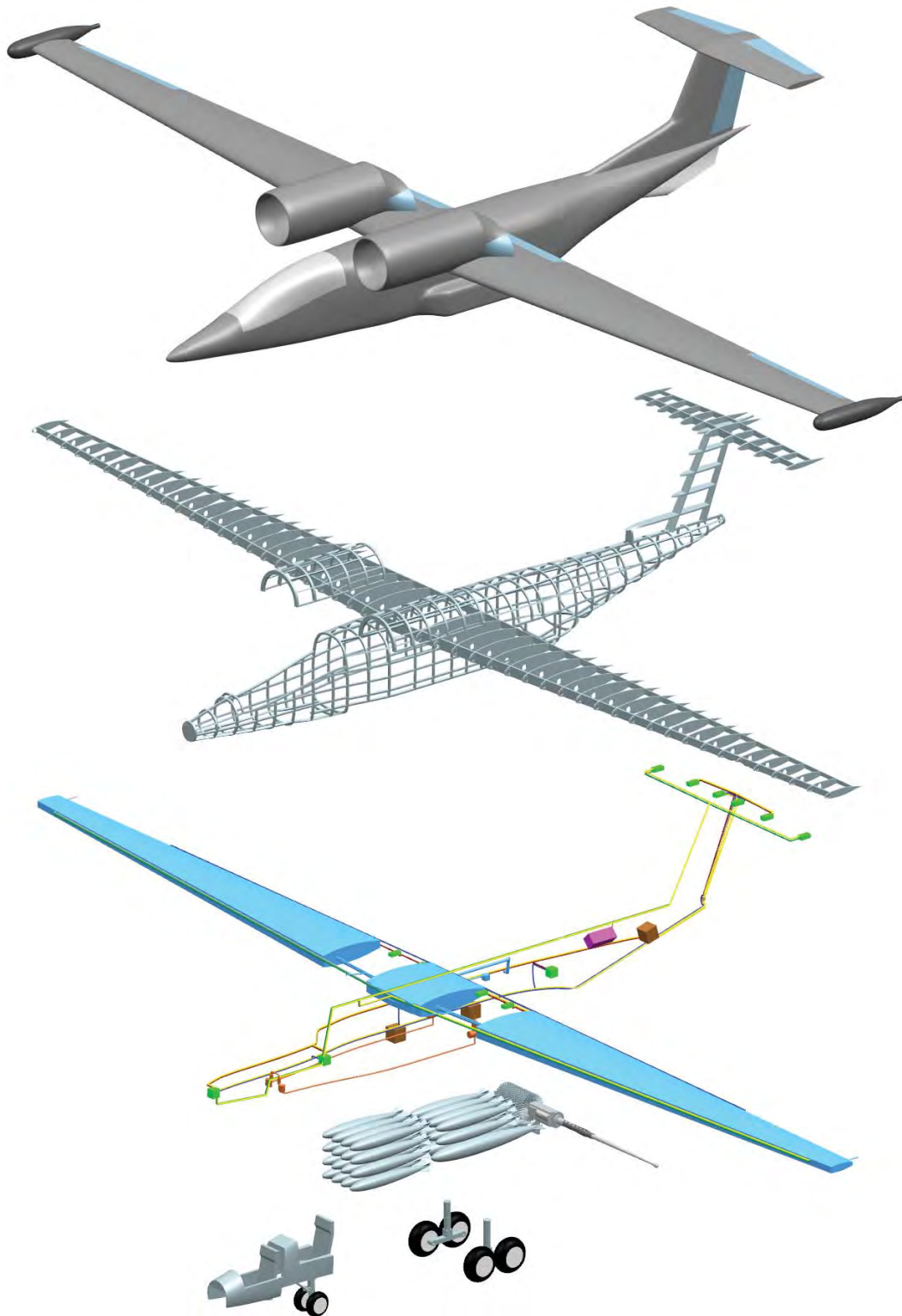


Figure 10.2: Exploded View of Subcomponents; NTS.

11. ARMAMENTS

The purpose of this chapter is to present the armaments featured on the Overseer and their accompanying systems. Hand calculations are provided on the accompanying website: <https://toledoph.wixsite.com/ae522/class-i-design>.

11.1. BUSHMASTER III CANNON

The primary feature of the Overseer is the ability to side fire using a 35 mm Bushmaster III cannon. Information on the Bushmaster III cannon is presented in Table 11.1. Three types of rounds are compatible with the Bushmaster III: Advanced Hit Efficiency And Destruction (AHEAD), High Explosive Incendiary (HEI), and Armor-piercing Discard Sabot (APDS-T). Table 11.2 provides specifications on three commonly used 35 mm rounds.

Table 11.1: Orbital ATK Bushmaster III Specifications [54]

Recoil (lb_f)	14,000
Weight (lb_f)	
Receiver (lb_f)	150
Feeder (lb_f)	80
Barrel (lb_f)	250
Total (lb_f)	480
Rate of Fire (min⁻¹)	20
Power Required	3 HP at 24 V

The cannon is placed on the port side of the aircraft between fuselage stations 460 and 490. The location of the cannon was dictated by placement of ordnance in the fuselage of the aircraft. The cannon will be mounted on a ball joint with a series of gears providing rotation along each aircraft axis. Slewing of the cannon for storage and targeting will be done by hydraulic

Table 11.2: 35 mm Rounds [55]

	AHEAD	HEI	APDS-T
Round Weight (lb_f)	3.9	3.48	3.19
Projectile Weight (lb_f)	1.65	1.21	0.84
Charge Weight (lb_f)	0.000661	0.25	0.666
Projectile Length (in)	15.23	15.23	13.39
Muzzle Velocity (ft/s)	3445	3854	4724

actuators. These actuators will also function as shock absorbers countering the forces and moments experienced by the structure of the aircraft. An active gust alleviation system will make minor adjustments during combat operations to ensure targeting accuracy using multiple hydraulic actuators connected to the primary targeting system.

Although the cannon will be able to fire forward utilizing strife runs, the primary mode of fire will be done through pylon turns. The use of pylon turns allows for continuous suppressive fire by orbiting above the target. A yawing force of 176 lb_f is experienced by the aircraft the cannon's maximum rate of fire. An increase of 0.0256 rad⁻¹ C_{L_V} is required to counteract this force and maintain the aircraft in trimmed flight. Crossbeams will span the width of the aircraft connecting the ring frames to provide support for the cannon and the ammo drum; these ring frames serve as the keel beams for the cannon support structure. The ammo drum will be placed inside of this support structure to consolidate space and serve as a counter balance. A hatch on the starboard side of the aircraft will

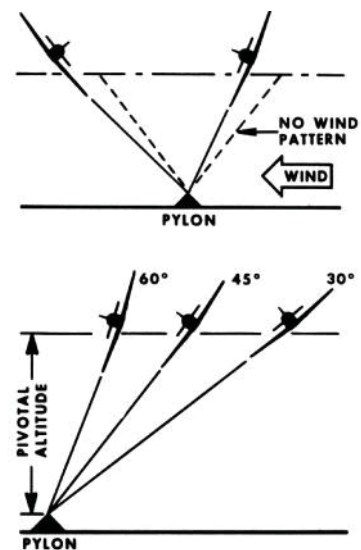


Figure 11.1: Pylon Turn and Pivotal Altitude [56]

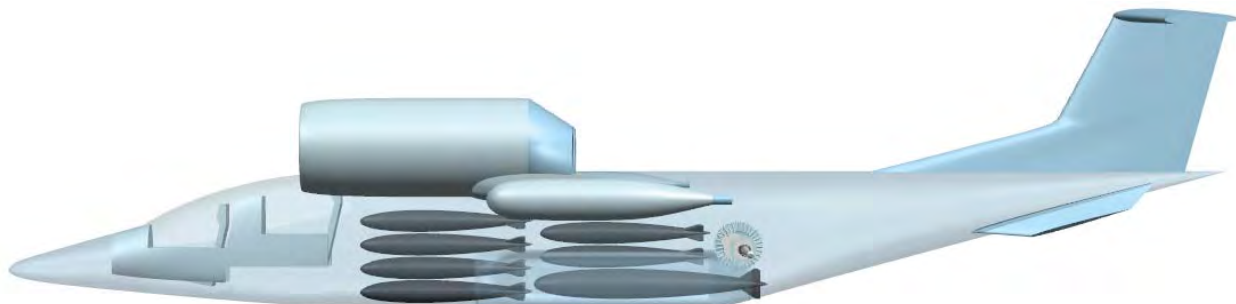


Figure 11.2: Ordnance Placement

allow for easy loading and unloading of the ammo drum.

11.2. ORDNANCE

A total of 15,000 lb_f of ordnance may be loaded onto the Overseer. Each weapons bay has accommodations for sixteen Mark 82 bombs. The presented configuration for optimum weight and balance places sixteen Mark 82 bombs in the forward weapons bay, and three Mark 83 with eight additional Mark 82 bombs in the aft weapons bay. Figure 11.2 displays ordnance placement on the Overseer.

11.3. ADVANCED ARMAMENT DEPLOYMENT

The Overseer features two advanced armament deployment methods: bomb lobbing and guided munitions. The use of bomb lobbing allows for increased range of bomb deployment alleviating the need to fly over a target. The use of bomb lobbing also allows for the deployment of armaments undetected by radar and away from heavy air defenses. This is traditionally done by flying low below radar altitudes and releasing ordnance in a Cuban 8 maneuver. The use of guided munitions provides benefits to both bomb lobbing and side firing. Traditionally gunships orbit at the pivotal altitude; the altitude which line of sight from the aircraft to parallel to the lateral axis of the aircraft remains stationary at a point on the ground. This altitude minimizes the need for targeting adjustments when firing at a stationary target. These altitudes are typically low forcing gunships to operate at night and with complete air superiority. Through the use of guided munitions, the operating altitude may be increased to lower chances of small arms ground fire. Guided bombs will also increase the precision of bomb lobbing.

12. ADVANCED TECHNOLOGIES

The purpose of this chapter is to present the advanced technologies the Overseer employs. The major systems discussed in this section are upper surface blowing and advanced target acquisition system..

12.1. UPPER SURFACE BLOWING

The defining characteristic of the Overseer is the implementation of upper surface blowing. The placement of the engines cantilevered off of the leading edge of the wing induces the Coandă Effect. This engine placement forces discharged exhaust gases to flow over the upper surface of the wing and high lift devices increasing the amount of lift generated. A flap system that creates a continuous and smooth curvature allows for the exhaust gas flow to stay attached to the upper surface while being redirected downwards. Through the use of upper surface blowing, the maximum lift coefficients in different flight stages may reach in excess of . The offset for the use of upper surface blowing is that the engine placement must be very close to the fuselage to reduce rolling and yawing moment in one engine inoperative situations and to maximize the efficiency of the Coandă Effect. Furthermore, a non-trivial weight penalty is taken due to structural support for cantilevering the engines. Several “tricks” used to support upper surface blowing also increase the assembly’s weight. Because of low pressure above the wing during cruise flight, the ideal nozzle has a small exit area; however, in low speed flight the ideal nozzle has a large exit area. To combat this an area reduction system is employed; A pair of “doors” open during take off and landing to increase the nozzle exit area for optimal performance. The use of heavier, high temperature materials are also used to protected the upper surface from hot exhaust gases. The basic design for upper surface blowing is mirrored that used in the Boeing YC-14 [53]. The figures below shows the door mechanism for variable exit area and a cutaway of the engine installation for upper surface blowing on the YC-14.

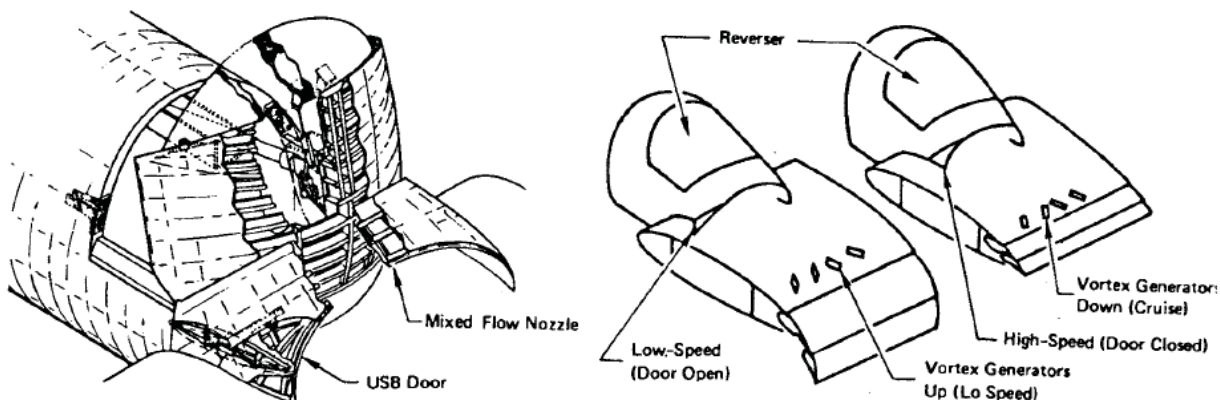


Figure 12.1: Upper Surface Blowing Nozzle and Thrust Reverser on YC-14 [53]

12.2. ADVANCED COMMUNICATIONS-ELECTRONICS SYSTEMS

A mix of targeting systems used on the AC-130U and F-35 Lightning II will be utilized to maximize mission performance. The Lockheed Martin AN/AAQ-39 Gunship Multispectral Sensor System (GMS2) is the primary fire control system used for the Bushmaster III on the Overseer. First outfitted for the AC-130U Spooky, the AN/AAQ-39 is an electro-optical and infrared control system that includes: “a large-aperture, Midwave Infrared (MWIR) sensor with four fields of view for long range target detection, recognition, and identification; two Image-Intensified Television (I²TV) cameras for situational awareness with the ability to detect light sources, markers, beacons, and personnel locators; a Near-Infrared (NIR) laser pointer for target identification and handoff; advanced image processing and algorithms for very high image quality and enhanced range recognition and identification; high accuracy line-of-sight pointing for ordnance delivery, and a laser designator/rangefinder,” [54]. This system will be placed in the aft seat for WSO use. The Northrop Grumman AN/AAQ-37 Electro-Optical Distributed Aperture System (EO DAS)



Figure 12.2: AN/AAQ-39 MWIR Magnification System [54] **Figure 12.3:** AN/AAQ-37 EO DAS Detection [57]

utilized on the F-35 Lightning II is also implemented on the Overseer for complete autonomous airborne targeting capability and situational awareness. The system’s six high resolution infrared sensors placed flush around the airframe provide unobstructed spherical coverage providing missile-warning including launch point detection, situational awareness Infrared Search and Track (IRST) and cueing, and day/night navigation [55]. The AN/AAQ-37 will work in conjunction with the AN/APG-81 Active Electronically Scanned Array (AESA) radar system, also manufactured by Northrop Grumman. Working together the two systems are capable of detecting and pin-pointing locations of artillery, anti-aircraft artillery, missiles, and rockets simultaneously past second stage burnout [56]. The AN/APG-81 allows for automatic target cueing and simultaneous radar display and detail expansion in a single Synthetic-Aperture Radar (SAR) display. The use of a touchscreen glass-cockpit further simplifies pilot and WSO workload [58].



Figure 12.4: AN/APG-81 Displays on Glass Cockpit [58]

13. RISK MITIGATION

The purpose of this chapter is to detail the various risk mitigation design choices prescribed for the Overseer.

Although a unique design, the Overseer does not pose many configuration design risks. The concept of upper surface blowing has been successfully fielding in both the Boeing YC-14 and the Antonov An-72/-74. Of concern is the use of a very high aspect ratio. The performance of the Overseer rests on its high aspect ratio and use of upper surface blowing. The risk of a very high aspect ratio is a rapid increase in wingspan and manufacturability. Aircraft with very high aspect ratios are often susceptible to instability due to gusts; this effect is due to high C_{n_u} values. To mitigate this effect spoilers on either wing will be used to alleviate gust loads during rolls. High bandwidths are attainable using spoilers due to their low inertia. A very high aspect ratio also makes the Overseer prone to high root bending moments. Figure 13.1 below show a Schrenk's approximation of the Overseer wings. The left plot shows a high increase in C_l due to upper surface blowing with total shear force at a given span wise location is shown on the right. The use of

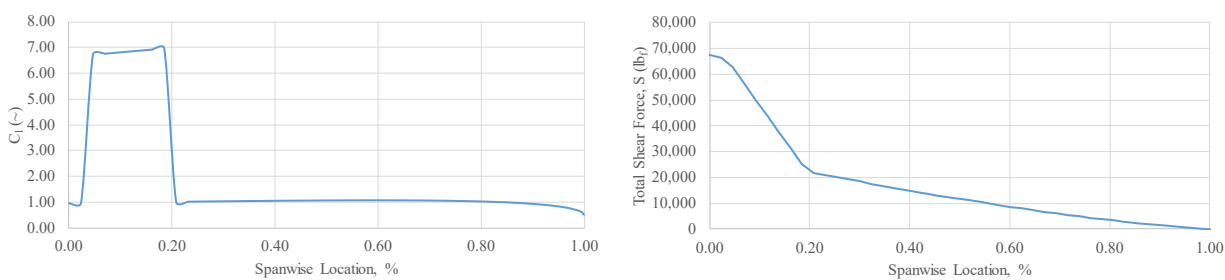


Figure 13.1: Schrenk's Approximation

very high aspect ratio wings creates a problem in manufacturing and transportation of long components. The use of a through spar is favorable in the structure of a wing. With a large wingspan manufacturing a straight, through spar that spans the entire wing becomes problematic. The Overseer is able to work around this problem through its modular wing design as detailed in the wing manufacturing plan in Chapter 14.

To achieve its mission as a gunship, the Overseer employs a number of target acquisition systems are discussed in Chapter 12. The integrity of these systems are vital to mission success. As such, the equipment place are currently fielded and proven their reliability through use in other platforms. Installation of these systems will be made such that future upgrades minimize impact on aircraft design.

Given the inherent dangers of a close air support aircraft multiple redundancies are placed to ensure mission success. As described in Chapter 8, the flight control and electrical systems both feature triply redundancies. Wiring from each of the three batteries and flight control systems provide complete independence from other systems. To further protect these two systems from damage, each of the wiring lines are placed along the structure of the aircraft. In the fuselage, all of the wiring is placed on the starboard side to minimize the risk of damage from ground fire during low pylon turns. These lines run along the top, upper side, and lower side of the fuselage. In the wing, two lines run aft of the aft spar, and a single line runs forward of the forward spar. Although running systems wiring inboard of the

spars increases protection, the trade off with maintenance and repair was deemed unsatisfactory. The wiring on the empennage follows the same layout as that of the wing. The hydraulic system does not form a closed loop; however, the main landing gears are exposed to the freestream in their fully retracted position. This provides protection to the belly of the aircraft in case of a failure in the hydraulic system. The anti-icing and de-icing systems are completely independent to minimize the risk of both systems failing. The anti-icing system is a by-product of the air bleed system from the engines. The air bleed system runs through the leading edge through tubing taking up the entire leading edge radius. This serves two purposes: to maximize volume flow rate of for thrust production (See Section 8.5); and, to serve as a barrier to systems lines running between the tubing and the forward wing spar. Due to the close proximity of the engine to the cockpit, reinforcement is added to the inboard section of the nacelle. This precautionary measure is to ensure engine blade separation does not strike the pilot nor the WSO.

14. MANUFACTURING PLAN

The purpose of this chapter is to present material selection and manufacturing plan of the Overseer.

The assembly of the aircraft will be done in a single location with components arriving as they are needed for optimization of space. Assembly facility is to be located in an area accessible by well established rail lines, and highways for maximum cargo accessibility. Manufacturing and acquisition of both structural and electrical components will be outsourced to companies throughout the nation. Although an increase in supply chain complexity, by utilizing companies from each state congressional support is increased.

The wing will be manufactured using a combination of metals and composites. Table 14.1 shows material selection for the wing components.

Table 14.1: Wing Material Selection

Component	Material
Spar	7075 Aluminium
Rib	5052 Aluminium
Inboard Skin	6A1-4V Titanium
Outboard Skin	Carbon Composite
Aileron	Carbon Composite
Flap	6A1-4V Titanium

The use of a continuous spar was considered however due the high wing span, manufacturing cost trade off was deemed excessive. The spars will be manufactured out of 7075 aluminum for its high strength. Ribs will be manufactured out of 5052 Aluminum for its strength. The wing is segmented into three sections defined by two spar breaks. The spar break occurs at $BL \pm 125$. The inboard wing section will require the use of Ti 6Al-4V (Grade 5) alloy due to the hot gases blowing over the upper surface. Similarly, the entirety of the flaps will be made using this titanium alloy. The outboard section of the wing will be made out of carbon fiber-epoxy layup to offset the use of heavier materials. Although composites skins have an increased complexity in repairability, the location of the spar break allows for the entire outboard section of the wing to be replaced in the event of battle damage. The use of smaller wing segments decreases manufacturing costs of replacement parts, shipping costs, and decreases grounded time for repair. Conformal fuel bladders are used in place of wet torque boxes allowing for self sealing. The wing will be delivered individually in its three sections for ease of transportation and system integration prior to mating. Figure 14.1 and 14.2 show wing assembly visualization and flow chart.

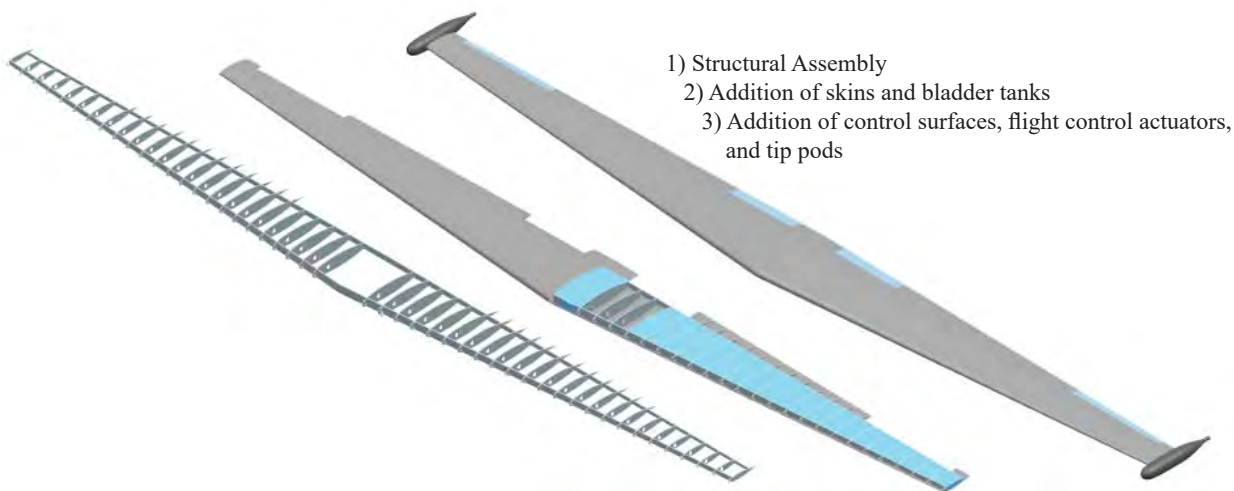


Figure 14.1: Wing Assembly Visualization

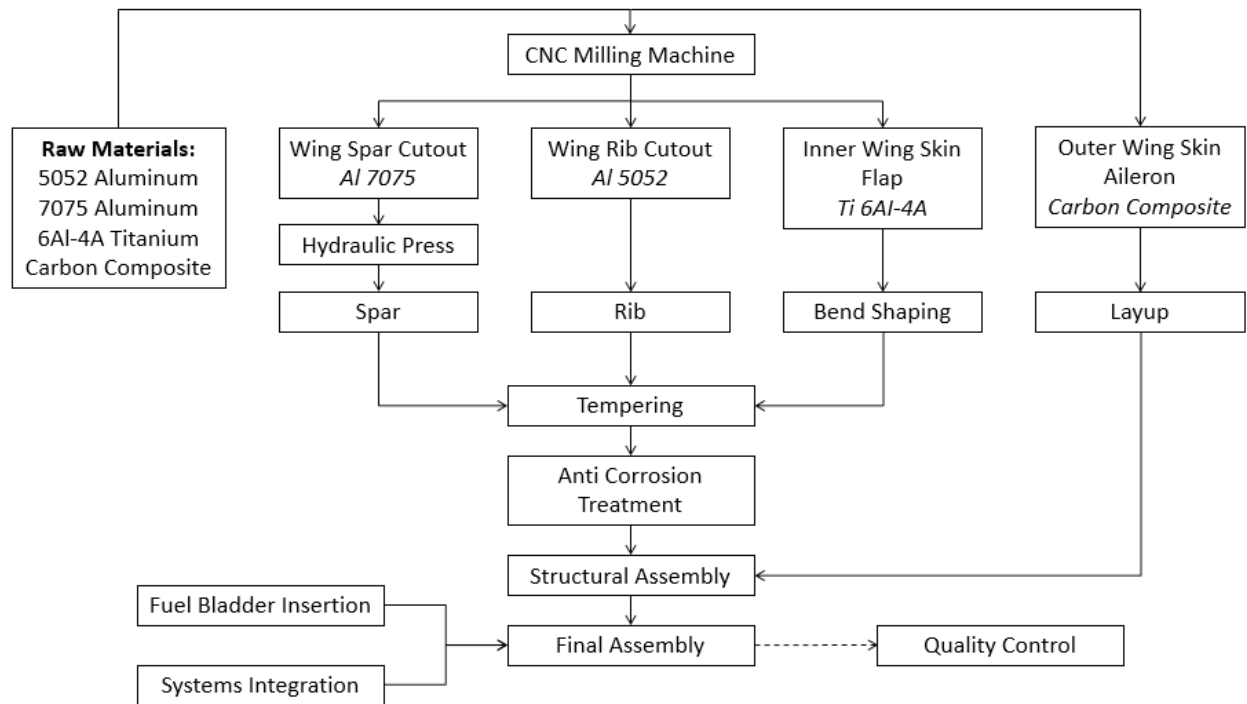
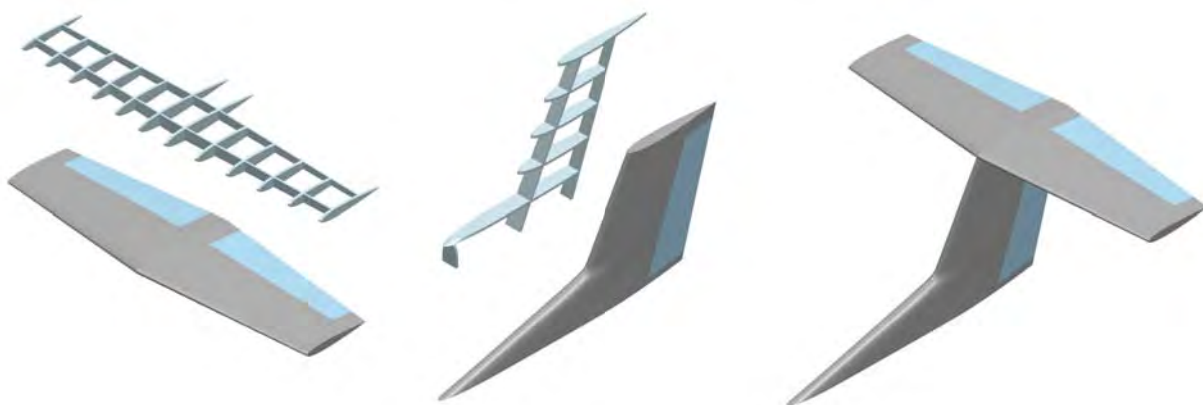


Figure 14.2: Wing Assembly Flow Chart

The empennage will be manufactured using an all aluminum assembly. Similarly to the wing, the main spars will be manufactured out of 7075 Aluminum with 5052 Aluminum ribs and 2024 Aluminum skin. A contiguous spar will be used for the horizontal stabilizer. Similarly to the wing, assembly between the vertical and horizontal stabilizers will take place at the final assembly building. Figures 14.3 and 14.4 show empennage assembly visualization and flow chart.

Table 14.2: Empennage Material Selection

Component	Material
Spar	7075 Aluminium
Rib	5052 Aluminium
Skin	2024 Aluminium
Control Surfaces	Carbon Composite



- 1) Structural Assembly
- 2) Addition of skins, control surfaces, and flight control actuators
- 3) Assembly of horizontal and vertical stabilizers

Figure 14.3: Empennage Assembly Visualization

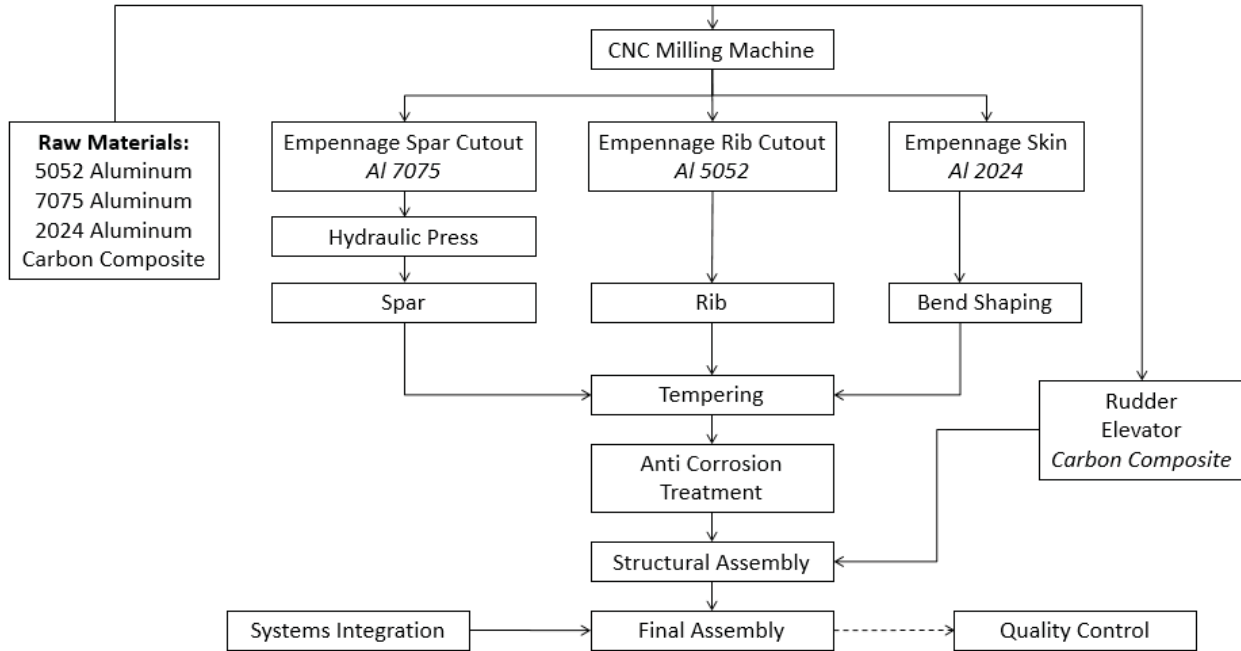


Figure 14.4: Empennage Assembly Flow Chart

The fuselage will be manufactured in three separate sections: cockpit, mid section, and tail. These sections are split at the firewall and aft bulkhead. The three section manufacturing will be utilized for the following reasons: additional safety structure require around the cockpit; ease and cost of manufacturing; and ease of transportation.

Table 14.3: Fuselage Material Selection

Component	Material
Ring Frame	5052 Aluminium
Longeron	5052 Aluminium
Stringer	Aluminium
Skin	2024 Aluminium

A semimonocoque construction will be employed with an all aluminum airframe. Material selection for the fuselage

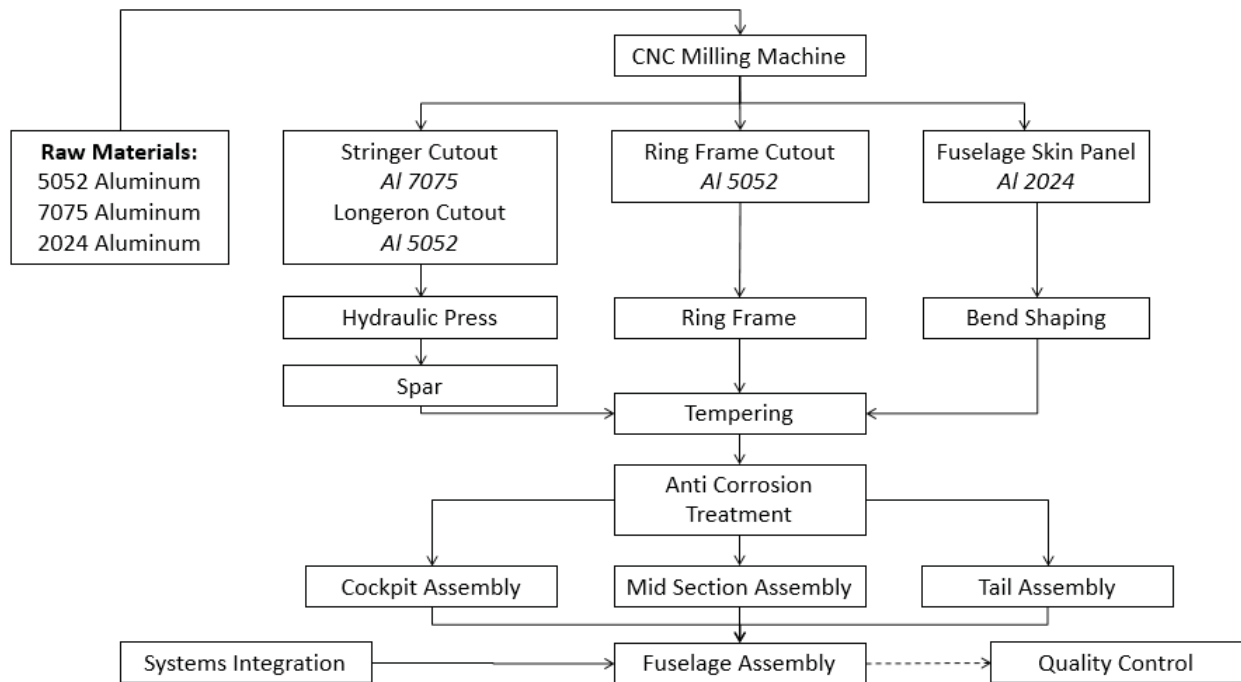


Figure 14.5: Fuselage Assembly Flow Chart

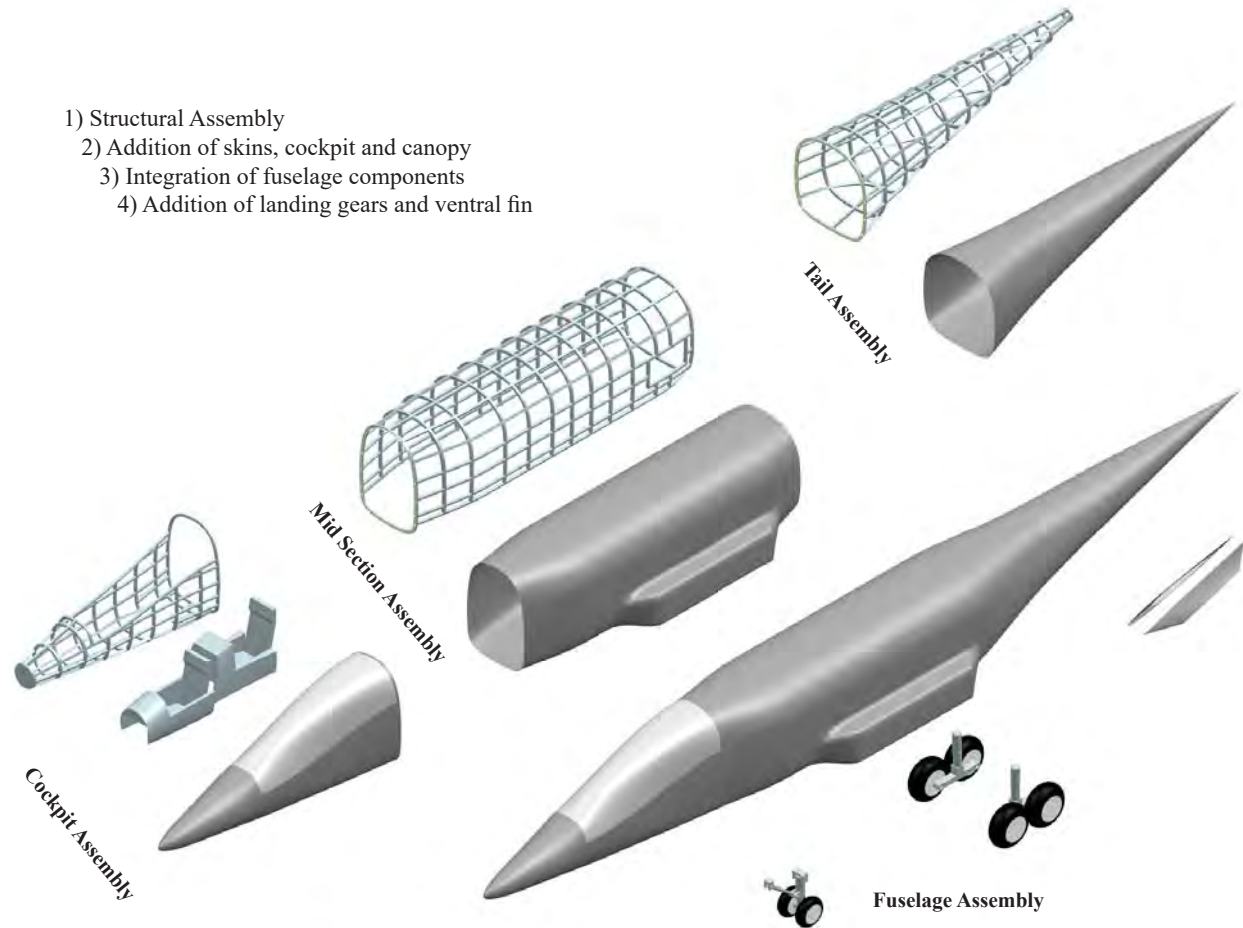


Figure 14.6: Fuselage Assembly Visualization

is presented in Table 14.3. Ring frames and longerons will be manufactured out of 5052 Aluminum for its strength and corrosion resistance, where are stringers will use 7075 Aluminum for its higher strength. The use of carbon composite skins was evaluated to be impractical in both the cost and ability to match thermal expansion with aluminum substructure. The three sections will be mated following delivery to the final assembly building.

Final assembly will occur at the main assembly building. The assembly will be modular to allow for single component replacement. Final assembly will begin by mating the fuselage sections together. Integration of subsystem will follow ensuring mating connections between fly-by-light, electrical wires, and fuel pipes are placed between components facilitating the modular approach. At this time all subsystems and landing gear will be integrated into the fuselage. The three wing sections and vertical and horizon stabilizers will be assembled simultaneously. The wing will be lowered onto the fuselage and attached using a series of steel alloy lugs. Installation of the engines already in their nacelles will follow. Following final assembly, a series of inspections and ground testing will take place ensuring complete mission capabilities.

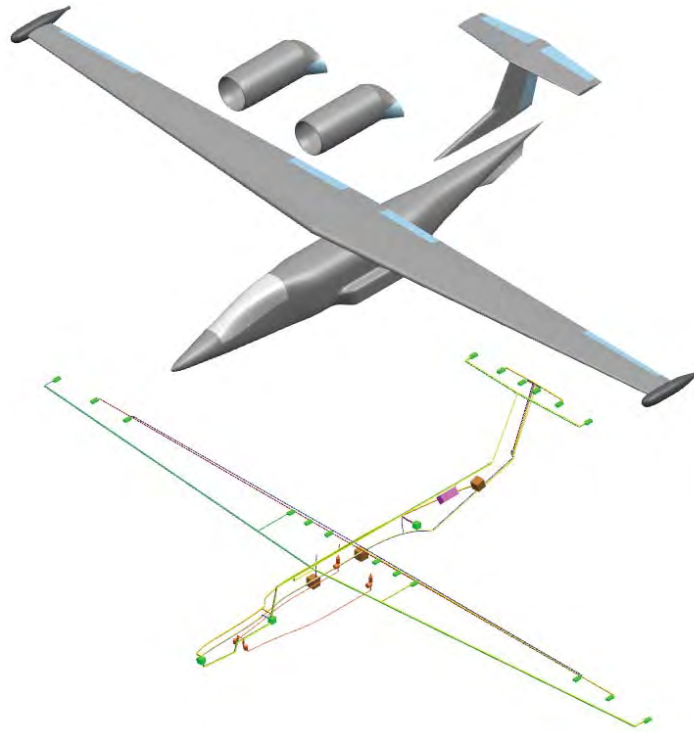


Figure 14.7: Final Assembly Visualization

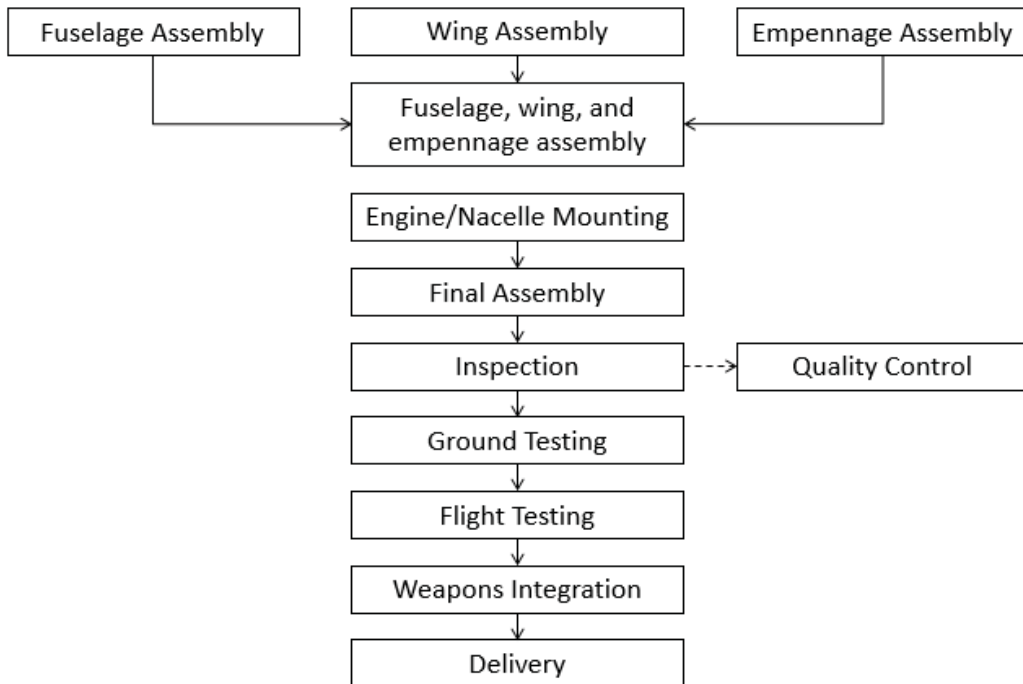


Figure 14.8: Final Assembly Flow Chart

15. COST ANALYSIS

The purpose of this chapter is to present the cost associated with the Overseer program. The cost module in AAA was used to assess the total program cost. Screenshots are presented on the accompanying website: <https://toledoph.wixsite.com/ae522/cost-analysis>.

Acquisition costs are presented in Table 15.1. Life cycle costs are presented in Table 15.2.

Table 15.1: Acquisition Cost (500 Units)

	Cost (\$)
Airframe Engineering and Design	\$83 million
Program Production	\$6,948 million
Flight Test Operations	\$139 million
Research, Development, Test, and Evaluation	\$762 million
Total Manufacturing Cost	\$7,966 million
Total Acquisition Cost	\$8,763 million
Estimated Price per Airplane	\$19.05 million

Table 15.2: Life Cycle Cost (500 Units)

	Cost (\$)
Fuel, Oil, Lubricants (500 flight hours/year)	\$2,500 million
Consumable Materials	\$2,745 million
Direct Personnel	\$19,006 million
Indirect Personnel	\$5,838 million
Operating Cost	\$44,909 million
Operating Cost per hour	\$3,476
Life Cycle Cost	\$288,468 million

An estimated price per plane based on production run is shown in Figure 16.1.

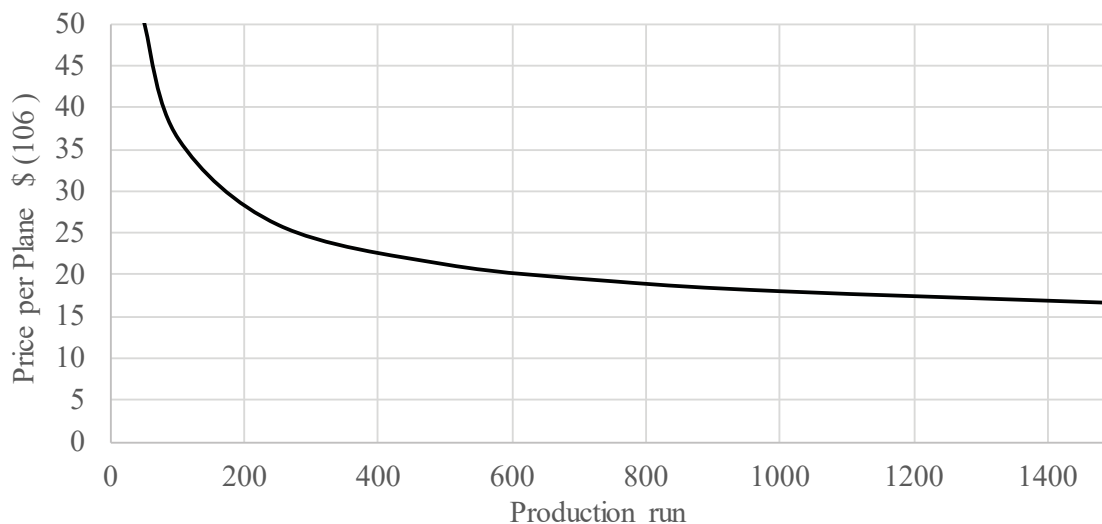


Figure 15.1: Aircraft Production Unit Costs

16. MARKETING PLAN AND PATH FORWARD

The purpose of this chapter is present how the Overseer will be marketed towards potential customers and the future of the platform.

16.1. MARKETING PLAN

Through the past several decades the need of a modern close air support aircraft has been continuously discussed. The aging A-10 fleet has required multiple systems overhauls and complete wing repairs. The Overseer has the capacity to serve not only a replacement, but also provide a wider range of mission capabilities. Given its superior capability and use of currently fielded advanced systems the Overseer’s customers will be limited to close allies with primary variants restricted to the United States armed forces. Historically, garnering public and congressional support for military assets have been a struggle. To appease these parties the Overseer will look to obtain components manufactured and designed from companies located in all 50 states and partner countries.

16.2. PATH FORWARD

The current design of the Overseer is that of a manned weapons platform. Military trends over the past few decades have looked to take make aircraft unmanned and autonomous. With today’s rate of technological advances the probably of an unmanned variant in the next two decades is high. By taking both pilots out of the aircraft multiple environmental systems will be unnecessary reducing the overall weight. No change in firing operations will occur as the WSO already remotely controls the system from the cockpit of the aircraft. The addition of autonomy to the aircraft will allow for multiple platform loiter over the airspace with only a WSO monitoring the combat zone until the need for weapons deployment arises; this system will completely negate the need for a pilot.

A variety of upgrades allow for greater versatility of the Overseer as a weapons platform. A reduction or complete replacement of the ordnance payload may be replaced with ammunition transforming the overseer in to a modern, high caliber AC-47. The offset of bomb payload with canon ammunition gives the Overseer the ability to provide extreme uninterrupted suppressive fire capabilities allowing trapped ground troops to extract. A second possible upgrade is the addition of folding wing tip to reduce the overall span of the Overseer. Current hangar sizes storing the A-10 are roughly 220’ by 180’, these accommodate five aircraft. Without the use of folding wingtips only two Overseers may be stored in existing infrastructure. Folding wing tips may allow for the three Overseer to be housed in current A-10 hangers.

17. SPECIFICATION COMPLIANCE

The purpose of this chapter is to present the compliance of the Overseer to the objectives outlined in the RFP.

Table 17.1 displays the compliance matrix.

Table 17.1: Specification Compliance Matrix

Specification Requirement	Threshold Specification	Objective Met?
AAO Radius & Endurance	4 hour at 500 nm	Yes
Weapons & Armaments	35 mm cannon with 750 rounds	Yes
	14,000 lb _f ordnance	Yes
Systems	Cat. 2 Targeting System	Yes
	Communications Array	Yes
Takeoff Runway Length	6,000 ft	Yes
Cruise Speed	200 KTAS	Yes
Max. Speed	300 KTAS	Yes
Service Ceiling	45,000 ft	Yes
Max. Load Factor	8 g	Yes
Flyaway Cost (500 Units)	\$40 million	Yes
Operating Cost	\$3,000/hr	No

Table 17.2 shows the final objective score achieved by the Overseer and the A-10. Chapter 3 presents weight factors suggested by military personnel. The selected weight factors place greater emphasis on minimizing cost and ability to operate from advance airfields. Using these factors, the Overseer scores higher than the A-10 in a number of categories.

Table 17.2: Objective Function Overview

Function	Weight	Overseer	Overseer Score	A-10	A-10 Score
AAO Radius	10.0%	500 nm (4 hrs)	0.10	250 nm (1.88 hrs)	0.03
Dash Speed	12.5%	400 KTAS	0.22	381 KTAS	0.20
Cruise Speed	12.5%	360 KTAS	0.41	300 KTAS	0.28
Flyaway Cost (500 Units)	15.0%	\$19.7 mil	0.62	\$18.8 mil	0.68
Operating Cost	15.0%	\$3,472	0.11	\$5,944	0.04
Minimum Runway Length	15.0%	4,750 ft	0.24	3,100 ft	0.34
Max. Load Factor	10.0%	8	0.10	8	0.10
Observables	10.0%	Internal (1)	0.10	External (0)	0.00
Objective Function Score			1.90		1.66

REFERENCES

1. Anon., "A-10 Thunderbolt II," U.S. Air Force Website, URL: <http://www.af.mil/About-Us/Fact-Sheets/Display/Article/104490/a-10-thunderbolt-ii/>
2. Anon., "Close Air Support Aircraft (A-10 Replacement); Request for Proposal," 2017-2018 AIAA Foundation Undergraduate Team Aircraft Competition, pp. [online RFP], 1-7, URL: <http://www.aiaa.org/UndergradIndividualAircraft-CAS-RFP/>
3. Roskam, J, *Airplane Design: Part I, Preliminary Sizing of Airplanes*, DARcorporation, Lawrence, KS, 2005.
4. Roskam, J, *Airplane Design: Part II, Preliminary Configuration Design and Integration of the Propulsion System*, DARcorporation, Lawrence, KS, 2005.
5. Roskam, J, *Airplane Design: Part III, Layout Design of Cockpit, Fuselage, Wing, and Empennage: Cutaways and Inboard Profiles*, DARcorporation, Lawrence, KS, 1989.
6. Roskam, J, *Airplane Design: Part IV, Layout of Landing Gear and Systems*, DARcorporation, Lawrence, KS, 2010.
7. Roskam, J, *Airplane Design: Part V, Component Weight Estimation*, DARcorporation, Lawrence, KS, 1999.
8. Roskam, J, *Airplane Design: Part VI, Preliminary Calculation of Aerodynamic Thrust and Power Characteristics*, DARcorporation, Lawrence, KS, 2008.
9. Roskam, J, *Airplane Design: Part VII, Determination of Stability, Control and Performance Characteristics: Far and Military Requirements*, DARcorporation, Lawrence, KS, 1991.
10. Roskam, J, *Airplane Design: Part VIII, Airplane Cost Estimation: Design Development, Manufacturing and Operating*, DARcorporation, Lawrence, KS, 1990.
11. Anderson, J., *Introduction to Flight*, 8th Ed., McGraw-Hill: New York City, NY, 2011
12. Anderson, J., *Fundamentals of Aerodynamics*, 5th ed., McGraw-Hill: New York City, NY, 2007
13. Barrett, R., "Dragonfly; Sample Report Block 1," Class Handout.
14. Barrett, R., "Statistical Time and Market Predictive Engineering Design (STAMPED) Techniques for Aerospace System Preliminary Design," *Journal of Aeronautics & Aerospace Engineering*, Omics Publishing, Vol. 3, No. 1, Feb. 2014.
15. Anon., "Ju-87G," Aircraft Aces, URL: <http://www.aircraftaces.com/images/junkers-87-stuka.jpg>
16. Dwyer, L., "Junkers Ju 87 Stuka," The Aviation History Online Museum, URL: <http://www.aviation-history.com/junkers/ju87.html>
17. Anon., "Stuka, deutscher Sturzkampfbomber Junkers Ju 87," Weltkrieg, URL: <https://weltkrieg2.de/stuka/>
18. Anon., "Junkers JU 87 Stuka," howstuffworks, URL: <http://science.howstuffworks.com/junkers-ju-87-stuka.htm>
19. Editors of Encyclopaedia Britannica, "Stuka," Encyclopaedia Britannica, URL: <https://www.britannica.com/technology/Stuka>
20. Anon., "Ilyushin Il-2 Shurmovik," Aircraft Aces, URL: <https://deanoinamerica.files.wordpress.com/2012/02/il-2-fhc-12-a.jpg> <http://www.aircraftaces.com/images/il-2-sturmovik.jpg>
21. Crellin, E., "Stalin's 'Essential Aircraft: Ilyushin Il-2 in WW2,'" Smithsonian National Air and Space Museum, URL: <https://airandspace.si.edu/stories/editorial/stalin%E2%80%99s-ilyushin-il-2-shurmovik>
22. Anon., "Republic P-47 Thunderbolt," Aircraft Aces, URL: <http://www.aircraftaces.com/images/p47-thunderbolt.jpg>
23. Dwyer, L., "Republic P-47 Thunderbolt," The Aviation History Online Museum, URL: <http://www.aviation-history.com/republic/p47.html>
24. Wyndham, B., "Republic P-47 Thunderbolt," Warbird Alley, URL: <http://www.warbirdalley.com/p47.htm>
25. Anon., "Fairchild Republic A-10 Thunderbolt II," Airfighters, URL: http://www.airfighters.com/profiles/a-10/A-10_74_FW.jpg
26. Pike, J., "A-x Attack Fighter - Design," GlobalSecurity, URL: <https://www.globalsecurity.org/military/systems/aircraft/a-x-1966-design.htm>
27. Tegler, E., "Why the A-10 Warthog Is Such a Badass Plane," Popular Mechanics, URL: <http://www.popularmechanics.com/military/a18236/why-the-a-10-warthog-is-such-a-badass-plane/>
28. Anon., "A-10 Thunderbolt II," Military.com, URL: <http://www.military.com/equipment/a-10-thunderbolt-ii>
29. Anon., "Douglas AC-47 Spooky," DeviantArt Deport, URL: https://pre00.deviantart.net/383c/th/pre/f/2017/152/d/8/spooky_cambodia_1_dev_by_ws_clave-dbb5s43.jpg
30. Eger, C., "The Spookiest story in Vietnam: The AC-47 gunship," Guns.com, URL: <http://www.guns.com/2015/08/07/the-spookiest-story-in-vietnam-the-ac-47-gunship-12-photos/25>
31. Anon., "Douglas AC-47D," National Museum of the U.S. Air Force, URL: <https://web.archive.org/web/20141011174350/http://www.nationalmuseum.af.mil/factsheets/factsheet.asp?id=3211>
32. Pike, J., "AC-47," Global Security, URL: <https://www.globalsecurity.org/military/systems/aircraft/ac-47.htm>
33. Anon., "AC-119k Stringer," <http://www.ac-119gunships.com/the119s/ac119k/gunshipk.htm>

34. Anon., "Fairchild AC-119G," National Museum of the U.S. Air Force, URL: <https://web.archive.org/web/20141025090520/http://www.nationalmuseum.af.mil/factsheets/factsheet.asp?id=3213>

35. Broyhill, M., "Fairchild AC-119 Gunship 'Shadow,'" Strategic-Air-Command.com, URL: http://www.strategic-air-command.com/aircraft/attack/ac119_gunship.htm

36. Anon., "Fairchild AC-119K," National Museum of the U.S. Air Force, URL: <https://web.archive.org/web/20141025090632/http://www.nationalmuseum.af.mil/factsheets/factsheet.asp?id=3214>

37. Petric, B., "A Gunship History," USAF AC-119 Gunships, URL: <http://www.ac-119gunships.com/history/hist1.htm>

38. Pike, J., "AC-119," Global Security, URL: <https://www.globalsecurity.org/military/systems/aircraft/ac-119.htm>

39. Anon., "AC-130J," Aviation Graphic, URL: https://www.aviationgraphic.com/4934-thickbox_default/ac-130j-ghostrider-1-sog-jp-2200.jpg

40. Anon., "Lockheed AC-130A," National Museum of the U.S. Air Force, URL: <https://web.archive.org/web/20141011171113/http://www.nationalmuseum.af.mil/factsheets/factsheet.asp?id=3216>

41. Anon., "Lockheed AC-130A 'Plain Jane'," National Museum of the U.S. Air Force, URL: <https://web.archive.org/web/20141011171113/http://www.nationalmuseum.af.mil/factsheets/factsheet.asp?id=3220>

42. Anon., "Lockheed AC-130A 'Surprise Package'," National Museum of the U.S. Air Force, URL: <https://web.archive.org/web/20141011171113/http://www.nationalmuseum.af.mil/factsheets/factsheet.asp?id=3221>

43. Anon., "Lockheed AC-130A 'Pave Pronto'," National Museum of the U.S. Air Force, URL: <https://web.archive.org/web/20141011171113/http://www.nationalmuseum.af.mil/factsheets/factsheet.asp?id=3224>

44. Anon., "Lockheed AC-130E 'Pave Spectre'," National Museum of the U.S. Air Force, URL: <https://web.archive.org/web/20141011171113/http://www.nationalmuseum.af.mil/factsheets/factsheet.asp?id=3216>

45. Anon., "AC-130U," U.S. Air Force, URL: <http://www.af.mil/About-Us/Fact-Sheets/Display/Article/104486/ac-130u/>

46. Anon., "AC-130W Stinger II," U.S. Air Force, URL: <http://www.af.mil/About-Us/Fact-Sheets/Display/Article/104485/ac-130w-stinger-ii/>

47. Anon., "AC-130J Ghost Rider," U.S. Air Force, URL: <http://www.af.mil/About-Us/Fact-Sheets/Display/Article/467756/ac-130j-ghostrider/>

48. Barrett, R., "Col. Roger Disrud," Photograph, Lawrence, KS, October, 2017.

49. Stirling, M., "Lt. Col. John Marks," 442D Fighter Wing, URL: <https://media.defense.gov/2016/Nov/23/2001671903/-1/0/161123-F-QV141-013.JPG>

50. Anon., "Prof. Adrian Lewis," University of Kansas Department of History, URL: <https://history.ku.edu/adrian-lewis>

51. Disrud, R. "Technical Discussion of A-10 and Replacement Aircraft," The University of Kansas, Aerospace Engineering Department,

52. Lewis, A. "Technical Discussion of A-10 and Replacement Aircraft," The University of Kansas, Aerospace Engineering.

53. Barrett, R. "Preliminary Weight Technical Discussion," Lawrence, KS, September, 2017.

54. Anon., "Bushmaster III," Orbital ATK, URL: https://www.orbitalatk.com/defense-systems/armament-systems/automatic-cannons-chain-guns/docs/Bushmaster_III_Fact_Sheet.pdf

55. Anon., "35mm/1000 KDG Millennium GDM-008," NavWeaps, URL: http://www.navweaps.com/Weapons/WNGER_35mm-1000_Millennium.php

56. Anon., "Pylon Turning," Dauntless-soft.com, URL: [http://www.dauntless-soft.com/products/freebies/library/books/flt/chapter11/eights%20on%20pylons%20\(pylon%20eights\)_files/imageri9.jpg](http://www.dauntless-soft.com/products/freebies/library/books/flt/chapter11/eights%20on%20pylons%20(pylon%20eights)_files/imageri9.jpg)

57. Wimpres, John K., Newberry, Conrad F., "The YC-14 STOL Prototype: Its Design, Development, and Flight Test," American Institute of Aeronautics and Astronautics, 1998.

58. Anon., "Q-39 (AN/AAQ-39)," Lockheed Martin, URL: <https://www.lockheedmartin.com/us/products/q-39.html>

59. Ray, Jonathan, "Industry Scan," AviationToday, 1 Aug. 2008, URL: <http://www.aviationtoday.com/2008/08/01/industry-scan-59/>

60. Anon., "AN/AAQ-37 Distributed Aperture System (DAS) for the F-35," Northrop Grumman, URL: <http://www.northropgrumman.com/Capabilities/ANAAQ37F35/Pages/default.aspx>

61. Northrop Grumman, "F-35 JSF Distributed Aperture System (DAS) Sensors Demonstrate Hostile Fire Detection Capability " YouTube, URL: <https://www.youtube.com/watch?v=fHZ00T5mDYU>

62. Northrop Grumman, "APG-81 AESA Radar for the F-35 JSF ," YouTube, URL: <https://www.youtube.com/watch?v=wIWA0upjMeM>

63. Petrenko, V. F, et al., "Pulse electro-thermal de-icer (PETD)," Cold Regions Science and Technology, Vol. 65, Is. 1, Jan. 2011, Pg. 70-78, URL: <https://www.sciencedirect.com/science/article/pii/S0165232X10001278>

64. Wang, Zhenjun, "Recent progress on ultrasonic de-icing technique used for wind power generation, high-voltage transmission line and aircraft," Energy and Buildings, Vol. 140, Apr. 2017, Pg 42-47, URL: <https://www.sciencedirect.com/science/article/pii/S0378778817302633>

65. Rae, Perry, "Overseer Technical Discussion," Lawrence, KS, March 26, 2018.
